Utilizing
Crosswise self-growing connection
As
Load-bearing element
In
Building Design

Zhinan Wu

Utilizing crosswise self-growing connection as load-bearing element in building design

By

Zhinan Wu

in partial fulfilment of the requirements for the degree of

Master of Science

in Building Engineering – Structural Design

at the Delft University of Technology,

to be defended publicly on November 27th, 2020.

Thesis committee:

Prof.dr.ir. J.W.G. van de Kuilen,	TU Delft
Drs. W.F. (Wolfgang) Gard,	TU Delft
Ir. L.P.L (Lennert) van der Linden	TU Delft
Xiuli Wang,	TU Delft

An electronic version of this thesis is available at http://repository.tudelft.nl/.

TUDelft

Acknowledgement

Abstract

Within the context of utilizing alternative materials to promote sustainable construction in the building industry, Living Architecture is a concept that uses living organisms as the building materials. As a rather unconventional approach, it possesses benefits such as low cost, not requiring considerable workforce or industrial material, carbon-free, and its ability to return to nature when no longer in use. As an essential part of Living Architectures, scientists and engineers have recognized the importance of fusion between trees. For instance, in projects such as the Baubotanik Tower and the Living Tree Pavilion, a design premise is that the structure becomes ready when the fusion between trees could provide sufficient strength to support the structure. However, little research has been conducted in terms of the fusion processes and the mechanical behaviours of tree connections, which is an essential step prior to designing Living Architecture. With crosswise tree connection as the main focus of this thesis, the following research question is formulated:

What are the mechanical behaviours of a self-growing crosswise tree connection when utilized as load-bearing elements in a building structure, and how can such connections be modelled during the preliminary design phase of a building structure?

To help answering the research question, literature studies are conducted. In chapter 1, from a botanical perspective, it is concluded that, in the event of two stems contacting with one another, the two stems would gradually fuse together. Such an event is triggered by the abrasion on the bark due to the rubbing between the stems; later, due to the secondary growth, fibers from both stems deviate and join together to form common growth rings, such event can also be verified by the micro-CT scans that have been conducted on the crosswise tree connections. Additionally, due to the nature of the connection, a certain eccentricity from the stems' piths exists, and it is important to acknowledge that the length of such eccentricity stays constant from the start of the fusion process.

To investigate the influence of tree growth on the mechanical properties of trees and tree connections, which is needed for design purposes, chapter 2 investigates the growth model and the tapering geometry of living trees. With the help of the Urban tree growth model published by the United States Department of Agriculture and a series of simple tapering equations, the growth parameters of a growing tree can be computed.

Part-II of the thesis explores deeper in terms of the mechanical behaviours of such crosswise connections. A simple analysis of two trees connected in a crosswise manner is first conducted in chapter 4. It is concluded that, under loading, the connection can be subjected to tensile stress perpendicular to the grain and rolling shear stress. As two of the weakest strength properties of wood, the crosswise connections should be treated with care by future designers.

As a part of an entire building structure, it is essential to determine the rotational stiffness and strength of a structural connection; therefore, in chapter 5, an experimental design is proposed for such purpose. Due to the irregular geometry of the crosswise connection, the experiment makes use of digital image correlation so that the rotational stiffness of the connection under loading can be obtained. Since conducting the actual experiment falls out of this thesis scope, a finite element modelling analysis with similar boundary conditions is conducted in chapter 6. With the results obtained from FEM, it is found that, due to the nature of the connection, complex torsional behaviours occur to the connection. Additionally, with the connection under loading, it is found that non-uniform stress distribution and stress concentration occurs along the interface between two stems. Comparing with the strength properties of wood, it is discovered that the first incident that causes failure is tension perpendicular to the grain, which is the weakest strength property of wood.

To conduct preliminary structural design and verification, wireframe modelling approach is often utilized. In chapter 7, it is concluded that it is most suitable to model the crosswise connection with a separate beam element that connects the two stems, for its ability to capture the complex torsional behaviours described in chapter 6.

Lastly, after investigating the local behaviours of crosswise connection, Part-III investigates the feasibility of conducting a preliminary structural design and verification with such connections. With the case study analysis conducted in chapter 8, it is concluded that, by appropriately capturing the load effects on growing trees and tree connections, designers are able to predict when the structure would reach sufficient strength to be in service.

This thesis positions itself as a part of a broader spectrum that examines the feasibility of utilizing tree connections as the load-bearing elements in structures, which can be seen as a step towards sustainable construction.

Contents

List of Figures

List of Tables

Introduction

1. Research motivation

1.1 Sustainability in the building industry

Sustainability plays a significant role in almost every professional industry around the globe. It is described as enhancing the quality of life, allowing people to live in a healthy environment, and improving social, economic, and environmental conditions for present and future generations[1]. Since the first mention of sustainability from the world commission on environment and development, entitled Our Common Future (1987), it has become one of the focal points in building sectors. The buildings that had been constructed beginning from the second half of the last century until the first decade of this century were characterized by the enormous consumption of energy and natural resources[2], which led to much criticism regarding the amount of waste produced and the pollution of air. Knowing that the construction industry is a significant consumer of non-renewable resources and responsible for half of the total CO2 emission[3], it becomes imperative for the building sector to move towards a more sustainable dimension. In the effort of incorporating sustainability in the building industry, many innovative strategies have emerged, including life-cycle assessment of building projects, re-purposing existing buildings, consideration of alternative materials, etc.

1.2 Alternative construction material: Living architecture

In the context of the use of alternative construction materials, a rather peculiar approach is Living architecture, which is defined as the use of forces and possibilities provided by natural living organisms such as trees to help and build low-cost and sustainable construction[4]. Implementing trees as a part of load-bearing components in a structure has been experimented with and applied throughout history. Here, the tree does not refer to the standardized engineering timber elements that engineers apply to structures, but itself has an organism. For instance, in India, there are numerous bridges like the Rangthylliang bridge across the region for people to access from one place to another. The bridges are realized by guiding roots in a hollowed branch across the river and pushing them into the soil on the other side. The 50-m long bridge takes 10 to

15 years to be fully functional[4]. Since the bridge only consists of Ficus Elastica as the structural member, the trees are responsible for both load-bearing and stability.

Figure 1. Rangthylliang bridge made with Ficus elastica[4]

Other examples of living architecture have also been experimented in the context of utilizing the mechanical properties of the living organism itself, such as the "living chair" built by John Krubsack in 1914. The chair was constructed entirely by forcing the trees to grow in the desired way as they were growing. His work had inspired other artists and builders to experiment with trees, such as Marcel Kalberer, who constructed the Auerworld Palace in less than a month. The structure was realized with living, bent, and shaped willows, which now serve as public facilities in schools and gardens along with about 10,000 other living willow construction[4].

Figure 2. Living Architecture: Living chair (left)[5] Auerworld Palace (right)[4]

Although building with trees has been experimented throughout history, it remains an uncommon concept in the modern building industry, possibly because the state of living trees depends on many factors such as light, temperature, water, humidity, and nutrition. More recently, Baubotanik, a research group based in Germany, aims to develop a so far missing theoretical and scientific basis of living architecture. It has been working on realizing an artificial tree tower utilizing the properties of inosculation and its time-dependent strengthening behaviour. Inosculation is a term used in the horticulture field, which refers to the state where tree members, for example, roots, branches, or stems, grow together so that individuals of the same species form a network in which water and nutrients are interchanged.

For such research, Baubotanik built a prototype for such research, a three-story building made of around 400 plants of Salix alba that were planted in the ground and on six levels in special plant containers, whose growth stages have been closely monitored. Although the structure is still under development, the design is based on the premise that both the trees and their self-growing connections will become strong enough to take over the loading from the structure[6].
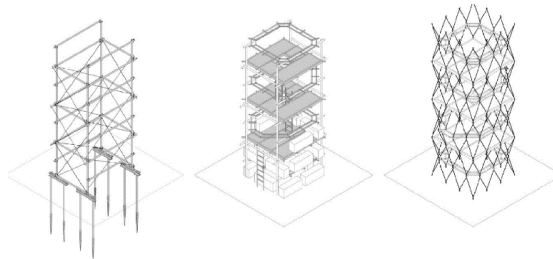
Figure 3. Baubotanik tree tower[4]

Of the examples illustrated above, it can be seen that the connections made with living organisms play a significant role in stabilizing the structure. Therefore, it is of interest to dive deeper into the mechanical properties of the tree connections.

1.3 Load-bearing tree connections

In his book, Design in Nature – Learning from trees[7], Mattheck discusses the phenomenon of trees connecting naturally without humans' interference. Depending on how two trees come into contact with each other, such as tree swaying due to wind, two types of connection could occur, namely axial welds and cross welds. Axial weld occurs when two parallel trees make contact with one another, and cross weld occurs when two crossing trees make contact with one another. Over the course of trees' growth, the distance between two trees will decrease, which means that the contact becomes more frequent and intensive. The contact between two trees would result in local growth to reduce contact stresses by enlarging the contact area [9], a well-known phenomenon associated with the mechanical self-optimization of trees, which is explained in detail in Section 1.2 in Part-I: Literature Study.
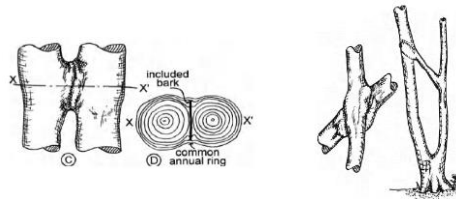
Figure 4. Axial weld (left) and cross weld (right)[7]

Examples of tree connections can also be found where human interference is involved. A Ficus cage, shown in Figure 5, interwoven by several Ficus Benjamina trees, is a popular plant often used for interior decoration. From an interview with a Ficus cage trader[8], it is learned that, in the beginning, the seedlings of Ficus Benjamina are planted in the land. The young plants will typically grow to about one meter in height after the first year; it is at this stage when an artificial cage made with iron is built; the workers then start to weave the young plants around the iron cage for the plants to form the desired shape. On average, the connected plants will be transplanted from the ground to the pot in the fifth year. During growth, the part of the trees where weaving takes place will fuse, and the Ficus cage becomes a stable structure by itself.

Figure 5. Ficus cage

Nuijten[9], a student from TU Delft, made a design proposal, and built a living tree pavilion in 2010. The structure was designed to be supported only by the trees and the tree connections, but until the trees have grown to sufficient strength, the structure is supported by temporary timber columns. Nuijten had predicted that in approximately ten years, the pavilion would grow into a structure with sufficient load-bearing capacity to withstand the proposed load combination. One of her innovative ideas is implementing different types of tree joints, illustrated in Figure 6; they are identified as cross-weld, axial-weld, and graft.
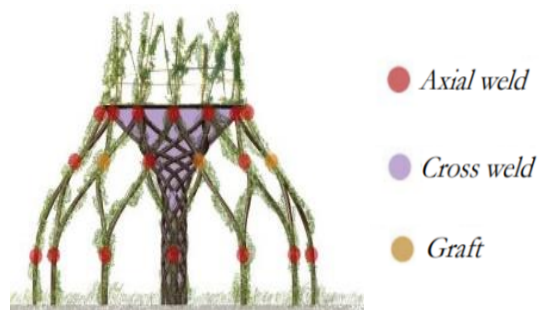
Figure 6. Living Tree Pavilion design concept[9]

Winterman[10], a student from TU Delft, performed micro-CT tests on the crosswise connection made by Ficus Benjamina. The study focused on the microstructure of a crosswise connection, which provided insights regarding a crosswise connection's inosculation process. Figure 7 provides the cross-sectional views of the connection in different planes.

5
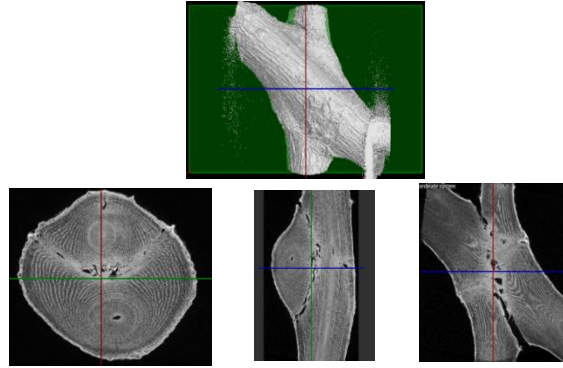
Figure 7. Cross-section of inosculated trees[10]

2. Research justification

As described above, many on-going research and experiments have focused on utilizing living trees and tree connections as a part of the load-bearing elements. A similar conclusion made by these designs is that, unlike standardized engineering materials such as concrete and steel, living trees and tree connections are subjected to growth, and their mechanical properties vary with growth. However, the following research gaps are recognized:

- To design with growing trees and tree connections, study should be made in terms of the fusion process between trees.
- To conduct design with growing trees, study should be made regarding the growth model of trees, as it directly influences the mechanical properties of trees and tree connections.
- In Nuijten's design of the Living Tree Pavilion, tree connections were treated as rigid moment-resisting connections, while in reality, a perfectly rigid connection does not exist; therefore, it is necessary to investigate further in terms of the mechanical behaviours of tree connections when utilized as a load-bearing element.

Additionally, during the preliminary design phase of a building structure, in order to capture the global behaviours of the structure, wireframe analysis is often conducted, where structural elements are modelled with 1-dimensional beam elements. However, it is unprecedented to incorporate self-growing crosswise tree connections during structural analysis; therefore, investigation should be made in terms of how the connection can be modelled in a wireframe finite element package so that the correct behaviours of the connection can be captured. These considerations lead to the main research question for this thesis project.

3. Research question

With crosswise connection as the main focus of this thesis, the main research question is:

What are the mechanical behaviours of a self-growing crosswise tree connection when utilized as a load-bearing element, and how can such connection be modelled during the preliminary design phase of a building structure?

To answer such research questions, a series of sub-questions need to be formulated so that the research can be done in a logical manner. The objectives as well as the sub-questions are defined in chapter 4 and 5, respectively.

4. Objectives

For a structural connection in building design, rotational stiffness and strength are two of the most important aspects; therefore, one of the objectives of this thesis project is to propose an experimental design that aims to investigate the stiffness and resistance of a crosswise tree connection. Since conducting the actual experiment falls out of the scope of this thesis, a 3-dimensional finite element modelling of the crosswise tree connection with similar boundary conditions is analysed, which would provide useful insights in terms of the connection's mechanical behaviours and strength characteristics. As a possible modelling approach, it can also be used to compare with the experiment results in the future.

Upon obtaining a basic understanding of crosswise connection's mechanical behaviours, another deliverable of this project is to conduct a preliminary structural analysis and verification of a building structure with growing trees and crosswise connections. For this, growth model of trees as well as a wireframe modelling approach of crosswise connection are investigated. And lastly, with a design case study, invesigation is made in terms of the feasibility of utilizing growing trees and tree connections as the main load-bearing elements in structures, which can be seen as an innovative method towards sustainable construction.

5. Methodology

The following flow chart illustrates the adopted methodology to carry out this thesis project. The content of each section is then briefly summarized hereinafter.
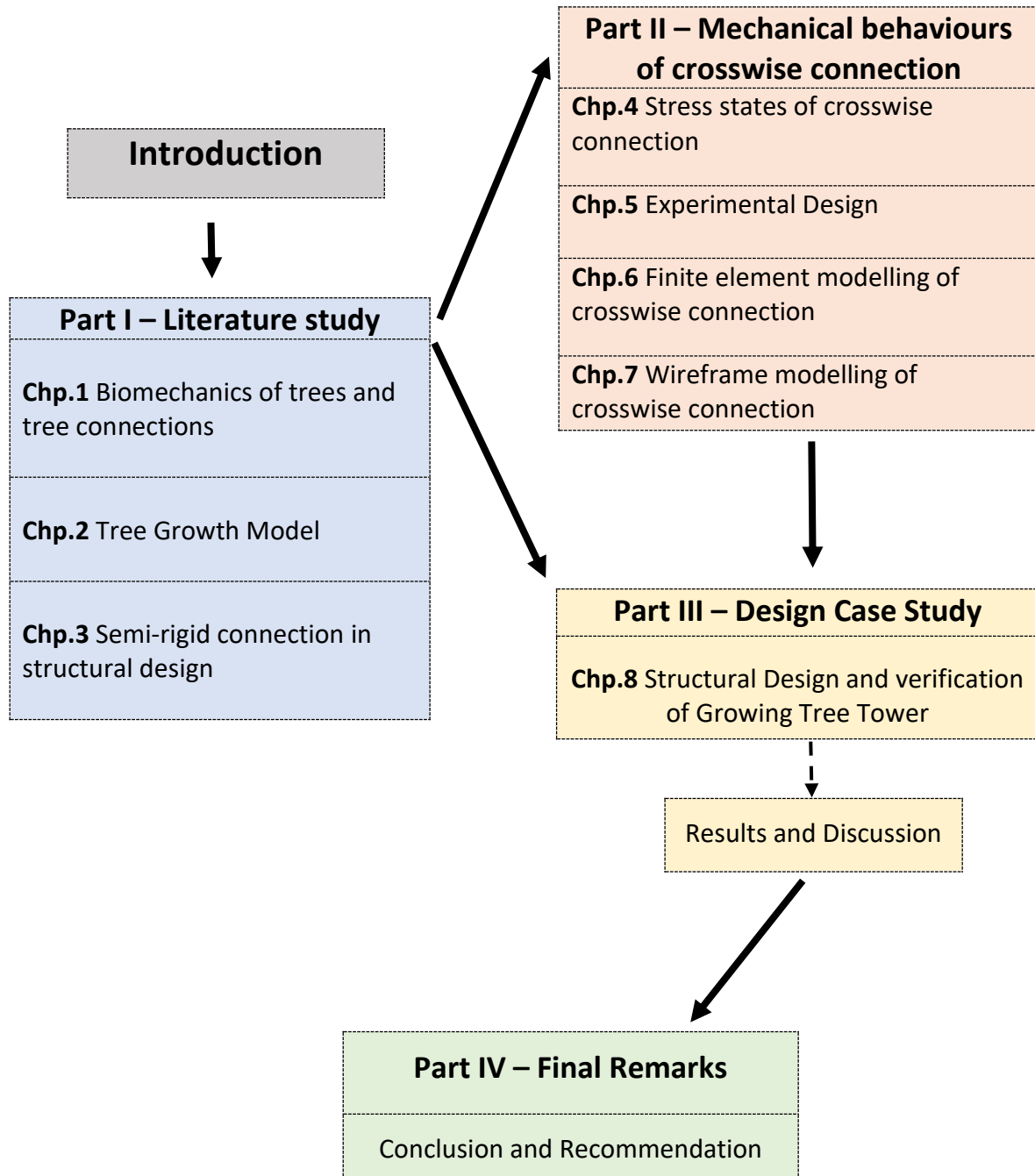
Figure 8. Flow chart of research project

Part I. Literature Study

Before utilizing crosswise tree connections as load-bearing elements, more comprehensive and fundamental knowledge regarding tree mechanics should be obtained. Therefore, through literature study, chapter 1 aims to answer the following research question:

- What are the main biomechanical properties of trees? How is the structure of wood composed, and what are the main material properties of wood?
- What events occur on a micro-level during inosculation between two trees?
- What are the unique characteristics of a crosswise connection?

As a preparation to investigate the feasibility of utilizing growing trees and crosswise connections in the preliminary structural design in Part III, chapter 2 investigates the growth model and the tapering geometry of trees, while chapter 3 investigates the mechanical behaviours and the most common modelling approaches of semi-rigid structural connections.

Part II. Mechanical behaviours of crosswise connection

The literature study made in chapter 3 provides the motivation for more in-depth research in Part-II, which focuses on analyzing and capturing the mechanical behaviours of a crosswise connection. First, a simple case of two trees connected in a crosswise manner is analyzed in chapter 4. With recognizing the importance of determing the rotational stiffness and strength of a semi-rigid connection, an experimental design with a corresponding finite element modelling approach is analyzed in chapter 5 and 6. The sub-questions to be answered are:

- What are the mechanical behaviours of a crosswise connection under loading?
- What are the hypotheses regarding the failure mechanism of a crosswise connection?

Learning from the mechanical behaviours of a crosswise connection in chapter 6, a wireframe modelling approach for the connection is proposed in chapter 7, which provides the opportunity in conducting the preliminary structural design of a building structure in Part-III.

Part III. Design Case Study

Inspired by projects like the Baubotanik Tower, a design case study is conducted in chapter 8. The main motivation for the case study is to investigate the feasibility of utilizing growing trees and crosswise connections as the load-bearing elements during the preliminary design phase of a building structure from a structural engineer's perspective. With the structural verification procedures proposed in the case study, designers are able to predict when the structure would be ready for service. The scope of this design case study is limited to the following criteria:

- The new design is proposed from a structural engineer's perspective, thus, the multidisciplinarity of the design is out of scope.

- The structural verification is based on linear-elastic static analysis under ultimate limit states, which only correlates with the structure's response such as internal forces/moments and internal stresses. Therefore, the verification with serviceability limit state or dynamic response of the structure is out of scope.

- Structural verification is based on Eurocode 1991-1-1

- A parametric design based on the proposed building design is analyzed at the end. The purpose of such analysis is not about offering an optimized structure, but to show designers with its capabilities of predicting the time it would take for the structure to be completed with different building configurations.

Part I – Literature study

1. Biomechanics of trees and tree connections

Implementing any material in structural design requires a comprehensive understanding of the material properties, especially organic materials such as wood because of its anisotropic properties and its complex microstructure. To utilize trees and crosswise connections as main load-bearing elements, chapter 1 provides a literature study on the fundamental knowledge about the material properties of wood, biomechanics of tree structures, and the inosculation process with a closer look at the crosswise connection.

1.1 Wood structure and material properties

1.1.1 Macroscopic and microscopic structure of wood

On a macroscopic scale, wood is composed of three main elements: heartwood, sapwood, and bark. Heartwood, although physiologically inactive, its formation is a regulatory process serving to keep the amount of sapwood at an optimum level[11]. Sapwood is responsible for the transportation of water and mineral from the roots to other parts of the plant, such as leaves; additionally, it provides mechanical strength to the plant due to the presence of lignified cells. The bark is responsible for the transportation of nutrients from leaves to storage organs and growing parts of the plant, such as cambium.
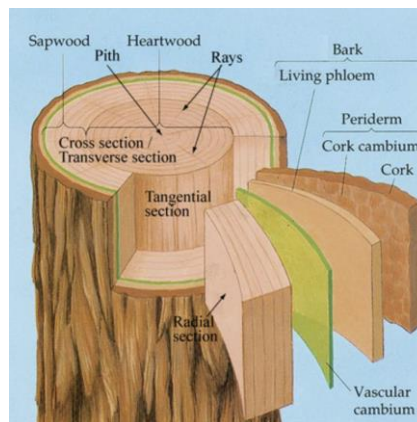
Figure 9. Cross-section of wood[12]

On a microscopic scale, a few terminologies of plant cells with their functions need to be described because of their critical roles during the inosculation process, which is discussed in section 1.3. The cell layers that will be addressed, from outside to inside, are the epidermis, periderm, cortex, phloem, cambium, and xylem.

Epidermis is the outermost layer of cells covering the stem of a tree; the vital purpose of epidermis is to serve as a protective barrier against mechanical injury, water loss, and infection[13].

Periderm is also referred to as 'outer bark,' which is the tissue providing protection, water conservation, insulation, and environmental sensing[14]. Periderm is generated as a result of secondary growth as epidermis cells are crushed in the process. It consists of three layers, phellem, phellogen, and phelloderm, from outside to inside, respectively. Phellogen, which is also referred to as cork cambium, is the middle layer that produces phelloderm (cork skin) to the inside and phellem (dead cork cells) to the outside. Phellem, sometimes referred to as dead cork cells, are hollow cells that serve insulation purposes; it is also essential in minimizing oxidation of living cells. Phelloderm can be referred to as the secondary cortex; it can be produced in thin-walled or thick-walled varieties, which affects the strength of periderm.

The aforementioned microstructures can be visualized in the diagram shown in Figure 10.
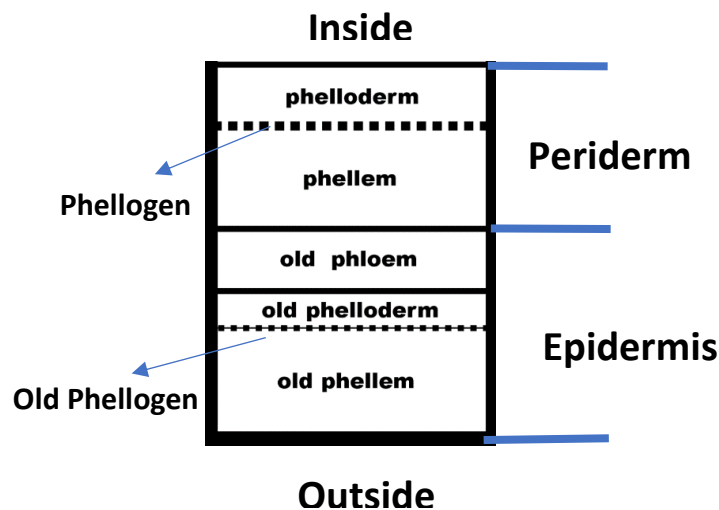
Figure 10. Layers of tissues in tree bark[14]

Cortex is a layer between periderm and vascular cambium; it is responsible for converting carbon dioxide and water that the plant absorbs into simple carbohydrates, which the plant then uses for photosynthesis.

Phloem, produced by the vascular cambium, is responsible for food, nitrogen, and growth regulator transport vertically and horizontally within a tree.

Cambium is a lateral meristem cell that produces xylem cells to one side and phloem cells to the other to form the vascular system.

Xylem, divided from cambium, is responsible for the transportation of water and mineral in the sapwood from the roots to other parts of the plant such as leaves. It also gives mechanical strength to the plant due to the presence of lignified cells.

1.1.2 Material properties of wood

1.1.2.1 Orthotropic elasticity of wood

Anisotropy is used to imply a material in which the mechanical properties differ in an infinite number of directions. Wood has extreme anisotropy because 90 to 95% of all the cells are elongated and parallel to the trunk, while the remaining 5 to 10% of cells are arranged in radial directions, with no cells at all aligned tangentially[12]. Thus, wood can be treated as an orthotropic material, in which the material properties vary in three principal directions: longitudinal, radial, and tangential.

Designers often assume that the mechanical properties along each direction remain constant throughout the entire element. With this assumption, twelve elastic constants are used to describe the orthotropic elasticity of wood: three moduli of elasticity E_L, E_R, E_T three moduli of rigidity G_{LR}, G_{LT}, G_{RT}, and six Poisson's ratios $\mu_{LR}, \mu_{RL}, \mu_{LT}, \mu_{TL}, \mu_{RT}, \mu_{TR}$, where the one-letter subscript L, T, and R indicate longitudinal, tangential, and radial axis, respectively. The following relationships hold to the material properties of wood:

$$\frac{v_{ij}}{E_i} = \frac{v_{ji}}{E_j} \qquad (1.1)$$

$$G_{ij} = G_{ji} = \left[\frac{\sqrt{E_i E_j}}{2\left(1 + \sqrt{v_{ij} v_{ji}}\right)}\right] \qquad (1.2)$$

In structural analysis, the importance of elastic properties along the grain is recognized, whereas the elastic properties in the radial-tangential plane are often considered as isotropic. Many of the studies[15][16][17] have followed this simplification while still being able to obtain satisfactory results. Therefore, the following assumptions could also be made:

$$E_R = E_T \qquad (1.3)$$

$$\mu_{LR} = \mu_{LT} \qquad (1.4)$$

$$\mu_{RL} = \mu_{TL} \qquad (1.5)$$

$$\mu_{RT} = \mu_{TR} \qquad (1.6)$$

$$G_{LR} = G_{LT} \qquad (1.7)$$

However, one thing that is often overlooked by structural designers is the fact that the material and physical properties vary even within the same tree due to the variation of growth rings' density. Such variation can be ascribed to the anatomical structure of wood, such as the characteristics of vessels and fibers[18]. As the tree grows, the rings that are farther away from the pith exhibit higher density than those near the pith until they reach a stable value in many years. As density increases, the mechanical properties such as the modulus of elasticity and the modulus of rupture increase.

The statements made above can be proved by the following figures, which were researches that have already been conducted in the field. Figure 11 shows that the density of Pinus radiata increases from the pith outwards until reaching a stable value at year 20[19], while Figure 12 indicates that the modulus of elasticity of black spruce keeps increasing until reaching a stable value at year 50[18].
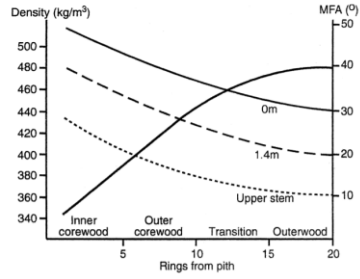
Figure 11. Schematic curves showing typical pattern of pith-to-bark variation for Pinus radiata in wood density, with progressive increase[19]
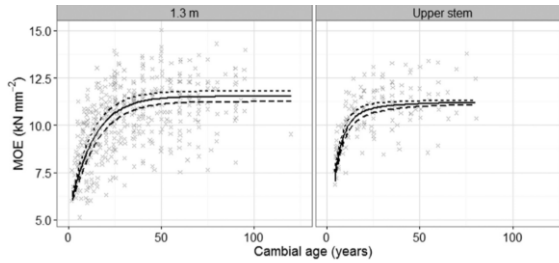
Figure 12. Modulus of elasticity (MOE) vs cambial age[18]

Uniaxial compression test[15] had also been used to illustrate the same phenomenon. The tests were conducted on two timber specimens cut from the same tree but at different radial coordinates, one closer to the pith, the other far away from the pith. Although being parts of the same tree, the results showed that the two elements have different mechanical properties. Young's modulus parallel to the grain of the center specimen is considerably lower than the peripheral specimen. The experimental value of young's modulus of elasticity obtained from the peripheral annual rings is almost identical to the real value obtained from other literature.
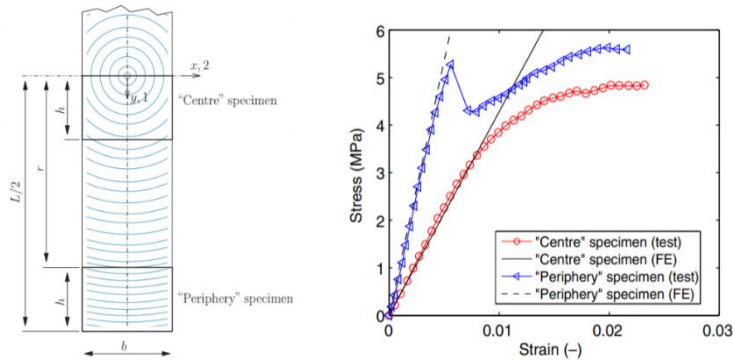
Figure 13. Results obtained from uniaxial compression test of wood[15]

1.1.2.2 Strength properties of wood

In terms of strength properties of wood, depending on the type of loading and the direction of the load, the strength of the wood exhibits very different characteristics. Five parameters are commonly measured for design purposes, including bending, compression parallel and perpendicular to the grain, tension perpendicular to the grain, and shear parallel to the grain, where the modulus of rupture is often substituted as a low or conservative estimate of tensile strength for timber[20].

Although the magnitude of these parameters varies depending on the wood species, the general behaviours are similar: tensile strength parallel to the grain is usually the highest, followed by compression parallel to the grain, then followed by shear parallel to the grain and compression perpendicular to the grain, the lowest strength property is usually tension perpendicular to the grain.

Several strength parameters of wood are much less investigated for various reasons; however, with a few assumptions proposed by researchers, they can also be implemented for design purposes. For example, because wood is highly orthotropic, it is very difficult to fail in shear perpendicular to the grain before another failure mode occurs. Still, limited literature suggested that shear strength perpendicular to the grain may be 2.5–3 times that of shear parallel to the grain [21].

Additionally, suggested by Eurocode 5[22], rolling shear strength is approximately equal to twice the tensile strength perpendicular to the grain. And lastly, the torsional strength of wood about its longitudinal axis can be approximated as the shear strength parallel to grain[20].

1.2 Biomechanics of trees: Self-optimisation

For conventional structural elements like steel or concrete beams, the strength and stiffness are designed before production according to the potential stresses that would be subjected to them during service life. However, it is a different case for a living tree because a growing tree is able to mechanically optimize itself through adaptive growth based on the typical loading conditions.

Such statements can be proved by several pieces of evidence, such as the formation of reaction wood, which is trees' response in minimizing stresses by reducing the length of the loaded lever arm[23] and grow in an upright manner. For trees subjected to frequent wind

loading, conifers form compression wood on the lee side, whereas broadleaves form tension wood on the windward side[7].
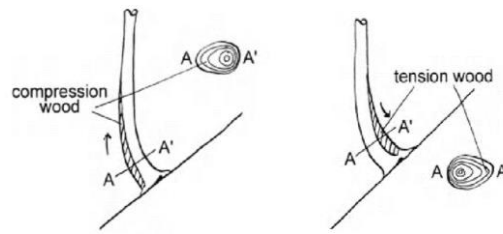
Figure 14. Tension wood on the broad-leaved trees, and compression wood on the conifers[7]

Self-optimization closely relate to a natural phenomenon called the axiom of uniform stress; it is a phenomenon possessed by trees in which they would make any effort to grow into a homogeneous state of stress on their surface. Mattheck[7] explains the shape optimization of a trunk for different loading scenarios in his book, shown in Figure 15. For instance, when the trunk experiences pure bending continuously, it forms into a shape that is similar to an I-beam, which is optimized to resist bending. And if the trunk experiences a combination of loads, local growth exacerbates on the area where stresses are the most.
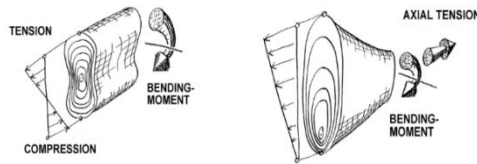
Figure 15. Shape of a trunk subjected to bending (left) and a combination of tension and bending (right)

Finally, adaptive growth can also be illustrated in the Baubotanik Tower. From observation, the trees are able to grow around the steel scaffolding placed next to them and finally merge so that the stresses experienced in the tree can be as uniform as possible.

Figure 16. Adaptive growth of trees in Baubotanik tower

1.3 Inosculation process of tree connection

A plain explanation of the inosculation process is that, at first, the bark tissues merge; afterwards, the wood bodies grow towards one another, merge, and subsequently form a continuous growth ring. After merging successfully, these "wood welds" from several individuals join into a single "hyper-organism", which develops a high mechanical strength[6]. The fusion process can be visualized in Figure 17, where r_1 and r_2 represent the radius of each tree, and e represents the eccentricity between the two trees.
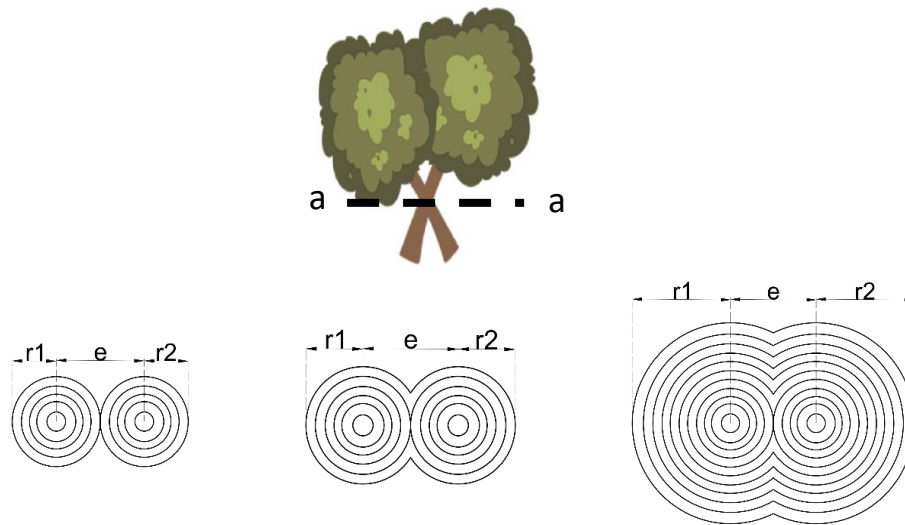
Figure 17. Cross-section a-a of inosculated trees during different growth stages

During the early phase of fusion, each tree is responsible for its own biological housekeeping (water transport, etc.) but sharing mechanical loading. However, as the connection continues to grow, mutual enveloping occurs where a certain arrangement of annual rings runs to the contact area from both sides, this is when the biological process of the two trees are also integrated[7]. Not many existing literatures elaborate on the inosculation processes of tree elements. A useful publication in 1932 written by M. Millner[24] on the topic of the natural grating in hedera helix is found, which provides a closer look at the inosculation process at a micro-level. Although not being strictly a tree, the basic principles could offer insights into this study. The following context is a summary of the publication.

At the location where the bark breaks due to the pressing and rubbing of stems to each other, breakage occurs in epidermis and cork cells. The fusion from two stems is essentially a result of the growth from phellogen and cambium.

18

Growth from phellogen

At the location where breakage occurs, phellogen is stimulated to form phelloderm (secondary cortex) consisting of several layers of small thin-walled cells; these cells around the grafting surface become loose and irregularly arranged. As the cork layers continue to break due to rubbing and friction, the thin-walled cells will begin to bulge outwards and push through the already broken bark. And finally, fusion takes place when the protuberances of one stem meet that of the adjacent stem, forming a narrow connecting band.

Growth from cambium

The first sign of growth around cambium cells is from the expansion of medullary rays due to pressure. Cambium across the medullary rays eventually begins to bulge outwards into the cortex, forming a protuberance of cells. Eventually, the protuberance gradually pushes its way through the cortex. And finally, the fusion takes place when the protuberances from the two stems meet. The cambium cells at the point where the two protuberances meet are simply converted into ordinary parenchymatous cells.

Summary

To better visualize the inosculation process, a list of diagrams from Figure 18 to 22 are provided below, which reflect the descriptions stated above.
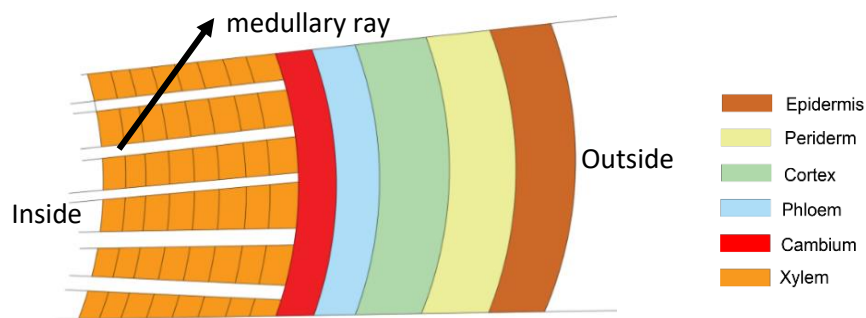
Figure 18. Schematics of exterior layers of wood
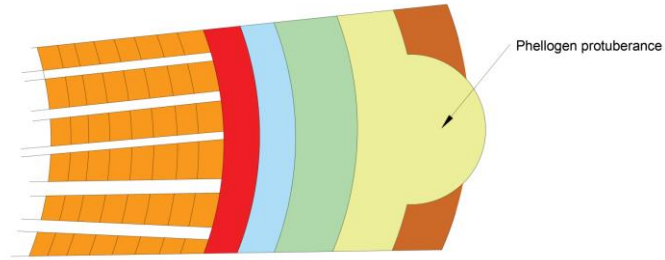
Figure 19. Formation of phellogen protuberance
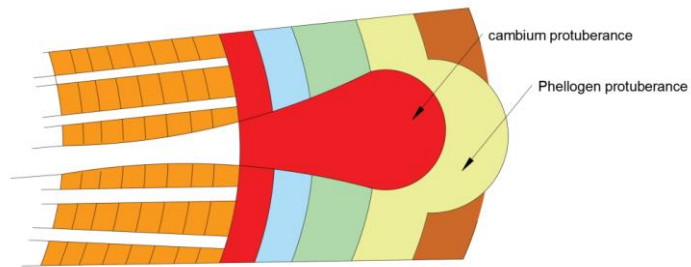
Figure 20. Formation of cambium protuberance
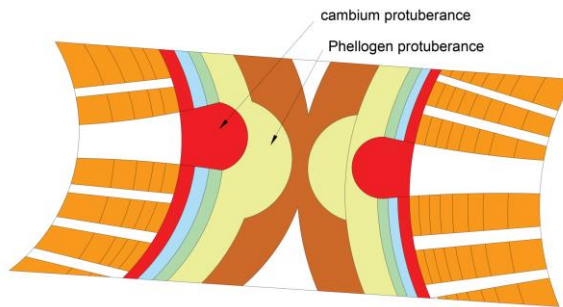
Figure 21. Merging of protuberances from two stems
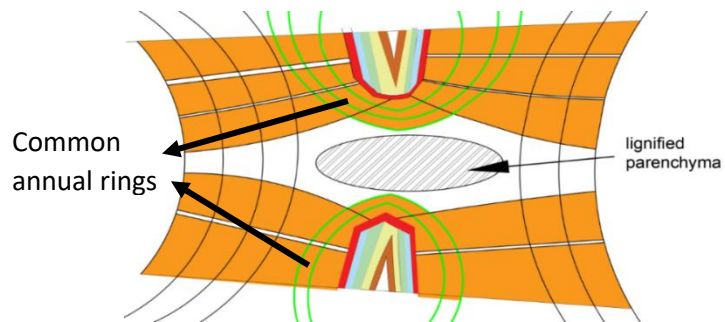
Figure 22. Fusion of two stems and formation of lignified parenchyma

The processes mentioned above take place pretty rapidly, within about one season of growth. After the fusion, growth goes on year by year in the same way that it does in the normal stem so that the graft gradually increases in thickness. Wood in the graft region is formed simultaneously, and common annual rings are formed around both stems.

As a final remark, inosculation usually does not take place to old trees or between two trees that are more than eight years apart, probably because it is more difficult for tree barks to injure when they make contact with one another[24]. Additionally, inosculation mostly occurs between the same species.

1.4 Crosswise connection

Since the focus of the thesis is on crosswise connections, it is vital to investigate its characteristics. A crosswise connection is developed when one of the tree elements makes contact with another for reasons such as wind load. As discussed in section 1.3, as the contact occurs continuously, abrasion wound on the bark occurs, and mutual enveloping of the wood fibers from two elements take place, which restricts their relative movements[7]. Such phenomenon is illustrated in Figure 23.
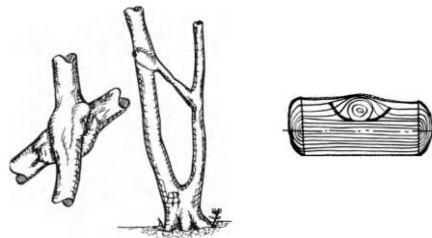
Figure 23. Inosculation process of crosswise connection[7]

From the CT scans performed by Winterman, it is possible to observe the cross-section of such a connection. Looking carefully at wood fibers over the cross-section in Figure 7, it can be observed that, instead of forming complete circles like regular trees, the fibers near the interface from one stem deviate and join the fibers of another stem. For a clearer view, this is illustrated in a 3-D sketch in Figure 24.
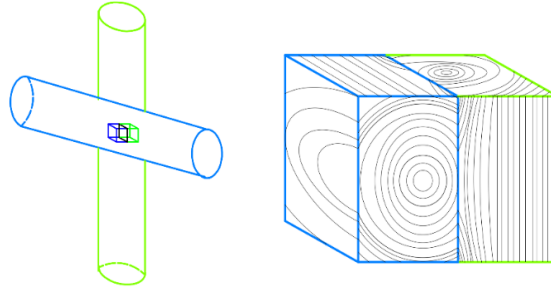
Figure 24. Fiber deviation in cross-welded tree connection

Recognizing the fiber deviation around the interface is essential because it is one of the most important factors affecting the ultimate strength of wood[25]. Correspondingly, it becomes necessary to recognize the stress state at the interface and investigate the strength property associated with that stress state so that the connection can be used as a reliable structural element.

From Figure 25, it can be observed that a certain eccentricity measured from the heart of two wood elements exists. Such eccentricity, which is inevitable for a crosswise connection, would raise additional challenges for the connection when implemented as a load-bearing element. Such challenges are explained in detail in chapter 4 of Part-II of the thesis.
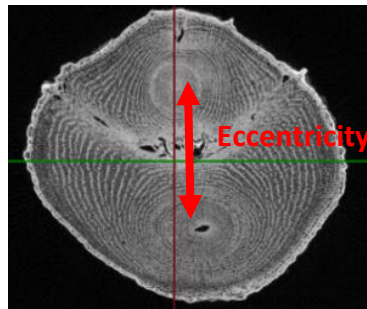
Figure 25. Eccentricity between two stems in a crosswise connection

Conclusion

Literature study is made in chapter 1 regarding the microscopic and macroscopic structure of wood, biomechanics and material properties of trees, and the inosculation process of trees with a closer look at the crosswise connection. A thorough understanding of these aspects helps to lay the foundation prior to analyzing the mechanical behaviours of crosswise connection. It also helps provide insights in terms of how trees can be used as structural elements during designs. After conducting the literature study, the following key conclusions are drawn:

- Wood exhibits extreme anisotropy because of its fiber orientation, it can be treated as an orthotropic material because its material characteristics vary in three principal directions: longitudinal, radial, and tangential.
- For design purposes, the importance of elastic properties parallel to the grain is recognized, whereas the elastic properties in the radial-tangential plane are often considered as isotropic.
- Trees exhibit unique biomechanical characteristics such as adaptive growth, in which trees tend to exhibit an optimized growth pattern to minimize the surface pressure.
- In general, inosculation is triggered by pressing and rubbing of two contacting stems, and the breakage occurs in epidermis and cork cells. Then the fusion from two stems is essentially a result of the growth from phellogen and cambium.
- A successful inosculation can be manifested by mutual enveloping, where a particular arrangement of annual rings runs to the contact area from both sides.
- Fiber deviation occurs as a result of inosculation. As an important factor that influences the strength of wood, this should be treated with care by future designers.
- From the start of the inosculation process, the eccentricity between two trees remains the same even though the connection continues to grow in diameter.

Since this thesis research deals with growing trees and tree connections as load-bearing elements, the next chapter aims to investigate the growth pattern as well as the tapering geometry of trees.

2. Tree growth model

For conventional structural elements made of concrete or steel, the mechanical characteristics are predetermined in the manufacturing process and are expected to be maintained during their service life. However, it is a different case for structures built with living trees, for their varying physical and mechanical properties with time. As mentioned in the Introduction, the projects that utilized trees and tree connections as the load-bearing elements all made an essential assumption, that the structure would be ready for service as soon as the trees and the tree connections have grown and reached sufficient strength. For instance, a tree forms a tapering geometry, and as it grows, its stem diameter increases, which affects its second moment of area, an essential factor for resisting wind load. As discussed in section 1.3 that the inosculation process is also a function of time, therefore, the same scenario should also apply to tree connections, that their stiffness and strength should increase over time.

Therefore, as a preparation to analyze how growth affect the mechanical properties of trees and tree connections with the case study in chapter 8 at Part-III of the thesis, investigation in terms of tree growth and its tapering geometry is conducted in this chapter.

As Ferdinand Ludwig, the scientific coordinator of Baubotanik Research Group, stated that if living trees are subjects to architectural design and construction, the basic patterns and conditions of plant growth have to be recognized as essential design parameters[9].

2.1 Primary and secondary growth

Plant exhibits primary and secondary growth during its life, where the former is vertical growth of stem and roots, which depends on the type of soil, the abundance of water, and so on, the latter represents lateral growth due to activities of vascular and cork cambium resulting in the growth of tree trunk, forming xylem and phloem.

Secondary growth can be manifested by the growth rings on the cross-section of a tree: in spring and early summer, the cells that grow are large due to the greater amount of moisture available, resulting in a light-colored and wide ring, while in late summer and fall, the moisture available decreases and the cells also decrease in size as a result, resulting in dark, narrow rings. The wide rings are referred to as earlywood, while the narrow rings are referred to as latewood, illustrated in Figure 26.

Figure 26. Formation of earlywood and latewood on the cross-section of a trunk[26]

When it comes to growth parameters of trees, two of the most obvious parameters are the height and diameter of the trunk. In his book[7], Mattheck argues that, assuming that the tree trunk is a component optimized over millions of years of evolution and satisfies the axiom of uniform stress, depending on the shape and location of the crown, a relationship between height and diameter can be obtained, shown in the Figure below:
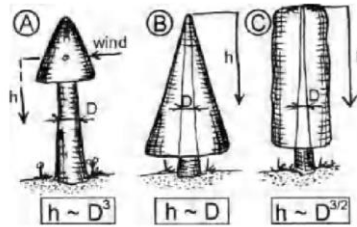
Figure 27. Relationship between tree height and trunk size depending on the shape of its crown

In Nuijten design of the living tree pavilion, she assumed that the trees grow 2 centimetres in circumference and 50 centimetres in height per year, and she used a general formula regarding softwoods in determining the weight. The formula is provided here as:

$$W = 0.26153 * (D^2)^{1.12422} * H^{0.93871} \qquad (2.1)$$

Nuijten concludes that how fast the trees will grow depends on the weather, light, water, nutrients supply, possible infections, damage done to the trees. Therefore, in her design, the suggested time that the trees need to carry the loads is consequently only a rough estimation based on average conditions.

2.2 Urban tree growth model

The usage of tree growth models developed by scientists and researchers often involves the calculation of an annual stream of benefits associated with energy effects, air pollutant uptake and emissions, carbon storage, rainfall interception, and effects on property values. Common tree growth model can be categorized as forestry model or urban model; it is essential to differentiate the two as they indicate very different growth behaviours. For instance, in forests, tree crowns compete for limited space and may not reach their maximum expansion potential[27], unlike urban trees that are exposed to more space.

Several publications describe the growth model of trees. From these publications, the most common parameters to be modelled include tree height, the diameter of the tree at breast height (D.B.H), which is often measured 1.4-meter from the ground, crown diameter, crown base height, leaf area, dry weight of the tree, and so on, as illustrated in Figure 28.
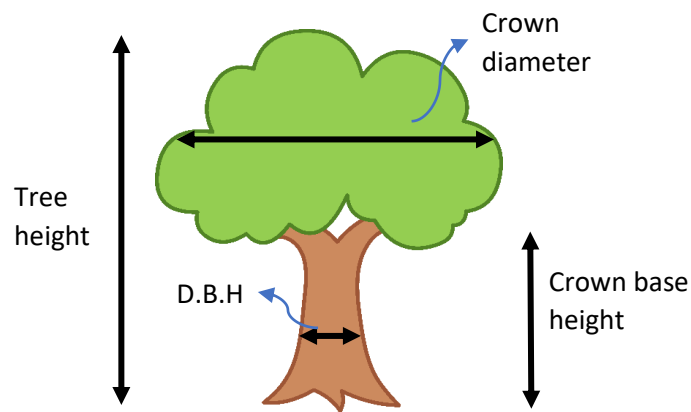
Figure 28. Essential growth parameters of tree

2.2.1 USDA urban tree growth model

Of the many publications regarding tree growth model, United States Department of Agriculture (USDA) has released a publication with an extensive database, namely Urban Tree Database and Allometric Equations, which includes 365 sets of tree growth equations developed for the 171 distinct species, scattered in urban settings of different climatic regions around the country[28]. With the extensive database, USDA has generated the best-fitting allometric equation for describing the tree growth model for each tree species at a specific climatic region. For instance, the growth model for the same species in the different climatic region would possess a different growth model.

Each growth model equation is examined through six mathematical models, in which the best-fitting model is selected. The six mathematical models include four polynomial models (linear, quadratic, cubic, and quadratic), log-log, and exponential[29]. For example, with age as input, output such as diameter at breast height (d.b.h), tree height, leaf area, and so on can be predicted. For illustration, the growth model for Ficus Benjamina from USDA documentation is illustrated in Table 2.1.

Table 2. 1. Growth model for Ficus Benjamina

Growth parameter	Formula	Constant
$D.B.H(cm)$	$a + b*(age) + c*(age)^2 + d*(age)^3$	$a = 2.24394$ $b = 1.91147$ $c = -0.02323$ $d = 0.00013$
$Tree\ height\ (m)$	$a + b*(D.B.H) + c*(D.B.H)^2$	$a = 0.49558$ $b = 0.28606$ $c = -0.00089$
$Crown\ height(m)$	$a + b*(D.B.H) + c*(D.B.H)^2$	$a = 0.20371$ $b = 0.18713$ $c = -0.00053$

With the expressions listed in Table 2.1, the development of D.B.H and the height of Ficus Benjamina every year can be calculated, which is shown in Figure 29. The exact numerical results are shown in Appendix 10.1.
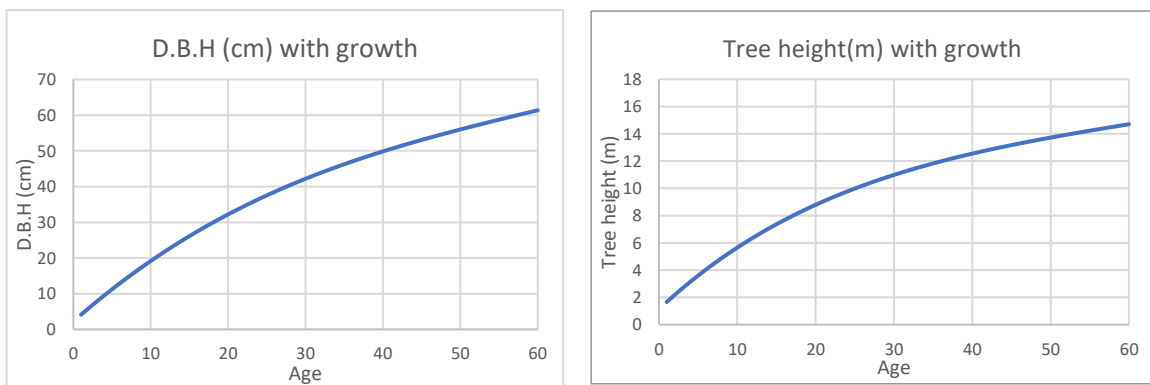
Figure 29. Development of D.B.H (cm) and tree height (m) of Ficus Benjamina based on the growth model

Another set of equations developed by USDA approximates the above-ground volume and biomass. Unlike growth parameters such as tree height and D.B.H, which are dependent on climatic region, tree volume and dry weight rely only on D.B.H or tree height, which can be acquired from the first set of equations listed in Table 2.1. The dry weight of the tree is obtained by multiplying a density factor of the specific tree species. The equations used to compute tree volume and weight for Ficus Benjamina is shown in Table 2.2:

Table 2. 2 Equations to obtain volume and dry weight of Ficus Benjamin

Growth parameter	Formula
$Volume(m^3)$	$0.0002835 * d.b.h(cm)^{2.310647}$
Dry Weight (kg)	$Volume * Density factor = Volume * 460kg/m^3$

Compared to the general model provided by Mattheck and Nuijten, the database provided by USDA is more attractive as it is region-specific and species-specific.

The growth model explained above is based on an extensive database, with each tree species having its own allometric equation. However, it is also stated in the literature that between 30 to 70 trees of each species were sampled for measurement; therefore, there is an upper and a lower limit in each measurement. For instance, the measurement of tree height for Ficus Benjamina ranges from 1.5 meters to 28 meters in the field, which means that the allometric equation is most reliable within this range. These upper and lower limits need to be bear in mind when utilized for design purposes.

2.3 Tree taper

Apart from the parameters obtained from the USDA documentation, to correctly assemble the trees as structural elements, the correct cross-sectional properties must be defined. Therefore, it is also essential to incorporate the tapering geometry of trees in the model.

Taper equation is an essential piece of information often used by forest biometrician for management purposes[30]; they are used to predict the diameter of a tree stem at any height of interest and can be useful for predicting unmeasured stem diameters. The exterior profile of a tree usually bends sharply near its base, then becomes linear along the central portion of the bole, and is variable along the upper stem[31]. Here, a simple linear tapering equation proposed by David

R. Larsen[31] is used. Larsen proposed an equation to estimate the diameter of the tree stem for the section below breast height (1.4m):

$$d_h = d\,b\,h + p_b * (h - b\,h) \qquad\qquad (2.2)$$

, while the diameter for the section above breast height and below crown base can be expressed by:

$$d_h = dbh + p_s * (h - bh) \qquad\qquad (2.3)$$

, and finally, the diameter for the section above the crown base, a cone is assumed with the following expression:

$$d_h = (ht - h)^* top\_ht\_\text{rate} \qquad\qquad (2.4)$$

In the expressions, p_b is the stump taper rate, p_s is the stem taper rate, h is the height at which a diameter prediction is desired, ht is the total tree height, bh is the breast height, dh is the diameter at height h on the tree, and top_ht_rate is the implicit parameter calculated in the following steps:

1. Determine the diameter at the crown base
2. Determine crown length as (total height – height to crown base)
3. Calculate the top_ht_rate as $\dfrac{\text{crown base diameter}}{\text{crown length}}$
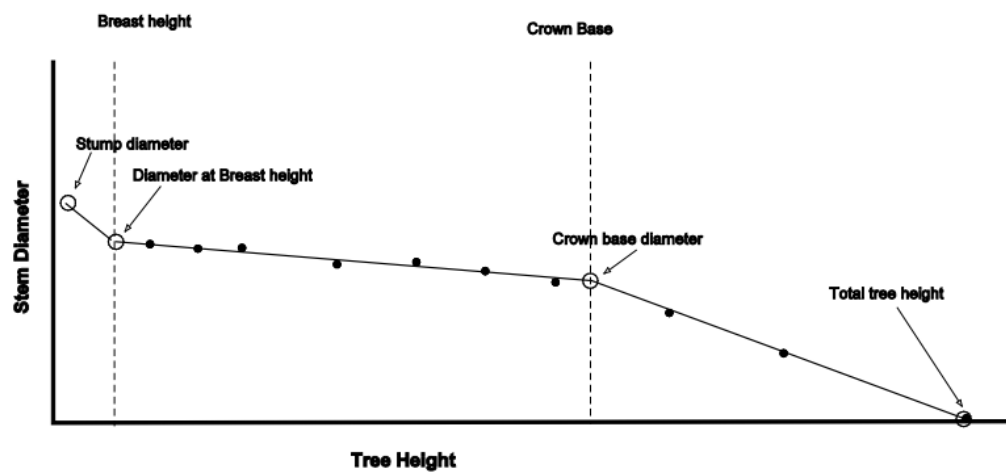
Figure 30. Tapering geometry of a tree[31]

Conclusion

Literature study is made in chapter 2 regarding the growth pattern and tapering geometry of trees. A thorough understanding of these aspects helps to lay the foundation prior to conduct structural designs with growing trees as the load-bearing elements. After conducting the literature study, the following key conclusions are drawn:

- Of the many growth model developed by researchers, the Urban Tree Growth Model published by USDA offers a practical model that is species-specific and climate-specific.
- Most common growth parameters include tree height, the diameter of the tree at breast height (D.B.H), crown diameter, crown base height, leaf area, and dry weight of the tree. With age as input, these parameters can be obtained from USDA growth model.
- Combining the tree growth model and tapering equations proposed by David R. Larsen, the geometry of a growing tree can be obtained, which is useful for design purposes.

3. Semi-rigid connection in structural analysis

In any structure designed with connections with a finite moment-resisting stiffness, it is essential to determine their ultimate strength and magnitude of stiffness, as they are responsible for ensuring the integrity of the entire structure and the transfer of forces from one element to another. Accurate determination of a connection's rotational stiffness is recognized, especially for timber structures, for the relatively low modulus of elasticity of timber[32]. Therefore, prior to utilizing crosswise tree connections as load-bearing elements in structures, it is essential to investigate how these connections provide stiffness to the structure under loading.

In the preliminary design phase of a structure, it is often more realistic and economically feasible to conduct structural analysis in a wireframe structural model, where most load-bearing members are constructed with 1-dimensional beam elements. However, modelling structures with tree connections as load-bearing elements in the structural analysis are almost unheard of in the past. Therefore, in this chapter, literature study is made in terms of the existing methods to model connections during structural analysis. Such research could offer insights to modelling the crosswise connection in chapter 7.

3.1 Rotational stiffness of connection

When implied on connections, rotational stiffness is a terminology used to define whether the connection can be categorized as a hinged connection, rigid connection, or semi-rigid connection. Accurate determination of rotational stiffness of connections is essential as it is vital for both the strength and serviceability of structures[33], because it influences distribution of internal forces and moments within a structure, and on the overall deformations of the structure.

When a connection is subjected to applied moments, the adjacent members rotate relative to each other and contribute additional deformations to the members. The degree of rotation of the connection with the corresponding applied moment is defined as rotational stiffness. The behaviour of the semi-rigid connection is characterized by a bending moment-rotation M-ϕ curve. A typical moment rotation curve is expressed in Figure 31, containing information about moment capacity, M_{Rd}, rotation capacity, φ_{Cd} and initial rotational stiffness S_{int}.
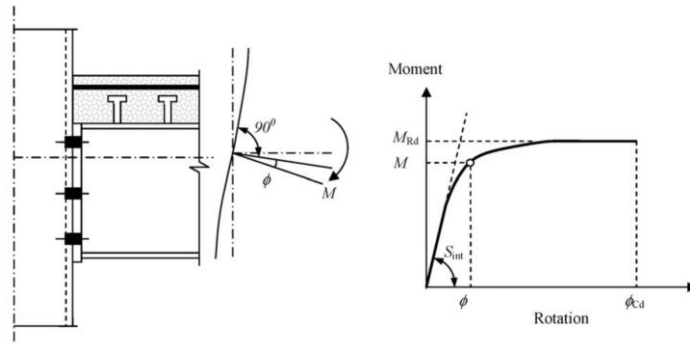
Figure 31. Moment-rotation characteristic for a typical bolted endplate joint[34]

The classification of a structural joint has been extensively researched in steel construction, for instance, in Eurocode 3 Part 1-8[35], a joint may be classified by comparing its initial rotational stiffness, $S_{j,int}$, with the classification boundaries shown in Figure 32. In the chart, zone 1 refers to a connection with rigid stiffness, while zone 2 and 3 refer to a connection with semi-rigid stiffness and zero stiffness, respectively.
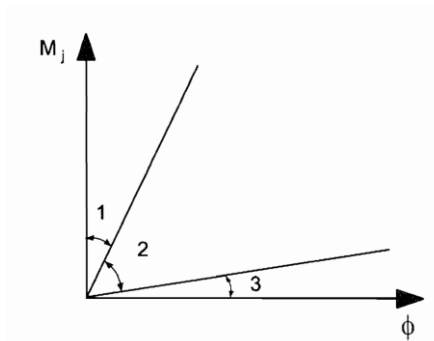
Figure 32. Classification of joints by stiffness[35]

3.2 Methods of modelling crosswise tree connection in wireframe model

During the design phase of a building, connections are usually applied with certain simplifying assumptions. For instance, a perfect pin connection or a perfect rigid connection is assumed for a multi-storey steel frame structure. Although such assumptions lead to rapid design calculation, they pose many undesired problems. For example, the bending moment of columns from frame action would be wrongly omitted when a perfect pin connection is modelled[36]. In contrast, a perfectly rigid connection would underestimate building sway and overestimating stresses at the connection[33]. Additionally, the rotational stiffness of the connection has a strong

influence on the distribution of bending moments and displacements of the analysed frame[32]. Therefore, study must be made in terms of how rotational stiffness of a semi-rigid connection is modelled during structural analysis.

3.2.1 Scissor's model

One of the methods to incorporate joint stiffness in structural modelling is Scissor's model. The most common application of scissor's model is to model the panel zone effect, which is defined as the region of the column web delimited by the column flanges and continuity plates at a beam-to-column connection[37], shown in Figure 33.
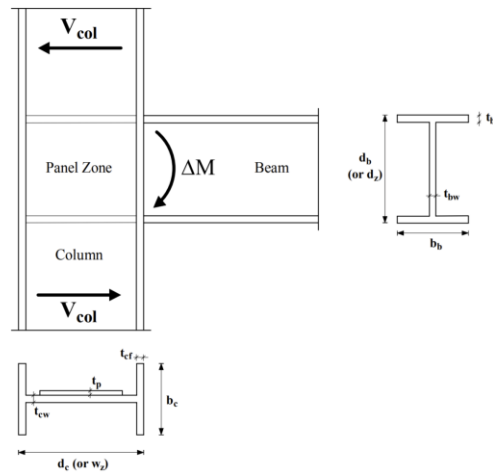
Figure 33. Schematic representation of a beam-to-column joint[37]

In such scenario, steel semi-rigid connections in a skeletal structure are usually modelled as pairs of scissors with a nonlinear relation between bending moment M and relative rotation γ, defined by the secant stiffness,

$$S_j = \frac{M}{\gamma} \qquad (3.1)$$

, where γ represents the shear deformation of the beam-column joint.

33

In a frame analysis program that consists only of line elements, panel zone behaviour can be modelled through the Scissors model. In this model, the sum of moments can be related to the joint shear force, and the spring rotation is equal to the panel zone shear distortion angle[38].
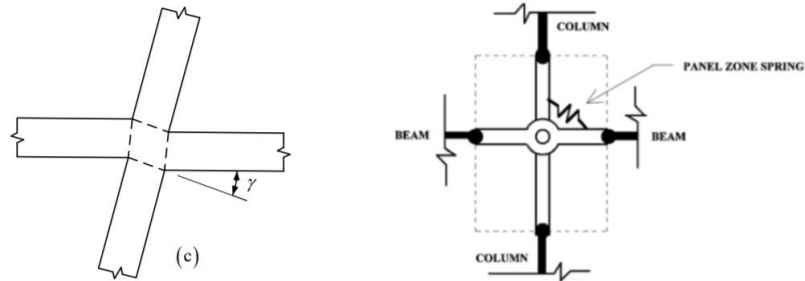
Figure 34. Scissor's model employed in moment-resisting frame[38]

Scissor's model is also applied to transformable structures, which possess revolute joints at all of its nodes, allowing a rotational degree of freedom about an axis perpendicular to the plane of the unit. Thus, at the centre or intermediate node, a rotational stiffness of 0 kNm/rad is assigned to the revolute joint that connects the two elements[39].
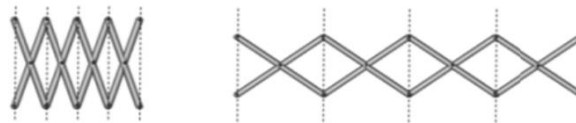
Figure 35. translational scissor structure[39]

Figure 36. Deployable cover for swimming pool in Seville designed by Escrig[39]

34

3.2.2 Two-noded spring element

Another method of incorporating joint stiffness in structural modelling is the use of a two-joint connecting spring. The link is a mass-less element composed of six separate springs, one for each of the six deformational degrees of freedom (one for axial, two for shear, one for torsion, and two for pure bending). The spring forces result from relative movement between the two end nodes of the spring:

$$F_k = c_k \cdot d_{u,k} \qquad (3.2)$$

, where $d_{u,k}$ stands for a relative translation or rotation in any of the three directions x, y, z, and c_k stands for spring stiffness specified for each of the six springs. The following equations and Figure 37 illustrate how the relative deformation is computed for axial action, shear action, and bending action:

$$axial: d_{u1} = u_{1\mathbf{j}} - u_{1\mathbf{i}} \qquad (3.3)$$

$$shear(1 - 2\ plane): d_{u2} = u_{2,j} - u_{2\mathbf{i}} - \text{dj2} \cdot r_{3\mathbf{j}} - (L - \text{dj2}) \cdot r_{3\mathbf{i}} \qquad (3.4)$$

$$bending(1 - 2\ plane): d_{r3} = r_{3}\mathbf{j} - r_{3\mathbf{i}} \qquad (3.5)$$
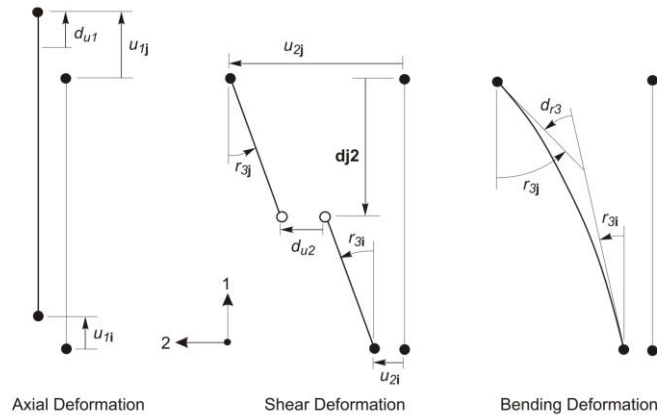
Figure 37. Relative deformation between two nodes for axial spring (left), shear spring (middle), and bending spring (right)[40]

Conclusion

Literature study is made in chapter 3 regarding the importance of determining the semi-rigidity of a structural connection. Investigation is also made in terms of the current modelling approaches of semi-rigid connections. A thorough understanding of these aspects helps to lay the foundation of utilizing crosswise connection in the preliminary design of a building structure. After conducting the literature study, the following key conclusions are drawn:

- Although simplifying the connections as perfectly hinged or perfectly rigid speeds up structural analysis, they never truly exist in real life, and such simplification could raise challenges such as underestimating building sway and overestimating stresses at the connection.
- The degree of semi-rigidity also has an influence on the moment distribution of a frame structure.

As a preparation to the design case study in chapter 8, where a wireframe modelling analysis is conducted, analysis is made into possible methods of incorporating semi-rigid connection in the wireframe modelling phase. From section 3.2, most common methods such as the Scissor's model and two nodded spring elements are discussed. It can be concluded that, by assigning a certain rotational stiffness, both methods can be used to model semi-rigid connections in a structure. However, considering the nature of the connection, as discussed in section 1.4, crosswise connection exhibits inevitable eccentricity between the center of the stems, therefore, comparing to the Scissor's model, two-nodded spring element is more suitable in modelling such connections.

Part II – Mechanical behaviours of crosswise connection

As discussed previously in the Introduction, connections made with trees as a part of living architecture have been experimented with throughout history and in several recent projects. However, there is a lack of research in terms of the mechanical behaviours of the connection when implemented as a part of the load-bearing structure. Since the focus of the thesis is on crosswise connections, it is vital to investigate the mechanical behaviours of such a connection when it is being loaded.

In Nuijten's design of the Living Tree Pavilion, tree connections were treated as rigid moment-resisting connections; however, as discussed in section 3.1, a fully rigid connection never truly exists, and she has suggested in her report that the actual stiffness and strength characteristics of tree connections should be investigated in the laboratory. Therefore, chapter 5 aims to propose an experimental design that aims to achieve such objective. Since conducting the actual experiment falls out of this thesis project, a 3-dimensional finite element modelling of the crosswise connection with a similar boundary condition as the experiment is analyzed in chapter 6, the results would help further contribute in the understanding of mechanical behaviours of crosswise connection as a part of a building structure. Lastly, to incorporate crosswise connection in the preliminary design phase of a building structure, a wireframe modelling approach is suggested in chapter 7.

4. Stress states of crosswise connection under loading

Depending on the source of the load, a crosswise connection could behave differently. Here, a simple case is illustrated, which is two identical trees connected in a crosswise manner. Two colours are used to identify the position of the trees, shown in Figure 38.
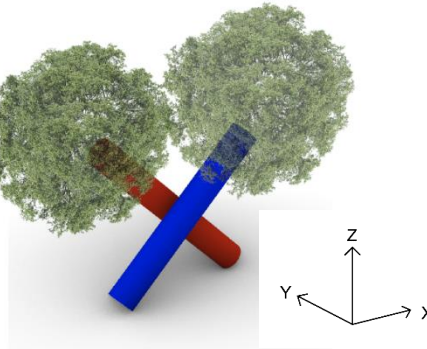
Figure 38. Two trees are crossly-connected

In general, for such a tree system, load scenarios can be categorized as in-plane or out-of-plane, where in-plane refers to the x-z plane, and out-of-plane refers to the y-z plane, as illustrated in Figure 39. In-plane loading could be resulted from self-weight and in-plane wind loads, while out-of-plane loading could be resulted from out-of-plane wind loads.
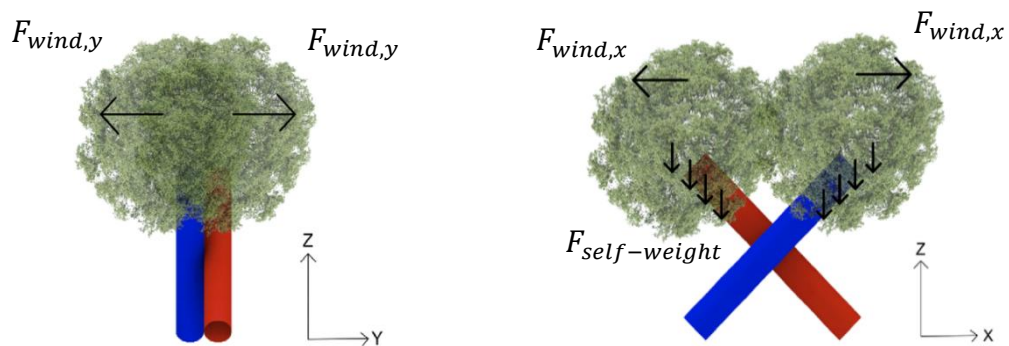
Figure 39. Out-of-plane loading (left) and in-plane loading for a crossly-connected tree system (right)

For a connected tree system, it is essential to realize that the center of gravity locates at the mid-point of the connected region, shown in Figure 40. Therefore, when loaded out-of-plane, except for flexural deformation due to the cantilever effect, torsion around z-axis is also present, shown in Figure 41.
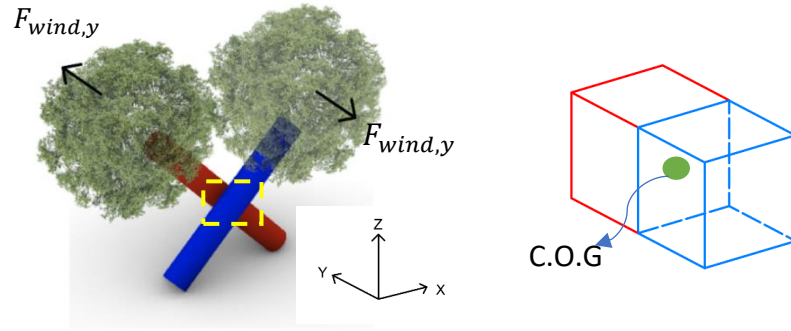
Figure 40. Position of center of gravity for a crossly-connected tree system
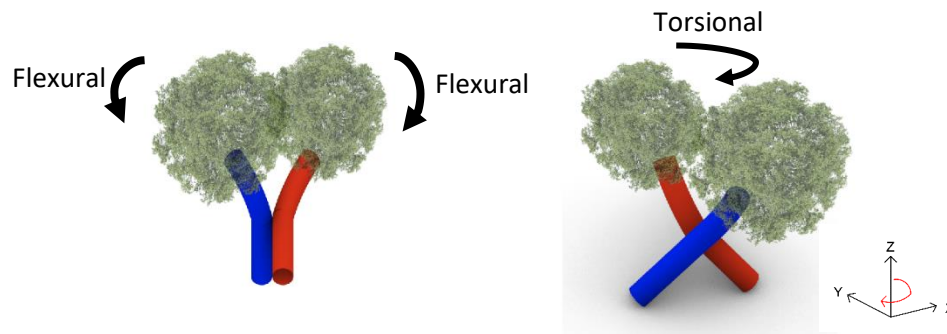
Figure 41. Flexural behaviour (left) and torsional behaviour (right) of the structural system under out-of-plane loading

Additionally, focusing on the connected region, due to the out-of-plane loading, it is as if the connection is being loaded axially in its own axis, illustrated in Figure 42. Under such loading scenario, it is important to recognize that, due to the fiber orientation, the axial force acts parallel to the grain. As one of the weakest strength properties of wood, such stress state must be treated with care by future designers.
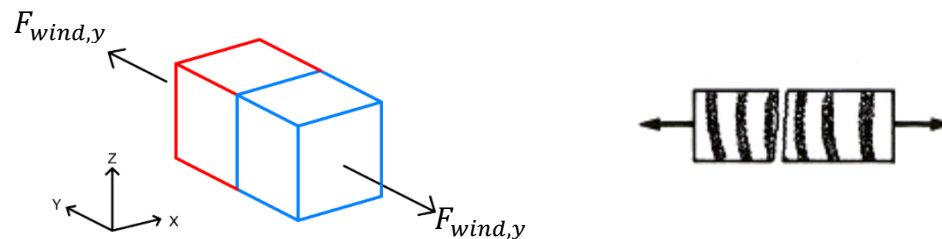
Figure 42. Connection loaded axially (left) axial force acts perpendicular to the grain (right)

When loaded in-plane, due to the eccentricity between the two trees, except for the flexural deformation due to the cantilever effect, torsion around the z-axis as well as y-axis occur to the connected region as well. Torsion around the z-axis is resulted from the fact that the neutral axis of the trees is not aligned with the center of gravity of the system, while torsion around the y-axis results from the in-plane bending moment from both trees.
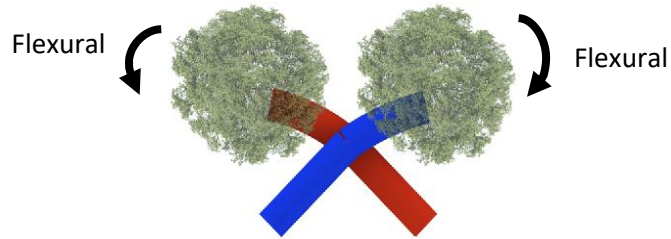
Figure 43. Flexural behaviour of tree system under in-plane loading
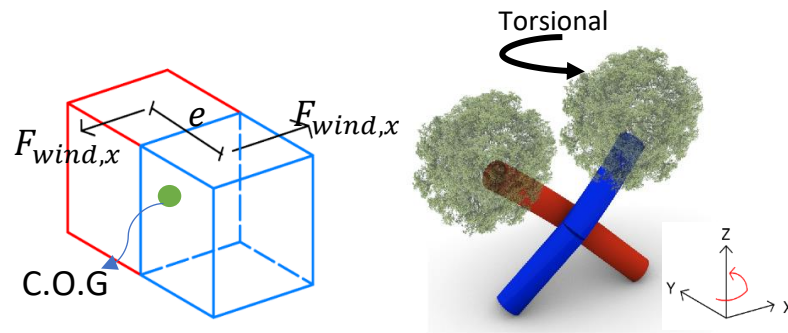
Figure 44. Torsion around z-axis of the tree system under in-plane loading
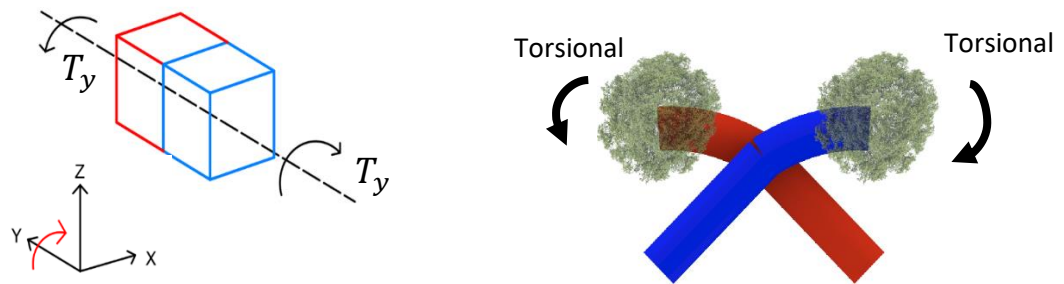
Figure 45. Additional deformation caused by torsion around y-axis under in-plane loading

It is important to note that, except for the bending and shear deformation of the stems, torsion around the y-axis in the connection would likely cause additional in-plane deflection to the stems. Additionally, it must be noted that, due to the fiber orientation of wood, the torsional moment in the connection acts in the radial-tangential plane, which would cause what is known as the rolling shear stress. Comparing to the longitudinal shear strength, rolling shear strength is very low, therefore, it should also be treated with care by future designers.
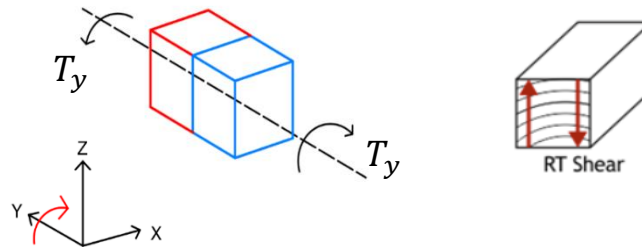
Figure 46. Rolling shear stress in the connection

The analysis above illustrates the mechanical behaviour of crosswise connection when only two trees are connection. However, when the connections are utilized as parts of a completed structure, such as Baubotanik Tower mentioned in the Introduction chapter, the swaying of tree crowns would be resisted by the adjacent moment resisting connections, which are also responsible for load transfer from one tree to another as well as providing stiffness to the entire structure.
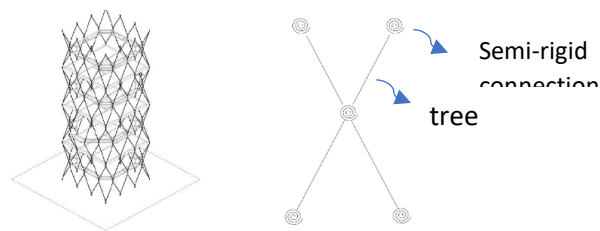
Figure 47. Structural scheme of Baubotanik Tower

The importance of obtaining the rotational stiffness and strength property of structural connection has been discussed in section 3.1, therefore, efforts are put into the next chapter in order to come up with an experimental design to achieve such objective.

5. Experimental Design

In this chapter, an experimental design is proposed, which aims to investigate the rotational stiffness as well as the ultimate bearing capacity of the crosswise connection when subjected to in-plane loading. The specimens to be tested are shown in Figure 48.

Figure 48. Crosswise connection specimens

5.1 Existing experiment scheme for measuring rotational stiffness of connection

The rotational stiffness of a structural connection is often expressed by a moment-rotation curve, which may be determined by different methods: laboratory experiments, numerical modelling, or code standards[32]. Study is made into various existing experiments that investigate the rotational stiffness of connections. Depending on the real-life application of the connection, experiments come with many forms; however, by studying several existing experiments that investigated the connection's rotational stiffness[41][42][43], a few similarities are found:

- Experiments usually involve fixing one of the members from the connection and applying monotonic/cyclic load onto another.
- To obtain the desired rotational stiffness around a pre-determined direction, possible rotational deformation around other directions are to be restricted.

5.2 Digital Image correlation

To obtain the connections' moment-rotation curve, it is essential to obtain the angular deformation during loading accurately. From the researches mentioned above, one or more measurement apparatus such as Linear Variable Differential Transformers (LVDT), strain gauge type transducer (SGTD), and inclinometer could be used. However, for crosswise tree connection, which exhibits irregular geometry, it could be challenging to measure such deformation with

42

conventional apparatus because these measurement apparatuses are usually applied to smooth surfaces.

During research, another useful tool is found, which is called digital image correlation (DIC), it is a tool that could be utilized to track deformation by cross-correlating a reference image with a stored image. For instance, ten images of the deformed specimen in ten load steps can be recorded by a high-resolution camera and transferred to the computer program for image interpolation. Based on the specific applications, two-dimensional or three-dimensional analysis is possible for post-processing. Results such as axial strain, displacement, shear strain, rotation, etc. can be interpolated by the computer program by comparing the deformed specimen in a specific load step with preceding load steps.

Since the technique relies on a comparison of discrete light intensity patterns obtained before and during deformation to obtain the shift of the images, test specimens must be marked with highlighters. There are two common types of marking methods, one of which is the use of point markers, which is often used to track the 3-D coordinate of the marked point; the other is the use of stochastic pattern, which is more often used to compute full-field displacement and strain.
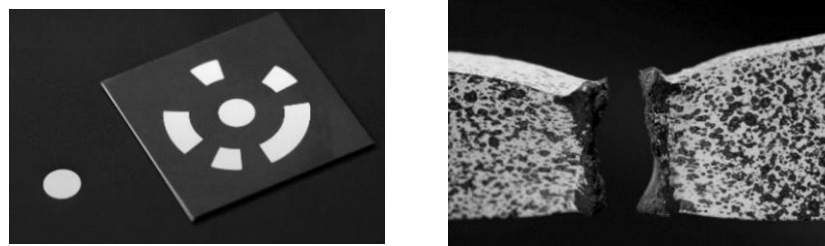
Figure 49. Point marker (left) and stochastic pattern (right)

5.3 Setup and procedure

Having determined the tools to be utilized in the experiment, the next step is to design the setup and procedures on the connection specimens. With the objective of the experiment in mind, which is to investigate the rotational stiffness of the connection, the experimental setup is proposed in Figure 50(a). Table 5.1 provides an overview of the function of each component in such a setup.

The experiment is to be performed on the Universal Testing System, shown in Figure 50(b). For the ease of loading, the connection is positioned so that one of the stems is horizontal while the other being tilted. One end of the horizontal stem is tied to a rope, which is attached to

the top jaw of the loading device at Point A, the other end of the horizontal stem is free. For the tilted stem, both ends are to be fixed from translation and rotation.
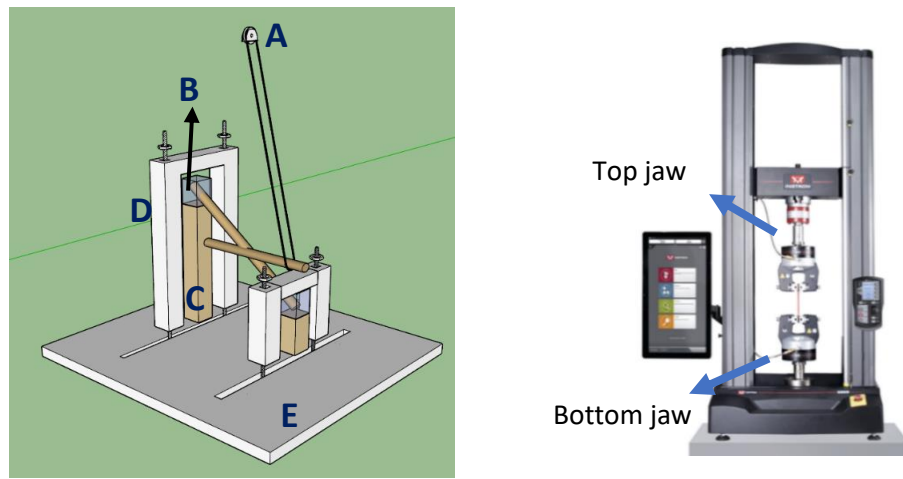
Figure 50 (a) Experimental set-up (b) Universal testing machine

Table 5. 1 Description of parts labelled in Figure 50(a)

Part	Description
A	Pulley attached to the top jaw of the loading machine. The other end is tied to one end of the specimen with an angle.
B	Resin used to fix the wood in place with Part D and Part C
C	A wooden block that is placed beneath the resin as vertical support.
D	A hollow U-shaped element used to secure the resin in place with the wooden block. By prestressing the U-shaped element to the bottom plate with bolts, both translational and rotational degrees of freedom are fixed.
E	Bottom plate attached to the bottom jaw of the loading machine. The two slots allow adjustment of the U-shaped element to compensate for the minor differences between specimens.

Without knowing the actual load-bearing capacity of the connection, the experiment is to be conducted in a displacement-controlled manner, where the ends of the tilted wood stem are forced downwards with the same rate. During displacement, one end of the horizontal stem is pulled by the rope at an angle, and the magnitude of the force applied will be recorded by the load cell from the Universal Test Machine. The experimental scheme is shown in Figure 51.
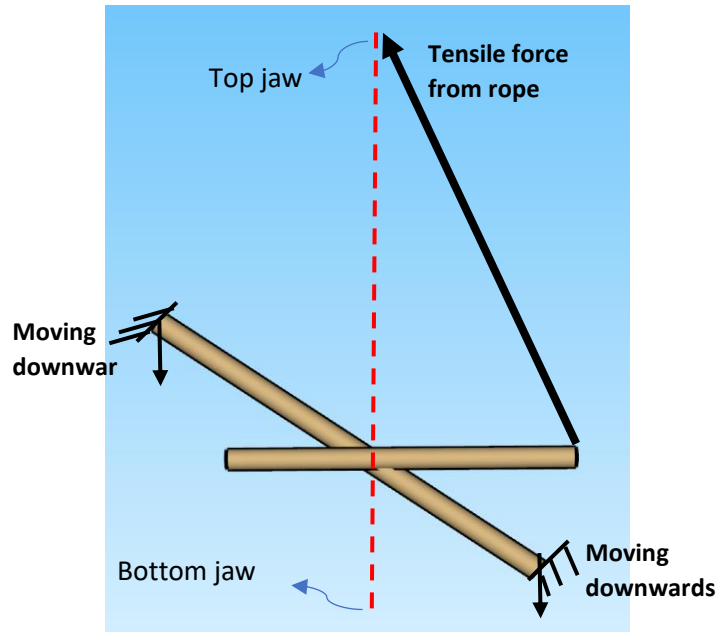
Figure 51. Loading and support scheme

The purpose of using a pulley in measuring the load is that, with such scheme, only axial force will be transferred to the load cells, which makes it more convenient in calculating the bending moment in post-analysis. The reason for pulling the end of the wood by the rope with an angle is to place the connection specimen perfectly between the top and bottom jaw of the loading machine, so that the loading points are aligned with the center of gravity of the connection. However, it can be seen from such setup that, the applied force at the end of the horizontal element would have a horizontal and vertical component. Typically, to obtain the rotational stiffness of a connection, pure bending is to be applied; therefore, further optimization on the setup should be made in the future.

5.3.1 Restraints

It is crucial to keep in mind that the experimental setup should reflect the actual behaviours of the connection when utilized in the actual structure. Referring to Baubotanik Tower again, it can be seen that all nodes possess a certain degree of rotational stiffness. Therefore, the support condition is defined so that both ends of the tilted stem are restrained in translation as well as rotation.

45
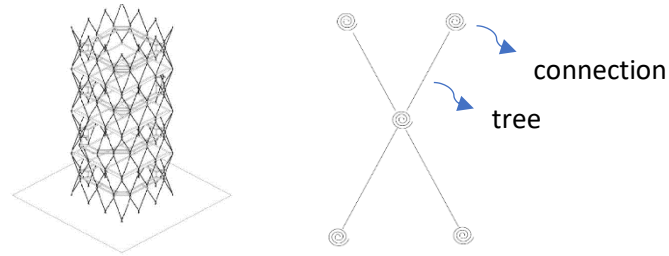
Figure 52. Structural scheme of Baubotanik Tower

The fixation on the two ends of the tilted wood stems is accomplished with the use of RenGel SW 404, which is a type of resin that could provide significant strength (80 Mpa to 124 Mpa[44]) when hardened. One of the advantages of using such resin is that the resin can be molded into a regular cubic shape, so that when the resin secures the ends of the stem, they can be tightly attached with other devices. As illustrated in Figure 50(a), the resin (Part A) is sandwiched between the hollow U-shaped element and the wooden block (Part C). By prestressing the U-shaped element downwards onto the bottom plate with bolts, the resin can be tightly secured in place, providing a rigid support reaction.

To compensate for the minor geometrical differences between specimens, as shown in Figure 48, the end supports are designed so that they can be adjusted both vertically and laterally. Lateral adjustment is realized by the slots on the bottom plate; while the vertical adjustment is realized by inserting additional pieces with the same dimension as the U-shaped element and the wooden block, which act as height increments. Such setup is illustrated in Figure 53.
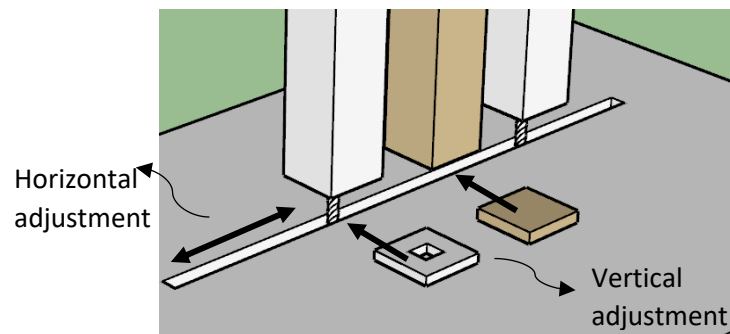
Figure 53. Slot on the bottom plate for minor adjustment

5.3.2 Loading scheme

As mentioned in the beginning of the chapter, the goal in conducting the experiment is to obtain the rotational stiffness of the connection, which would be reflected by the moment-rotation diagram. Therefore, the method to track the bending moment during the loading process needs to be found.

Without knowing the ultimate angle of twist for the specimen, it is difficult to determine the loading rate beforehand; additionally, there are no standards correlated with such testing. Therefore, to safely conduct the experiment, in terms of the loading rate, it is proposed to follow the procedure described in EN 408:2010 - Test methods for Structural timber, in which it has mentioned that the rate of movement of the loading head shall be not greater than (0,003 h) mm/s. For our case, h equals to the diameter of the stem.

During the loading process, the applied load at the end of the tilted stem is recorded by the load cell located in the top jaw, and the bending moment incurred at the connection can be simply calculated by multiplying the perpendicular component of the tensile force with the moment arm:

$$M = sin\alpha \cdot F_{90} \cdot L \qquad (5.1)$$
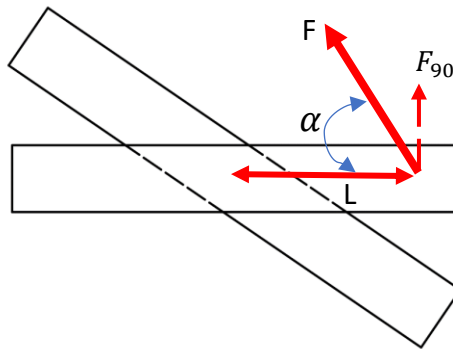
Figure 54. Connection loaded with axial force from the rope at an angle, α

During the loading process, the horizontal wood stem is expected to deform in-plane, which would affect the calculation of bending moment at the conneciton. Therefore, it is necessary to find a means to track the in-plane displacement of the end of the horizontal stem that is being loaded.

47

As suggested in section 5.2, DIC offers the ability to obtain displacement and rotation of an object with the use of a point marker. Therefore, it is proposed to utilize such a technique in measuring the rotation of the end of the horizontal stem to compute the correct bending moment. By attaching a point marker near the end of the horizontal wood element that is being loaded by rope, the rotation of the element can be tracked, and the calculation of bending moment at the connection can also be adjusted. For instance, before the horizontal stem starts to deform, the bending moment can be calculated using Equation 5.1. As the horizontal element starts to deform, the angle between the rope and the horizontal element would change, which would then affect the bending moment at the connection. However, by obtaining the original coordinate of the point marker and tracking its displacement, the change in angle, β, could be computed.
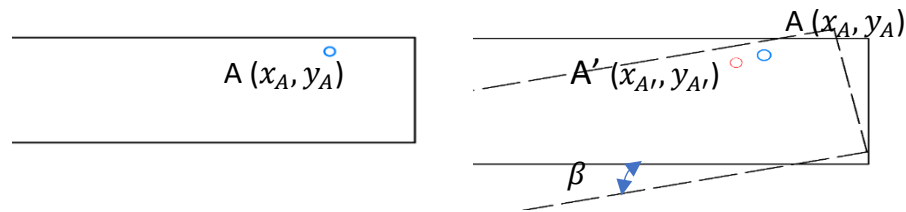
Figure 55. Original point marker (left), Displaced point marker during loading (right)

By tracking the tensile force, F, and the angle change, β, the bending moment for each load step can be computed:

$$M_n = sin(\alpha + \beta_n) \cdot F_n \cdot L \qquad (5.2)$$

DIC can also be utilized in measuring the angular deformation at the connected region. With the discussion made in section 5.2, a stochastic pattern is more suitable in tracking the full-field dispalcement or rotation of the entire area of interest. By marking the connection with paint, shown in Figure 56, the goal is to obtain the average rotation during each load step.
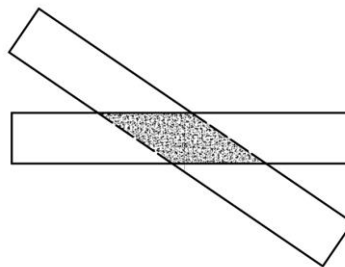
Figure 56. Stochastic pattern marked at the area of interest

Using the procedures provided above, Table 5.2 can be formulated, and subsequently, the moment-rotation curve can also be obtained for each connection. By obtaining the moment-rotation curve for each connection, the rotational stiffness as well as its capacity can be obtained.

Table 5.2. Data to be obtained from experiments

Load step	Tensile force F_i (kN) from load cell reading	Moment M_i (kNm) $M_n = sin(\alpha + \beta_n) \cdot F_n \cdot L$	Angular deformation θ_i (rad)	Moment-rotation stiffness (kNm/rad)
1	F_1	M_1	θ_1	M_1/θ_1
2	F_2	M_2	θ_2	M_2/θ_2
3	F_3	M_3	θ_3	M_3/θ_3
4	F_4	M_4	θ_4	M_4/θ_4
n	F_n	M_n	θ_n	M_n/θ_n

5.4 Hypothesis

According to the micro-CT scans conducted by Winterman, it is discovered that, during the fusion process between two stems, the fibers are subjected to flattening and deviation[10]. Considering that fiber deviation could significantly influence the strength of the wood, it is reasonable to predict as one of the hypotheses, that the strength of the connection is governed by the failure due to fiber deviation at the connection. The location of the predicted failure region is marked in Figure 57:
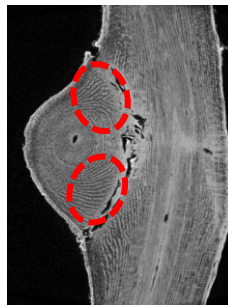
Figure 57. Location of fiber deviation in the connection

During the loading process, bending moment would occur in the elements. Therefore, another hypothesis is that, as the connection continues to grow and merge, the connection will be stronger than the stem itself, so the failure would be governed by the bending of the stem instead of the connection. The hypothesized failure mechanism is illustrated in Figure 58:
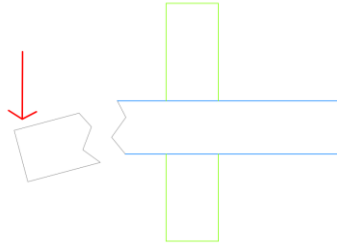
Figure 58. Bending failure of individual stem

With the proposed experiment performed on the specimens, the goal is to obtain the moment-rotation curve for each specimen, illustrated in Figure 59. Key parameters to be obtained include ultimate bending moment capacity (kNm), ultimate angular deformation (rad), and rotational stiffness (kNm/rad).
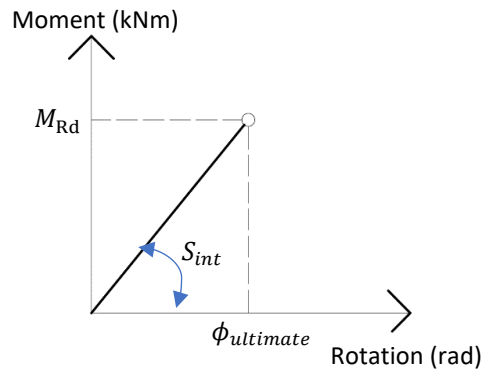
Figure 59. Moment-rotation curve of connection

6. Finite element modelling of crosswise connection

To gain the confidence of a specific material or a structural element in a structure, analysis is conducted prior to construction. The most straightforward method is to construct the entire physical prototype and test it under a specific loading scenario, however, economically speaking, during the design phase of a project, it is much more realistic to design and optimize the components using other means.

As one of the most popular solutions, finite element analysis could offer solutions to problems that involve heat transfer, fluid dynamics, electromagnetic potential, and structural mechanics. In these problems, engineers are often required to solve a series of partial differential equations (PDE), which are complicated equations used to compute relevant quantities of a structure such as stresses or strains to estimate the structural behaviour under a given load.

During finite element analysis, the entire structural element that is of interest is divided into a finite number of small pieces called mesh elements. Depending on the interpolation function (linear, quadratic, cubic, etc.) assigned to the elements, each possesses its own stress formulation. The elements are coupled by the coinciding nodes at their boundaries, where their degrees of freedom are shared. Combining the results from each mesh element, the global behaviour of the entire structure can be obtained.

A finite element model of a crosswise connection with similar boundary condition as the experimental design is analyzed in this chapter. The motivation for conducting such analysis are:

1. With a properly defined finite element model, it is the most useful tool besides actual experiments that could provide valuable insights in terms of the mechanical behaviours of the crosswise connection.
2. As one of the modelling approaches, by constructing the finite element model with similar dimensions and boundary conditions as the described in chapter 5, it can be used to compare with the results obtained by the actual experiment in the future when available.

The scope of the finite element modelling analysis is limited to linear elastic analysis, the results obtained are also useful in providing insights regarding how the connection should be modelled using wireframe approach, which is discussed in chapter 7.

6.1 Modelling wood with FEM

Modelling wood structures is a difficult task because of many reasons, for instance, its mechanical behaviours are dependent on many factors including the loading scenarios, the temperature, and moisture content. Additionally, the non-uniform ring density described in section 1.1, which affects the material properties in a single piece of wood also creates difficulties in modelling wood structures. Finally, the anisotropy of wood causes different responses under different loading directions. Therefore, a proper finite element modelling of wood requires taking into account all the quoted aspects as well as the geometry of the structure.

As described in section 1.1, wood consists of different macrostructures, the most important being sapwood and heartwood. Although having different functions and mechanical properties, it is difficult to be incorporated in a computational tool[45]. Nevertheless, many of the finite element modelling software such as DIANA FEA provides the option of modelling timber structures with certain simplification. The most basic material model for wood is linear elasticity, for which the Hooke's Law has defined that the strain is linearly proportional to the stress that acts on the material:

$$\sigma = E * \varepsilon \qquad (6.1)$$

In a three-dimensional analysis, a constitutive matrix that links stress and strain for a material can be defined as:

$$\varepsilon = D^{-1} * \sigma \qquad (6.2)$$

$$where \; \boldsymbol{D^{-1}} = \begin{bmatrix} 1/E_1 & -v_{21}/E_2 & -v_{31}/E_3 & 0 & 0 & 0 \\ -v_{12}/E_1 & 1/E_2 & -v_{32}/E_3 & 0 & 0 & 0 \\ -v_{13}/E_1 & -v_{23}/E_2 & 1/E_3 & 0 & 0 & 0 \\ 0 & 0 & 0 & 1/G_{12} & 0 & 0 \\ 0 & 0 & 0 & 0 & 1/G_{13} & 0 \\ 0 & 0 & 0 & 0 & 0 & 1/G_{23} \end{bmatrix} \qquad (6.3)$$

As discussed in section 1.1.2.1, wood is defined with orthotropic material properties, where Young's moduli (E_i), Shear moduli (G_{ij}) and Poisson ratios (v_{ij}) in longitudinal, radial, and tangential directions are assigned.

6.2 Modelling crosswise connection

For its irregular geometry, a 3-dimensional finite element modelling is constructed for the connection. Two stems with identical dimensions are used for analysis; the dimensions are labelled in Figure 60. In order to incorporate the fusion between the two elements, the intersected portion between the elements are subtracted, as illustrated in the Figure 61.
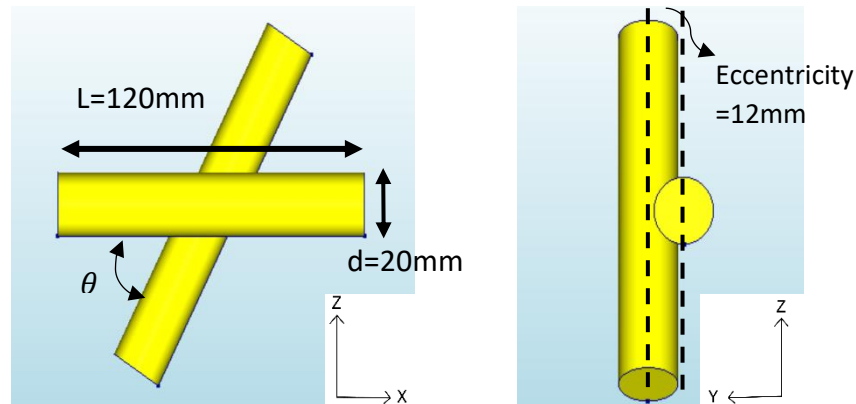
Figure 60. The dimension of the crosswise connection built with finite element model
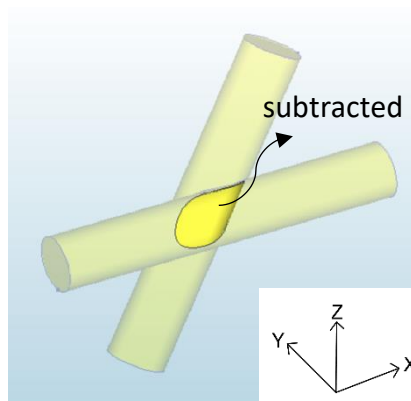
Figure 61. The intersected portion between two elements is subtracted

As one of the modelling approaches used to compare with actual experiments in the future, similar boundary conditions such as restraints and loading schemes are applied to the connection. From section 5.3, the loading scheme for the connection designed for the experiment is realized by an inclined rope, which is to place the loading jaws and the connection's center of gravity in one line. However, as conducting the experiment falls out of the scope of this thesis, the exact angle of the inclination is still to be worked on in the future. Since the purpose of

conducting the experiment and analyzing the finite element model is to investigate the rotational stiffness and strength of the connection, which is associated with its neighbouring stems loaded in bending, a vertical load upwards perpendicular to the horizontal element is applied. This approach also aims to offer qualitative insights to other researchers in terms of the mechanical behaviours of crosswise connection loaded in bending.

Since the analysis in this chapter is done qualitatively, a force with a magnitude of 100N is applied. The load is defined so that it is uniformly distributed over the end face of the horizontal element. Applying a concentrated point load is avoided because it would likely result in overloading of individual mesh element, which would lead to inaccurate results. The boundary conditions defined to the model are illustrated in Figure 62.
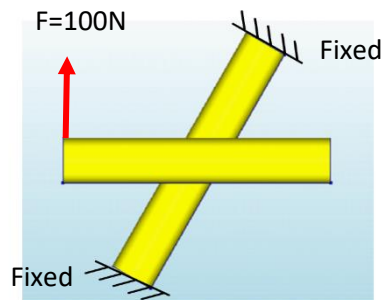
Figure 62. Support condition and loading scheme of FEM

Because of the lack of information regarding the material properties of Ficus Benjamina, linear elastic material properties of an arbitrary wood (Sitka Spruce) are used for the analysis. Following the assumption of transverse isotropy of wood described in section 1.1.2, the following material properties are assigned to the elements.

Table 6.1. Material properties assigned to the element

Parameter	magnitude
E_L	8500 Mpa
$E_R = E_T$	663 Mpa
$G_{LT} = G_{LR}$	544 Mpa
G_{RT}	25.5 Mpa
$\mu_{LR} = \mu_{LT}$	0.467
μ_{RT}	0.245

With three-dimensional analysis and the connection's irregular geometry, solid brick elements are used for meshing. Although a smaller size of the mesh element would provide more accurate results, for the size of the crosswise connection, it is found that element size of 4mm would provide fair results, because the connection with mesh size smaller than 4mm provides almost identical results in terms of deflection. The connection after meshing is illustrated in Figure 63.
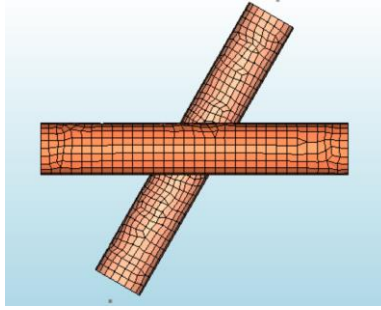
Figure 63. Connection after meshing

For its irregular geometry, it is difficult to assign the elements with one unique meshing element. With the automatic meshing option in DIANA FEM package, to create a meshed geometry that is as uniform as possible, four element types are generated, including HX24L (8-noded brick element), PY15L (5-noded pyramid element), TE12L (4-noded pyramid element), and TP18L (6-noded wedge element), shown in Figures 63. All elements are based on linear interpolation, and each node contains three translational degrees of freedom, u_x, u_y, and u_z.
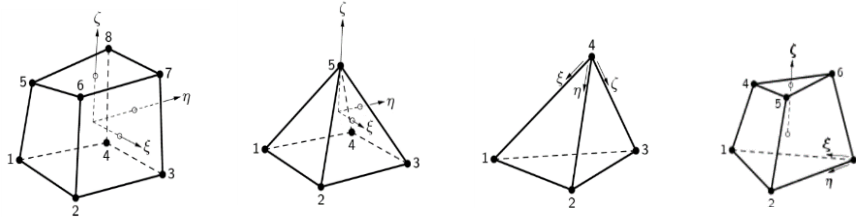
Figure 64. HX24L, PY15L, TE12L, TP18L mesh elements

By default in DIANA FEM package, the local axes x, y, and z are assigned parallel to the global axes X, Y, and Z. However, because of the orthotropic material properties of timber and the irregular geometry of the connection, it is essential to define the local axis of each element carefully. Figure 65 illustrates the local axes definition of the element in both horizontal wood and tilted wood.
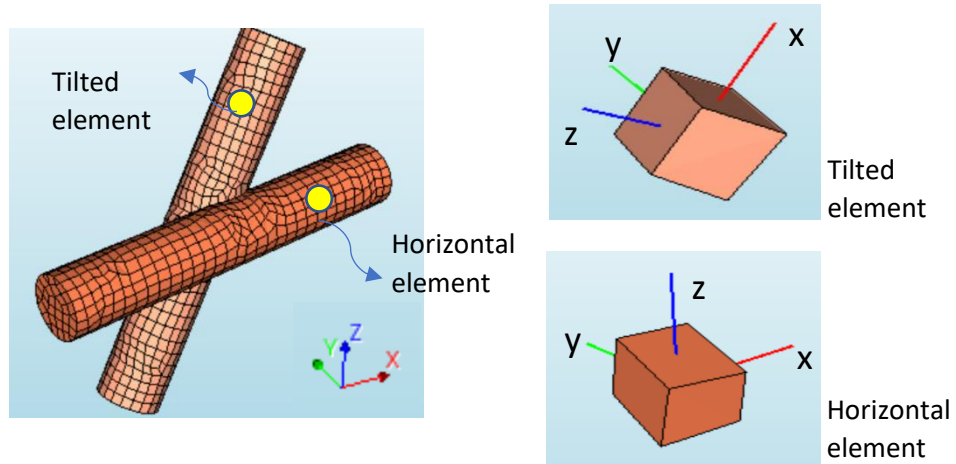
Figure 65. Local axes definition for horizontal element and tilted element

6.3 Non-uniform stress distribution at the interface

After running linear elastic analysis, it is found that non-uniform stress distribution is located near the interface where the two elements are connected, where stress concentration also occurs. Figure 66 illustrates the in-plane principle stress diagram of the connection, location A is where concentrated compressive stress occurs, and location B is where concentrated tensile stress occurs.
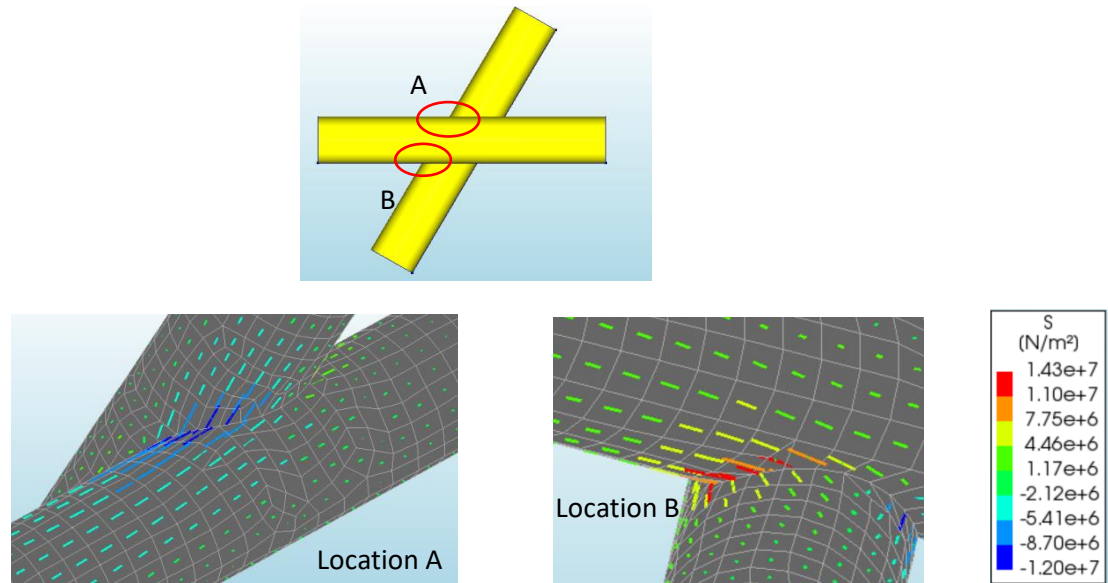
Figure 66. Stress concentration located at the interface of the connection

In terms of the magnitude of the principle stress, the concentrated tensile stress is about 1.2 times larger than then concentrated compressive stress. Such behaviour is reasonable because the lever arm from the applied load to point B is shorter than the lever arm from the applied load to point A, shown in Figure 67.
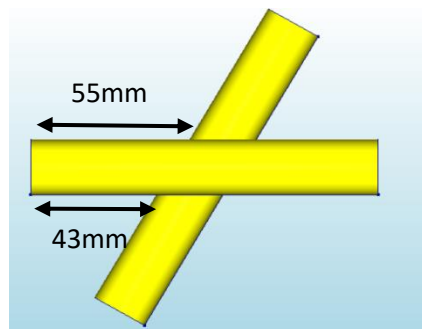
Figure 67. Moment arm from applied force to locations of concentrated stresses

In terms of the strength characteristics of a crosswise connection, question arises in terms of the maximum load applied when the failure occurs to the connection and the corresponding strength property that governs such failure mechanism. Again, since no literature is found in terms of the strength properties of Ficus Benjamina, which is the specimen used for the experiment, Sitka Spruce is chosen for such analysis. Although not being Ficus Benjamina, the verification procedure is useful as an approach for future studies. The strength properties are listed in table 6.2.

Table 6.2. Strength properties of Spruce Sitka

Strength properties	Magnitude (Mpa)
Compression parallel to the grain	18.4
Compression perpendicular to the grain	1.9
Shear parallel to the grain	5.2
Tension perpendicular to the grain	1.7
Modulus of rupture	39

To investigate the magnitude of stresses and the corresponding applied load at the event of failure, 100 load steps with 1-N increments are used for the analysis. By analyzing different stress components with their corresponding strength listed in table 6.2, it is found that the failure of the connection is governed by yielding of wood from tensile stress perpendicular to the grain, which also happens to be the weakest strength property of wood. The corresponding applied load at the end of the stem is 20 newtons. Such behaviour is illustrated in Figure 68, where it is possible to observe that, the yielding failure is again, due to the localized stress along the interface, similar to the observations made earlier in this section from Figure 66.
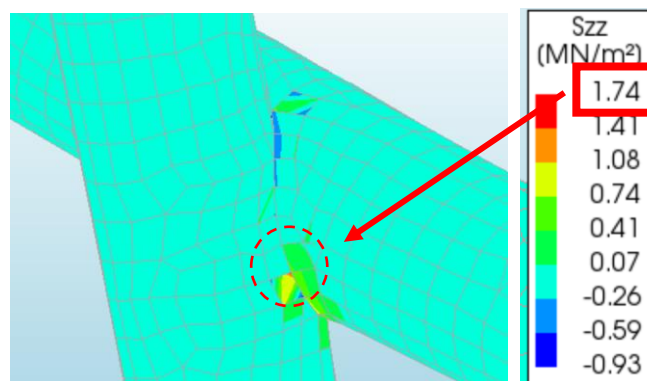
Figure 68. Yielding of connection along interface

6.4 In-plane & out-of-plane deformation

Another observation from the analysis is found, during the linear elastic analysis, when loaded with in-plane forces, both in-plane and out-of-plane behaviours can be observed from the connection, shown in Figure 69.
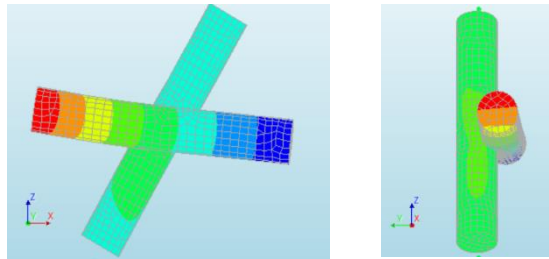
Figure 69. In-plane deformation of the connection (left) and out-of-plane deformation (right)

For the in-plane deformation, except for the bending and shear deformation contributed from the stem itself, eccentricity also results in additional torsional deformation. The reason for such torsional deformation has been discussed in chapter 4.

The out-of-plane deformation results from the torsion of the wood element that is being fixed. Such torsion in the stem itself is also due to the eccentricity between the two stems. This behaviour can be explained by imagining a beam that connects the neutral axes from the two stems, shown in Figure 70. The red and blue element represent the stems, while the green element represents the imaginary beam. Since the red element is fixed on its two ends, when the blue element is loaded, the green element acts as a moment arm, which transfer forces to the red element and cause torsion. The torsional deformation in the red element then causes the blue element to rotate with it. Such behaviours are discussed again in chapter 7 when wireframe modelling approach is proposed.
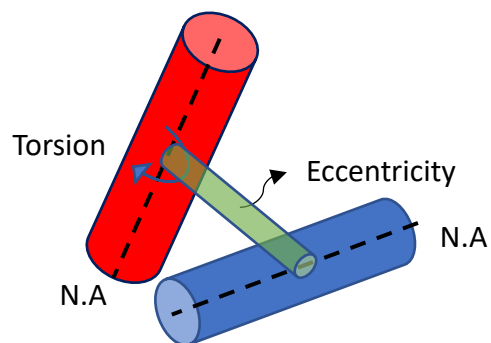
Figure 70. Imaginary beam connecting the neutral axis from two stems

To investigate how eccentricity contributes to both in-plane and out-of-plane deformation, a reference connection is constructed. The reference connection is loaded with the same loading scheme but does not possess any eccentricity. For comparison, more models with increasing eccentricity are built, as illustrated in Figure 71. The analysis is made with increasing eccentricity from 11mm to 16mm. Results are shown in Table 6.3 and Figure 72.
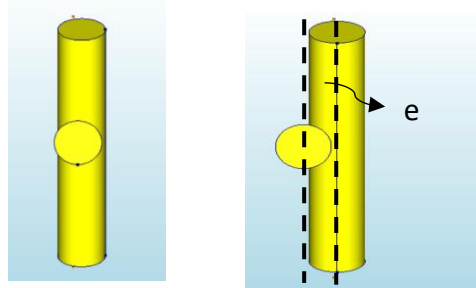
Figure 71. (a) Reference model without eccentricity (b) models with eccentricity

Table 6.3. Results of in-plane / out-of-plane deflection

Eccentricity (mm)	In-plane deflection (mm)	Out-of-plane deflection (mm)
0	0.232	8.87E-04
11	0.415	8.24E-02
12	0.458	9.45E-02
13	0.536	0.11
14	0.637	0.127
15	0.777	0.148
16	1.02	0.17
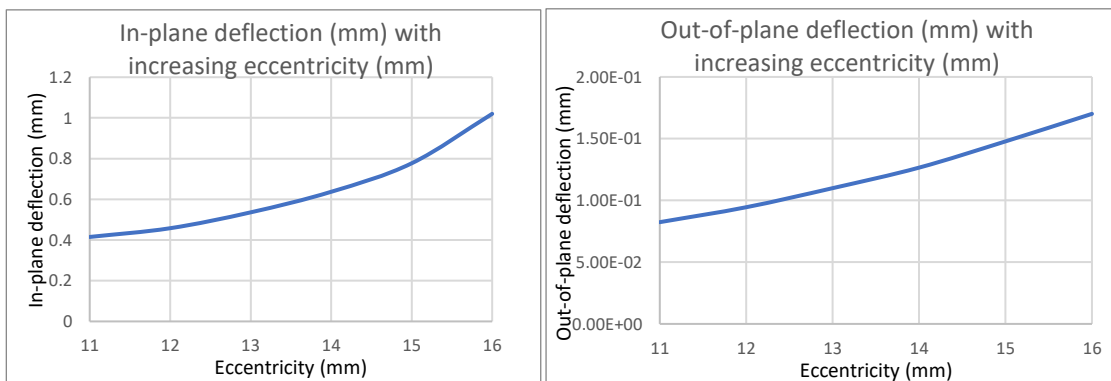
Figure 72. (a) In-plane deflection with increasing eccentricity (b) out-of-plane deflection with increasing eccentricity

From the results, it can be observed that, with increasing eccentricity, both in-plane and out-of-plane deformation increase. For instance, compared to the reference connection, which has an in-plane deformation of 0.232 millimetres and hardly any out-of-plane deformation, the in-plane deflection for the connection with 11 millimetres of eccentricity almost doubled, and the out-of-plane deflection almost becomes 100 times greater. It is also observed that, with 1-cm increment to the eccentricity, the deformation both in-plane and out-of-plane vary non-linearly.

Without the support of experiments, it is difficult at the stage to explain how exactly does the eccentricity influence the stiffness of the connection, however, it is discovered that, as the eccentricity increases, the intersecting surface, which is responsible for providing stiffness to the connection, varies in terms of its geometry and surface area. Figure 73 illustrates the 3-dimensional curved surface that is generated by intersecting the two stems together, and it can be seen that the surface area generated from the model with 16-millimeter eccentricity is smaller than the model with 11-millimeter eccentricity. Figure 74 shows the nonlinear relationship between the length of eccentricity and the intersecting area formed by the two stems.
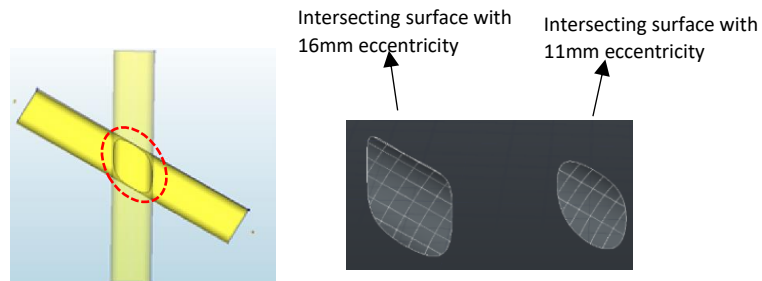
Figure 73. 3-dimensional curved surface representing the contact area between two stems
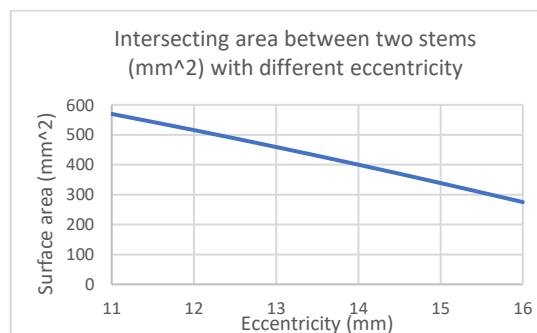
Figure 74. Varying contact area between two stems with changing eccentricity

7. Wireframe modelling approach of crosswise connection

To conduct global structural analysis of a building structure with crosswise connections as the load-bearing elements, they should be appropriately modelled during the preliminary design phase. As discussed in section 3.2, although modelling semi-rigid connections is well incorporated in many structural analysis packages, implementing crosswise connection is unprecedented. Therefore, efforts must be put into searching for a proper method for modelling crosswise connections so that its mechanical behaviours can be captured, and the design can be conducted with confidence.

Referring to the findings in section 6.4, it has been discussed that, due to the eccentric center of gravity, in-plane loading would cause torsional moment in both the connection and the stem. Looking at the conventional modelling approaches of structural connections discussed in section 3.2, it can be argued that both the scissor's model and the two-nodded spring element are not suitable for capturing such behaviours. For instance, the scissor's model is unable to model the eccentricity between the neutral axis of the two trees, which makes it an invalid approach. For the spring element, as discussed in section 3.2.2, a spring force is only activated with a corresponding deformation its degree of freedom, which means that, using the spring element, when the connection is loaded in-plane, out-of-plane behaviour would not occur. Therefore, although having the ability to model the eccentricity between tree elements, spring element is also an invalid approach.

7.1 Modelling crosswise connection with beam element

To capture the eccentricity between the tree elements as well as the interaction of in-plane and out-of-plane behaviours, another unconventional approach is investigated in this section, which is the use of beam elements.

Using a beam element between the connected trees makes it possible to incorporate eccentricity and transfer forces from one tree to another. For illustration, a simple structure shown in Figure 75 is analyzed. The structure consists of two straight beam elements (element 1 and 2) representing trees at an angle, θ relative to each other. To model the eccentricity, two beams are placed some distance apart and connected with another beam element (element 3) from the center. The blue and red beams represent the trees, while the green beam represents the connection. To prove that this modelling approach would correctly capture the mechanical behaviours of the connection, similar boundary conditions as the FEM approach are applied, shown in Figure 75.

62
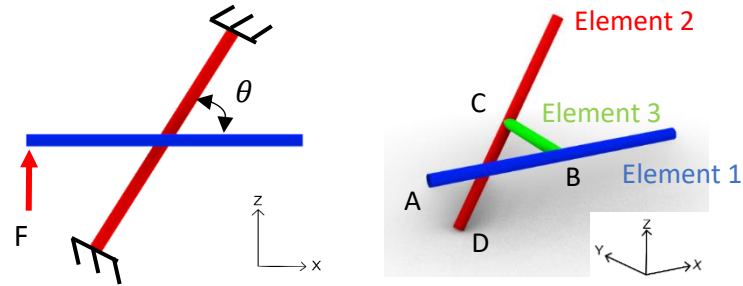
Figure 75. Simple structure used to illustrate the structural behaviours of crosswise connection

From the deformed shape of the system, illustrated in Figure 76, it can be observed that element 1 shows both in-plane (x-z plane) and out-of-plane (y-z plane) behaviours.
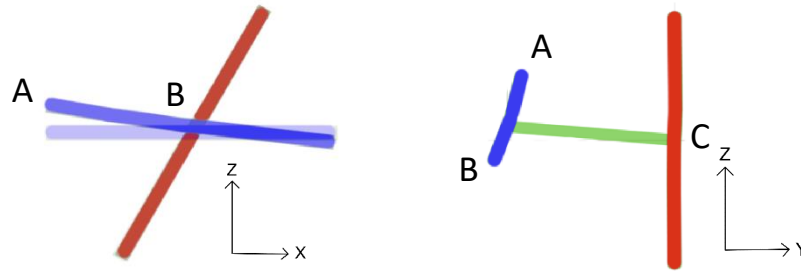
Figure 76. (a)In-plane deformed shape, (b)out-of-plane deformed shape of the structural system

The in-plane deformation illustrated in Figure 76(a) results from the following series of actions: the bending moment (M_y) in element 1 at point B results from the load at point A, which causes cantilever flexural deformation as well as shear deformation for segment AB; subsequently, this bending moment is then transferred from point B to point C through element 3 via torsion (T_x), which occurs around its own axis. This torsional effect on the connecting beam results in additional in-plane deformation. These statements are summarized in the bending moment diagram illustrated in Figure 77.
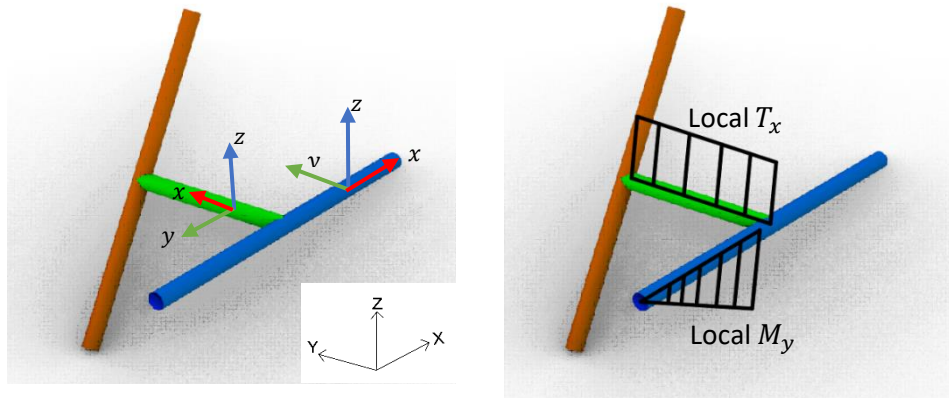
Figure 77. Local axes coordination (left) and local bending moment diagram (right) of the structure

The out-of-plane deformation illustrated in Figure 76(b) results from the torsional moment (T_x) of element 2 around its own axis, which is a transferred from the bending moment (M_y) of the connecting element (green beam). With the bending moment diagram shown in Figure 78, it can be observed that the center of the red element is subjected to the most torsional moment, which causes the connecting element (green beam) to deform with it. Such behaviours can also be visualized in Figure 79.
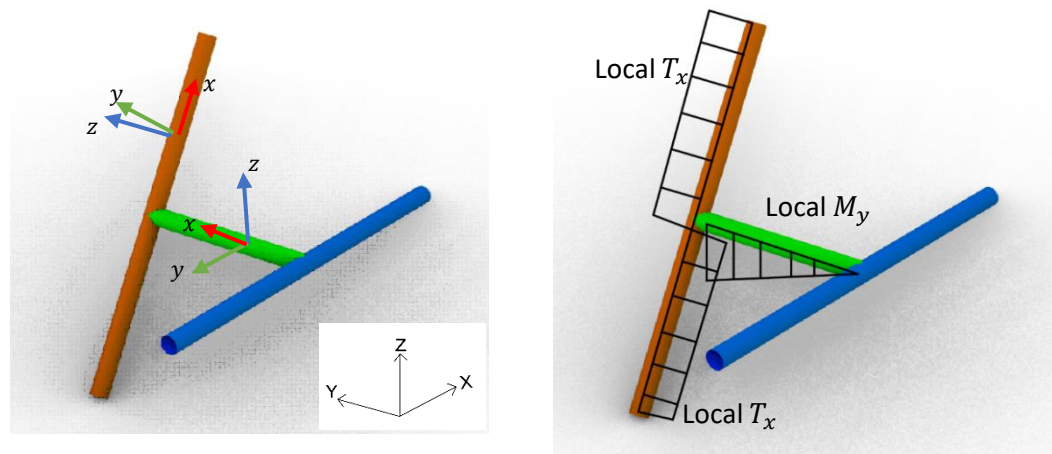
Figure 78. Local axes coordination (left) and local bending moment diagram (right) of the structure
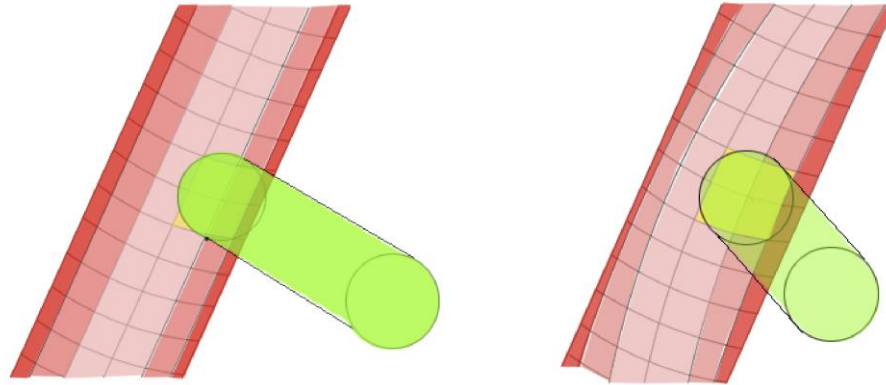
Figure 79. Torsional deformation of the red element

7.2 Modelling assumption: assigning crosswise connection with ellptical cross section

Having proved that the complex behaviours of a crosswise connection can be captured with a beam element, it is then necessary to assign such element with corresponding beam properties. For instance, a geometrical definition must be assigned to the cross-section of the connecting beam element. Looking at the micro-CT scans provided in the Introduction chapter, it can be observed that the part of the tree elements that are being connected forms an ellipse-like shape.
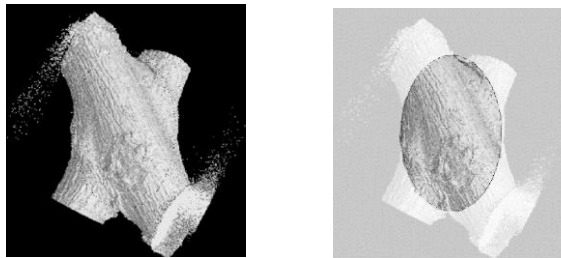
Figure 80. Elliptical cross-section assigned to the crosswise connection

Therefore, a modelling approach is proposed in this thesis project, that the beam element connecting the two trees possesses an elliptical cross-section. Based on this premise, it is possible to develop the geometrical relationship between the connection and the trees, which also becomes handy for design purposes, because it is then possible to incorporate how the mechanical properties of the connection vary with growth.

Knowing the diameter of the tree stem, D, and the intersecting angle made by the two trees, θ, the major and minor radius of the ellipse can be computed using basic trigonometry.
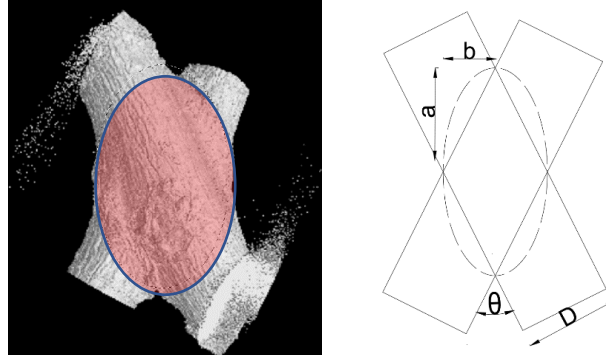
Figure 81. Dimension of the elliptical crosswise connection

$$a = \frac{D}{2 \cdot sin(0.5\theta)} \tag{7.1}$$

$$b = \frac{D}{2 \cdot sin(180° - \theta)} \tag{7.2}$$

Due to the fiber orientation of wood, when modelling the crosswise connection with wireframe modelling approach, one thing to pay attention to is the axes definition of the structural elements. In most wireframe modelling software, such as SAP2000 and Karamba 3D, by default, the longitudinal axis of a beam element is recognized as parallel to grain, while axis 2 and axis 3 are radial and tangential, respectively. Referring to Figure 82, with an acceptable assumption of transverse isotropy described in section 1.1.2.1, it is suitable for the tree elements, but it would cause an undesired error to the connecting beam element because the longitudinal axis of the connecting beam is no longer parallel to the grain.
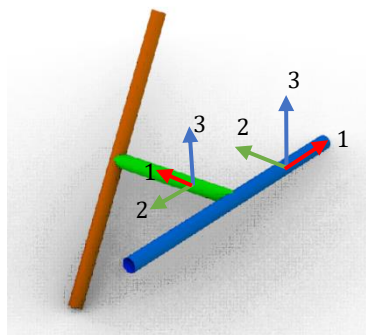
Figure 82. Local axes definition of tree element and connection element

Therefore, it is essential to assign each stiffness property with the correct elastic modulus. For instance, when loaded with axial force in its longitudinal axis, the young's modulus that are responsible for resisting such forces should be E_L for tree elements, while it should be E_R for the connection element. Similarly, when loaded with torsional moment about its longitudinal axis, the shear modulus that is responsible for resisting such forces should be G_{LR} for the tree element, while it becomes G_{RT} for the connecting element; this is because, under torsion around tree element's own axis, the material property that is responsible for providing resistance is shear modulus in both longitudinal-tangential (LT) and longitudinal-radial (LR) planes, as shown in Figure 83. Referring to Wood Handbook, for the timber element subject to torsion around fiber direction, shear modulus can be approximated as $\sqrt{G_{LR}G_{LT}}$[20].
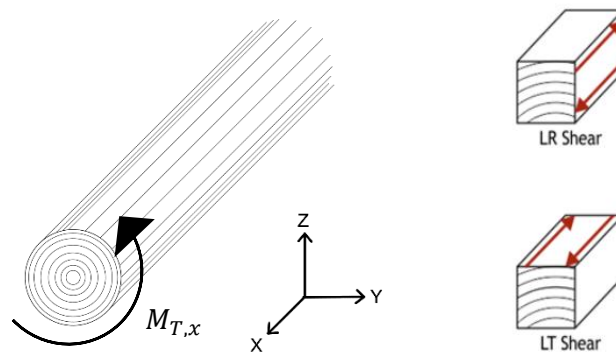
Figure 83. Tree element subjected to torsional moment

However, when the connection element is subjected to torsion, since the connection is still part of the individual tree, the shear modulus responsible for resisting torsion now becomes G_{RT}, shown in Figure 84.
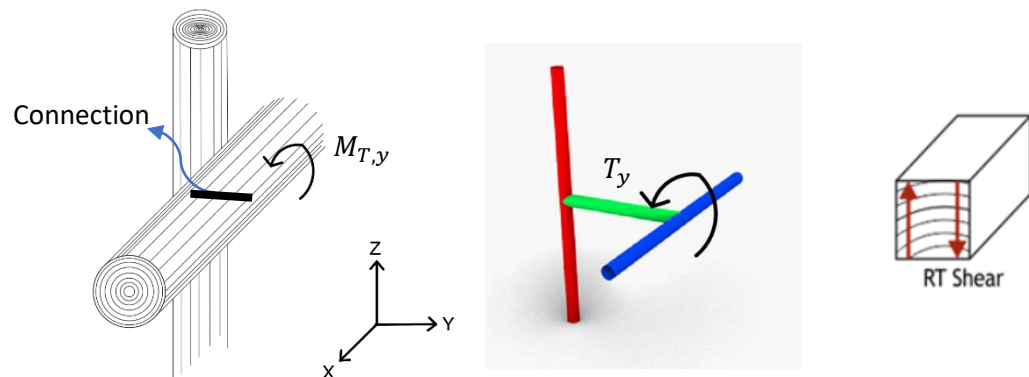
Figure 84. Connection element subjected to torsional moment

From the statements made above, manual adjustment to the material properties is needed so that the local axes match the correct fiber orientation. Table 7.1 illustrates the definition of the orthotropic material properties with its corresponding local axis to the tree element and the crosswise connection.

Table 7. 1 Material definition for stem and crosswise connection

Material properties for tree stem	Material properties for crosswise connection
$E_1 = E_L$	$E_2 = E_L$
$E_2 = E_3 = E_R$	$E_1 = E_3 = E_R$
$G_{12} = G_{13} = G_{LT}$	$G_{12} = G_{32} = G_{LT}$
$G_{32} = G_{RT}$	$G_{13} = G_{RT}$

7.3 Comparison with finite element model

To comment on this modelling approach, a comparison is made with the results obtained from FEM in section 6.4. To make a constructive comparison, the setup for the wireframe model is exactly the same as the FEM model, which means that the element dimension, boundary condition, loading scheme, and material properties from the two model are all identical.

The comparison between two models is made in terms of the in-plane and out-of-plane deflection with varying eccentricity. From Figure 85, it is found that, the relationship between the length of eccentricity and deformation is linear, which is different from the results shown in section 6.4, where nonlinear relationship is found.
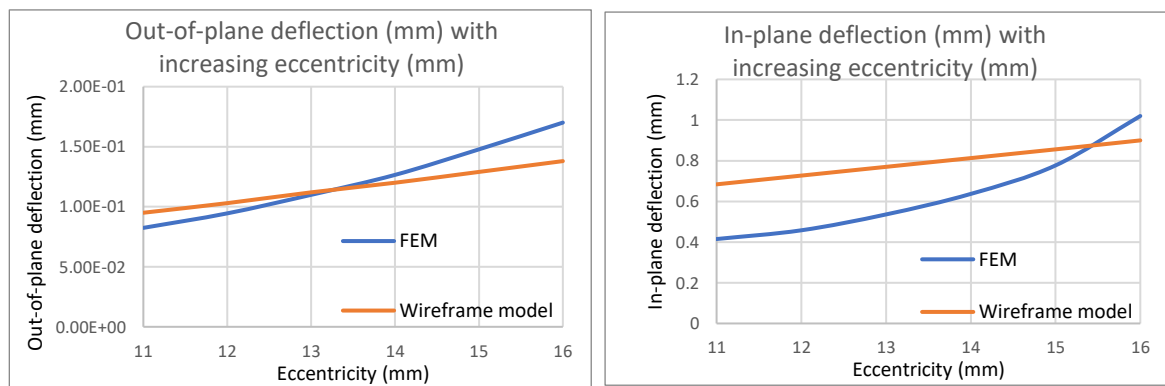
Figure 85. Results obtained from the simplified model and FEM for comparison. (a) In-plane deflection with increasing eccentricity (b) out-of-plane deflection with increasing eccentricity

The linear relationship found here with the wireframe model is reasonable, because linear elastic analysis is conducted for wireframe model, and the incremental deformation of the stem is linearly related to the connecting beam's length. For instance, the in-plane torsional deformation contributed from the connecting beam element is related to its torsional stiffness:

$$\frac{G_{RT} \cdot J}{L} \qquad (7.3)$$

, where J and L represent the torsional constant and the length of the connection beam element, respectively. The torsional constant is affected by the cross-section, which stays constant with the varying eccentricity, while L is directly related to the magnitude of eccentricity. Therefore, by linearly increasing the length of eccentricity, the torsional stiffness linearly decreases, which then leads to the linear increase of in-plane deformation, shown in Figure 85(a).

As discussed earlier in section 7.1, the out-of-plane deformation is directly influenced by the length of the moment arm, which is the length of the eccentricity. Therefore, by linearly increasing the length of eccentricity, the torsional moment linearly increases in the fixed stem, which then leads to a linear increase of the out-of-plane deformation in the free stem, shown in Figure 85(b).

With the explanation stated above, although the wireframe modelling approach exhibits differences with the finite element modelling approach, it is able to capture similar mechanical behaviour of the crosswise connection as well as transmitting forces from one stem to the other.

Conclusion

In part-II of the thesis report, efforts are put into investigating the mechanical behaviours of a crosswise connection when utilized as a load-bearing element in a building structure.

In chapter 4, with a simple case of two trees connected in a crosswise manner, it is found that, depending on the loading scenario, the connection can be subjected to different stress states. Two important stress states that occur in the connection are axial stress perpendicular to the grain and rolling shear stress. As two of the weakest strength properties of wood, they should be treated with care by future designers.

In chapter 5, an experimental design is proposed to investigate the rotational stiffness and strength of the crosswise connection. Learning from the literature and existing practices, the following aspects are included for the design:

i.   To capture the actual behaviour of the crosswise connections when utilized in actual structures, fixed supports are used on the ends of the one stem.

ii.   Due to the irregular geometries of the crosswise connections and minor differences from specimens, the setup is designed so that it could fit specimens with varying dimensions.

iii.   To obtain the moment-rotation curve for each specimen, DIC is to be utilized for its ability to track full-field deformation on irregular geometries.

In terms of bearing capacity of the crosswise connection, one of the hypotheses is that, due to the fiber deviation at the connection, which is be an important source of strength reduction for wood, failure would occur first at the interface of the connection, where fiber deviation takes place. Another hypothesis is that that failure would occur to individual stems if the bearing capacity of the connection is greater than the bending strength of individual stems.

Since conducting the actual experiment falls out of the scope of this project, chapter 6 focuses on providing a finite element modelling approach which could provide insights to how crosswise connection behaves under similar loading scenario as the experiment. Since the investigation focuses on the rotational stiffness and strength of the crosswise connection, which is associated with its neighbouring stem being loaded with bending, without knowing the exact loading angle for the experiment, a perpendicular load is applied to the stem for the finite element model. The finite element modelling approach aims to offer insights in terms of the mechanical behaviours of the crosswise connection subjected to bending.

By running linear elastic analysis of a crosswise connection under in-plane loading, it is found that both in-plane and out-of-plane deformation occurs to the connection, the in-plane deformation is contributed from bending and shear deformaiton of the cantilevered stem, and the torsional deformation of the connection due to eccentricity, while the out-of-plane deformation is due to the torsional deformation of the fix stem around its own axis.

From the results illustrated in section 6.4, a nonlinear relationship is discovered between the magnitude of eccentricity and connection's deformation. Such behaviour could be related to the fact that, with decreasing eccentricity, the intersecting 3-dimensional curved surface which is responsible for providing stiffness, varies in terms of its geometry and area.

Finally, it is discovered that, under loading, non-uniform stress distribution and stress concentration are found near the interface of the connection, which is a result of the irregular geometry around the interface at the connection. Since material properties of Ficus Benjamina, which is the target specimens in the experiment could not be found from literature, an arbitrary wood species (Sitka Spruce) is used for analysis, and it is found that when being loaded in-plane, the strength property that governs the strength of the connection is tension parallel to the grain, which is also the weakest strength property of wood.

Finally in chapter 7, based on the findings from chapter 6, a wireframe modelling approach for the crosswise connection is suggested, which is to incorporate a separate beam element that connects the neutral axis of the two trees at the location of the inosculation. By comparing with the results obtained by FEM, although it does not produce the exact same results, for design purposes, its role in terms of capturing the mechanical behaviours as well as transmitting forces from one stem to the other is fulfilled. Without the support of the actual experiment, it is difficult at this stage to conclude in terms of the accuracy of the results from the two models. However, with engineering judgement, it is assumed that the results obtained with finite element analysis offer more accurate results than the simplified wireframe model in terms of local behaviours, because of the following reasons:

1. the wireframe model is proposed based on a hypothesis that the connecting element formed by the two stems has an elliptical shape.
2. Finite element modelling takes into account of the irregular geometry of the crosswise connection during the analysis.

Part III – Design Case study

Structures such as the Baubotanik Tower and the Living Tree Pavilion introduce researchers and engineers to the possibilities of designing with trees and tree connections. However, since these structures are still under development, it remains uncertain in terms of the reliability and strength of these structures.

From the previous chapters, literature studies are made in terms of the biomechanics of trees, the inosculation process of tree connection, and the tree growth model. With the wireframe modelling approach proposed in chapter 7, it is possible to combine and implement such tools to design or verify building designs with growing trees and tree connections as the main load-bearing elements.

Inspired by the existing Living Architectures, with a design case study, Part III of the thesis project aims to propose a preliminary design and verification procedure of a structure supported mainly by the growing trees and tree connections. With the analysis procedures defined in the case study, designers are able to predict when the structure will be ready to provide service to the public.

This design case study can be seen as the study regarding the feasibility of utilizing growing trees and crosswise connections as the load-bearing elements during the preliminary design phase of a building structure. Since many studies of this thesis are based on Ficus Benjamina, it will be used as the tree species for analysis.

8.1 Objective

Every building design is orientated from different objectives that come from different parties involved. As the designer of the case study, objectives are set from a structural engineer's perspective. From Part-I of this thesis, an important conclusion is made, which is when two trees inosculate, fiber deviation occurs near the interface of the connection, as an important factor that influences the strength of wood, it should be treated with care by designers. From Part-II of this thesis, it is concluded that, when utilized as a load-bearing element, important stress state such as torsional shear stress occurs to the connection. Due to the fiber orientation, such torsional shear stress results in rolling shear stress. As one of the weakest strength properties, such strength property should also be treated with care by designers. With the statements made above, the objective of this design case study aims to provide a structural design that minimizes such torsional effects in the connection.

In order to take the time-dependent properties of trees and tree connections into account during the analysis, it is then reasonable to perform the analysis in a way that the inputs are adjustable. For its ability to control the parameters in great flexibility, Rhinocero, along with its plugin, Grasshopper and Karamba, will be utilized as the tool to assemble the geometrical model and perform structural analysis.

8.2 Growing Tree Tower description

8.2.1 Structural scheme

As discussed continuously in the previous analysis, the torsional effect of the crosswise connection results from the adjacent tree elements under bending. Therefore, to minimize such a torsional effect at the connection, the most straightforward and logical solution would be to utilize a structural scheme that does not rely on elements' bending to provide strength and stability.

To fulfill such requirements, conventional structural schemes such as a frame structure are not applicable for two reasons. Firstly, frame structures resist both lateral and gravitational load through bending action of the orthogonal elements, and the stiffness of such structure is mainly provided by the combination of bending rigidity of orthogonal elements as well as the rotational stiffness of the connections. Secondly, considering trees' growth pattern and geometry, the orthogonal configuration is unrealistic to be achieved by the growing trees.

Resisting gravitational and lateral load is also possible with a structural scheme that does not rely on either orthogonal elements or bending action, such as a diagrid system. Diagrid structures are the ones that make use of an exterior frame comprised entirely of diagonal members as the primary means of combined gravity and lateral support[46]. If conditions allow, the diagonals could be the only structural elements for the structure, which provide sufficient load-bearing capacity while also providing maximum interior spaces. Many skyscrapers have successfully employed diagrid as their structural scheme; examples are Swiss Re in London, UK and Hearst Tower.

Figure 86. Diagrid structures. (a) Swiss Re[47] (b) Hearst Tower[48]

Compared with conventional framed tubular structures, diagrid structures are more favourable to be employed as the structural system for the growing tree structure, as they are much more effective in minimizing bending action, because they carry shear by axial action of the diagonal members due to the triangulation formed repetitively. The triangulation configuration is illustrated in the force diagram in Figure 87.
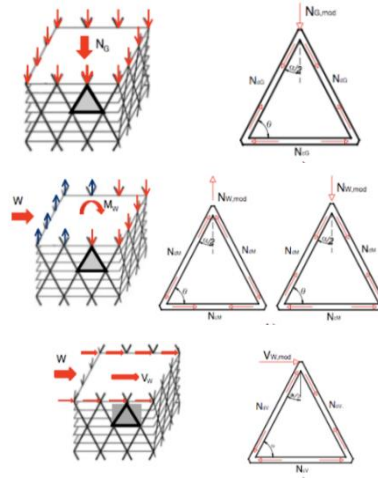
Figure 87. Gravitational force (top), overturning moment (middle), and horizontal force (bottom) resulted in axial forces in the diagonals[49]

It is important to note that the diagrid "tube" triangulation is not sufficient to achieve full rigidity in the structure in resisting lateral loads. A rigid diaphragm reaction from floor slabs and ring beams at the floor edges is required to transfer the horizontal load to the diagonals through axial action. The ring beams should be tied into the diagrid to integrate the structural action into a coherent tube[50]. Therefore, incorporating horizontal tie beams should be kept in mind while designing the structure.

With the consideration discussed above, a proposed diagrid growing tree tower built with Ficus Benjamina is illustrated in Figure 88. The structure has a cylindrical form, with a floor diameter of 6 meters. The reason for setting the height of the tower as 10.5 meters relates to the growth rate of Ficus Benjamina, which is discussed in section 8.2.3. The tower is supported on 6 points, each point planted with 2 trees that grow in a spiral matter in the opposite direction; therefore, a total of 12 trees are planted. A cylindrical form, like Swiss Re, is chosen as the tower's geometrical configuration because it allows a more natural and organic growth pattern for the tree elements, instead of having sharp turns at the corners, like the Hearst Tower.
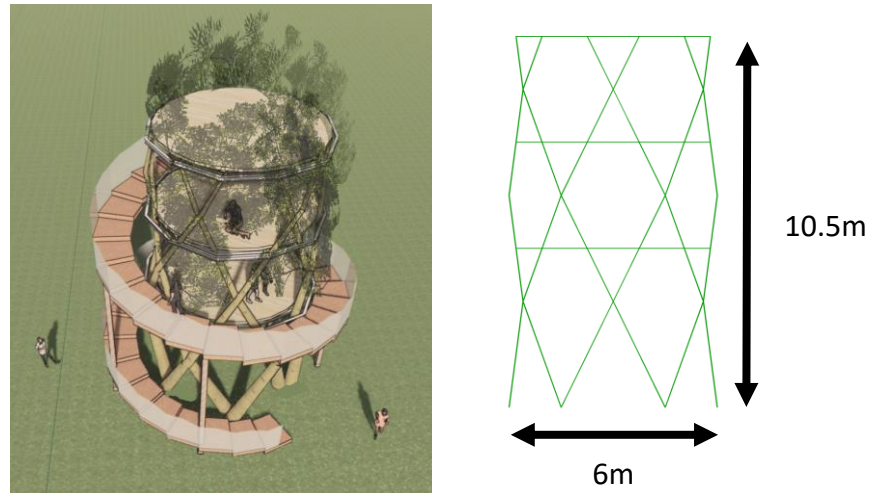
Figure 88. Growing diagrid tree tower

As mentioned earlier, the perimeter floor beams together with the floor slab are essential in transferring horizontal wind load through a diaphragm reaction. Therefore, the question arises in terms of how the perimeter beams can be incorporated with tree elements in the structure.

Studying from a publication by Baubotanik research group[51], which aimes to investigate the growth process and mechanical properties of the semi-artificial organism, it is learned that, due to trees' secondary growth and their ability to grow adaptively, trees have the ability to grow around foreign objects to optimize surface stresses, which can be related with the study of the self-optimization of trees made in the Literature study (section 1.2). With results from several experiments, Baubotanik has concluded that:

- Technical components with small cross-sections are incorporated within the plants much faster than those with wider cross-sections.
- Due to form-fitting as a result of optimization at a macroscopic level, 'interlocking' between the technical component and the growing wood could take place.

Figure 89. Development of tree growing around a steel tube[8]

Learning from this research, it is proposed to place the ring beams at the mid-height between connections for the growing tree tower. Baubotanik does not mention how long it takes before the technical component can be fully embedded in the trees; therefore, to carry out the analysis, a simple assumption is made that it would take two years before the technical parts are fully embedded with the tree elements.

Figure 90 illustrates the connection detail; it consists of two parts: the first part is a branch plate-to-circular structural section, shown in Figure 90(a), where the circular element is embedded in the tree element, while the plate element is welded with the circular element. The second part is an I-profile beam that serves as the perimeter floor beams of the tree tower, shown in Figure 90(b). The I-beams are installed on both sides of the trees to avoid torsion of the tree elements when the horizontal force is transferred from floor beams to the trees.
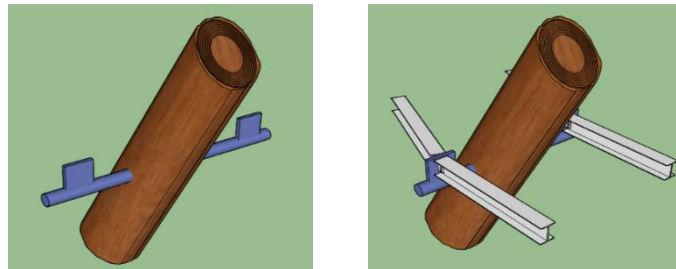
Figure 90.(a) Branch plate-to-circular section fused with tree (b) connected with I-profile beams

Another connection detail is provided in Figure 91; it illustrates the simple connection made between the two parts. The fin plate, which connects the rectangular plate and the I-profile, allows rotation of the I-profile when loaded with gravity loads. The main motivation of such design is to only transfer axial force from the floor to the trees.
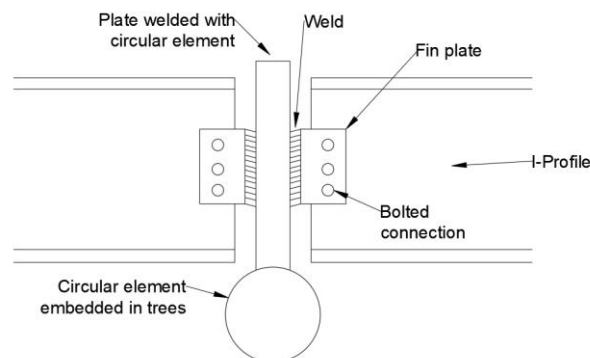
Figure 91. Connection detail

After the circular elements are successfully embedded into the trees, floor beams will be attached to the perimeter beams. To uniformly distribute the live load to the perimeter beams, a floor plan shown in Figure 92 is designed; it is assumed that the floor beams and the floor panels provide sufficient rigid diaphragm action for the transfer of horizontal force.
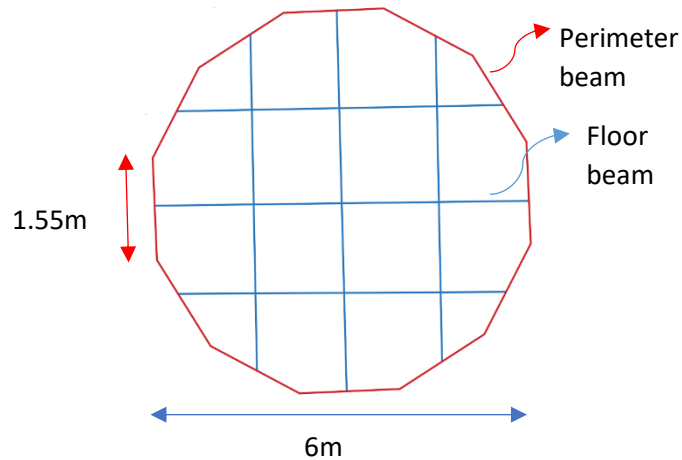
Figure 92. Floor plan

With the proposed floor plan, each set of perimeter beam spans 1.55 meters. With the load combination described in section 8.5.1, IPE-80 will be implemented as the perimeter beams profile, which could provide sufficient strength. The calculation procedure for such analysis is provided in Appendix 10.5.

8.2.2 'Growth' of the tree tower

One of the unique features of the self-growing tree tower is that, whenever the trees have grown to the predefined storey height and are connected with the perimeter floor beams, that storey is ready for use, unlike conventional buildings, which only becomes ready for service when the entire structure has completed construction.

With the urban tree growth model and tapering geometry of trees described in section 2.2, scripts are written in Rhino which makes it possible to visualize and keep track of the tree tower's growth stages. The scripts are shown in Appendix 10.2 and 10.3.

Combined with the assumption that trees can be fully bonded with perimeter beams in two years, the growing tree tower's construction can be visualized in Figure 93. Year 5, 14, and 26 are

the years when the crosswise connections are made, while year 11, 21, and 37 are the years when a specific storey is completed.
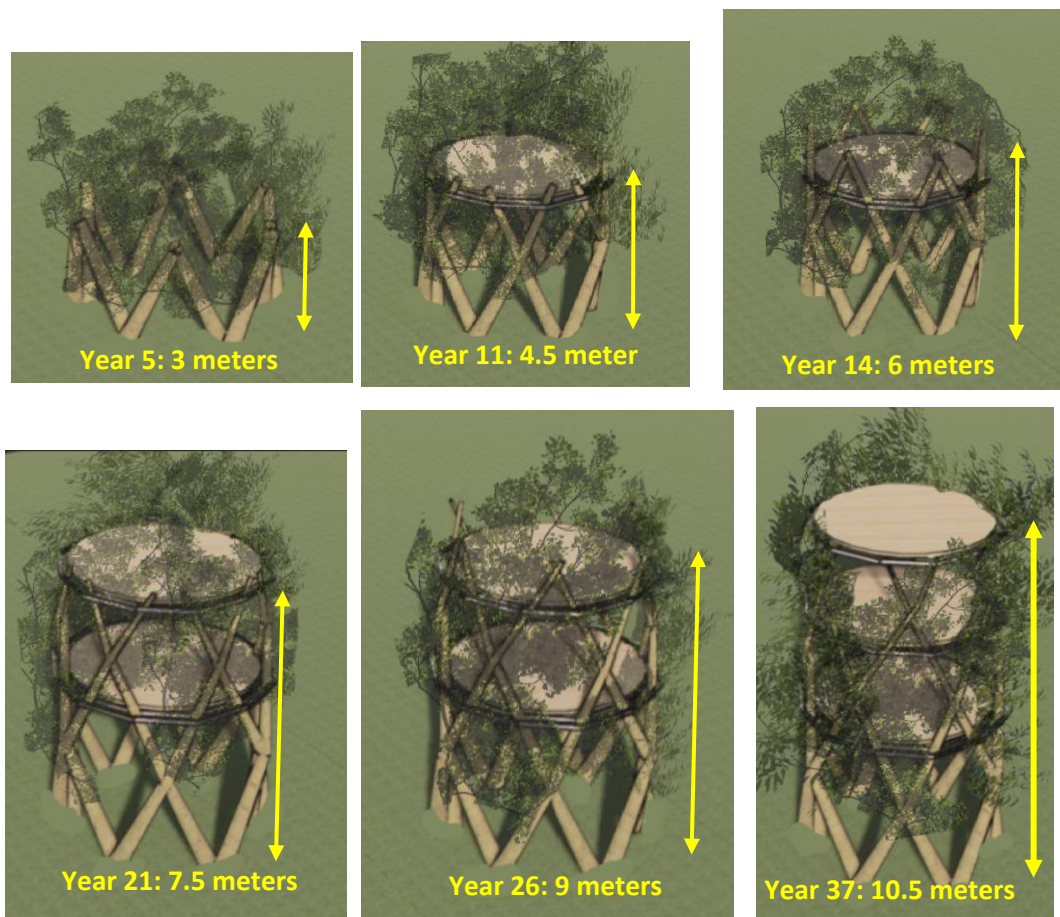
Figure 93. Growth stage of diagrid tree tower

According to the upper limit of tree height from the growth model of Ficus Benjamina, although the trees can continue to grow, it is proposed that the tree tower is completed in Year 37. The reason being, due to the declining growth rate of Ficus Benjamina, it would take another 30 years before the next storey can be installed on 13.5m. Therefore, it is decided that, after Year 37, the height of the tower is to be controlled by pruning the growing parts.

8.2.3 Structural behaviour of growing tree tower

Just after perimeter beams and floor slabs are attached for one storey, and before the attachment of the next set of perimeter beams and slab on the next storey, the cantilevered crown generates bending moment along the diagonals due to wind loading, shown in Figure 94. As discussed in chapter 4, with the tree elements subjected to bending moment, torsion can be expected at the connection. However, with the help of the triangulation scheme from the diagrid structure, the bending effect is expected to be diminished and turned into axial action when the growing trees reach the next storey and connect with another set of floor beams. This behaviour is to be discussed again in section 8.5 with the results obtained from structural analysis after the geometry and applied loads are defined in section 8.3, 8.4.

Cantilevered Crown

Completed diagrid

P_{wind}

F_{wind}
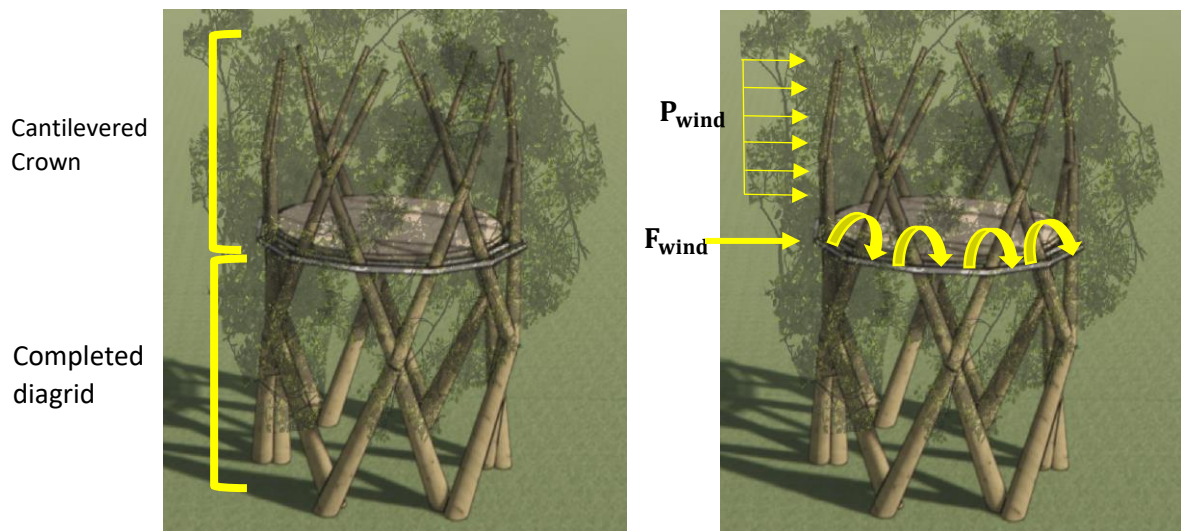
Figure 94. Horizontal wind load transfer from tree crown to the diagonal structural elements beneath

As a final remark for the crosswise connection in the growing tree tower, an interesting analogy can be made with the structural nodes of contemporary diagrid structures: for many existing diagrid structures, one of the key assumptions is that, the connection at the vertices of each triangulation act as a hinge, which only permits the transfer of axial loads to its adjacent members, similar to that of a truss-type design; however, in reality, for constructability purposes, the connections are made just stiff enough to assist with the safe erection processes without the use of temporary shores, where members can cantilever with little deflection from the node in anticipation of further connections to complete their triangulation[46].

8.3 Geometric definition for structural element

8.3.1 Tapering tree diagonals

Since element taper is not readily available in Karamba 3D, it is proposed that each diagonal tree member is to be divided into segments with varying diameters, and each segment has a uniform diameter along its length. Therefore, a question is raised regarding the minimum number of segments required to be modelled before conducting the structural analysis.

For such investigation, a simply supported tapered circular beam subjected to uniformly distributed load will be analyzed using analytical calculation. The obtained deflection will be used as a reference value for the identical beam analyzed in Karamba3D. The goal is to obtain the minimum number of segments that need to be modelled in Karamba3D so that the difference between the two results falls under 5%.

The beam to be analyzed is shown in the Figure 95. In the diagram, 'w' represents the magnitude of the uniform distributed load; for illustration, it is assigned with 1 kN/m. 'dA' and 'dB' are the diameters of the two ends of the tapered beam, 'L' represents the length of the beam, and 'ξ' represents the normalized length of the beam. To relate with the tree tower model, the length of the beam, L, is assigned as 1.5 meters. It is found that when the trees have grown to a new storey height, the ratio of the diameter at two ends of the tapered element (dB/dA) is about 4. To relate with the early growth stage of a tree, dA will be assigned as 0.05m, and dB assigned as 0.2m.
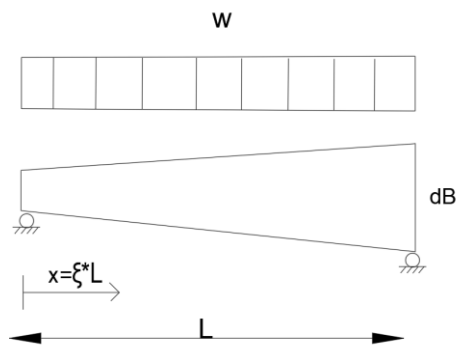
Figure 95. Simply supported tapered beam subjected to uniformly distributed load

<u>Analytical method</u>

For a simply supported beam subjected to uniformly distributed load, the bending moment at any position along the beam is:

$$M = \frac{1}{2}wL^2\xi(1 - \xi)$$

(8.1)

The curvature of the loaded beam can be expressed as:

$$\frac{d^2y}{dx^2} = -\frac{M}{EI}$$

(8.2)

Here, it is essential to note that the moment of inertia, I, at any position along the beam, becomes a function of the tapering ratio, r, and it can be expressed as:

$$I = I_A[1 + (r - 1)\xi]^4$$

(8.3)

, where I_A represents the moment of inertia at the thinner end of the tapered beam. Thus, the curvature expression then becomes:

$$\frac{d^2y}{dx^2} = -\frac{M}{EI} = \frac{wL^2}{2EI_A}\frac{\xi(\xi - 1)}{[1 + (r - 1)\xi]^4}$$

(8.4)

The expression for deflection can be obtained by integrating the curvature expression twice:

$$y = \frac{wL^4}{2EI_A(r - 1)^4}[-\ln K - \frac{(r + 1)}{2K} + \frac{r}{6K^2} + A\xi + B]$$

(8.5)

, where $K = 1 + (r - 1)\xi$; A and B are the integration constants.

By applying the boundary conditions of a simply supported beam (y=0 at $\xi = 0$ and $\xi = 1$), A and B can be determined:

$$A = \ln(r) - \frac{(r^2 - 1)}{3r}$$

(8.6)

$$B = \frac{1}{6}(2r + 3)$$

(8.7)

With the known information provided earlier:

$$L = 1.5m$$

$$r = 4$$

$$w = 1\ kN/m$$

$$I_A = \frac{\pi}{64}d_A^4 = 3.07E(-7)m^4$$

, deflection can then be solved:

$$y = (4.46E - 5)m$$

Calibration with wireframe structural model

This value of deflection is then taken as the reference value for the same analysis carried out in Karamba3D. Again, the goal is to find out the minimum number of segments that need to be modelled so that the result obtained falls within 5% compared to analytical solution.

After trial and error, it is found that, to obtain a 5% accuracy, the minimum number of segments to be modelled is 64. During the investigation, it is also found that elements with a longer span or higher degree of tapering form require a greater number of segments to be modelled to achieve accurate results.

8.3.2 Crosswise connection

As discussed in chapter 7, with eccentricity and the interaction between in-plane and out-of-plane behaviours in a crosswise connection, a beam element connecting the adjacent tree elements is suitable for such analysis.

In Karamba, the modelling of crosswise connection is achieved by offsetting the diagonal tree elements, which creates a gap between them. The gap is then connected by a beam element assigned with an elliptical cross-section, which the dimensions vary with the growing geometry of the trees, as discussed in section 7.2. The eccentricity between the tree elements is assigned as 12 millimetres, and such eccentricity will remain constant throughout the entire growth stage of the structure. Figure 96 illustrates how the connection is modelled in the program.
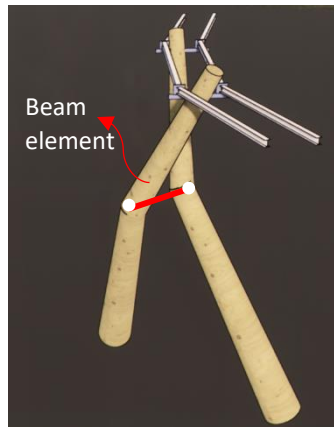
Figure 96. Eccentricity modelled in Grasshopper, linked by beam element

In Karamba3D, it is possible to modify the mechanical properties of a beam element manually. With the simplified wireframe model proposed in chapter 7, a beam element with elliptical cross-section is defined for the connecting beam element. How the cross-sectional properties of the structural elements (diagonal trees, crosswise connection) vary with growth is discussed in the next section.

8.3.3 Effect of growth on the cross-sectional properties of structural elements

The behaviour of a structural member is dictated by its material and its geometry, where the cross-section and the length of the structural member affect how much that member deflects under a load, and the cross-section affects the stresses that exist in the member under a given load. Since the goal of this design case study is about utilizing growing trees and tree connections as load-bearing elements, further analysis should be conducted in terms of how growth would affect their mechanical properties.

<u>Diagonal tree elements</u>

The effect of growth on individual trees is investigated first. On a cross-sectional level, the tree could be subjected to different forces such as axial force, bending moment, shear force, as well as torsional moment, illustrated in Figure 97.
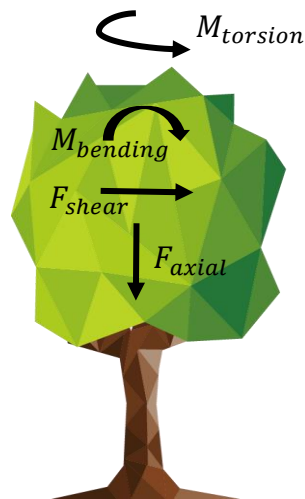
Figure 97. Potential forces that could act on a tree element

Assuming that the cross-section of a tree forms a perfectly circular shape, the corresponding stiffness should be investigated, as formulated in Table 8.1

Table 8. 1 Mechanical properties of a single tree

Mechanical parameter	Expression	Cross-sectional parameters
Axial stiffness (k_{axial})	$\dfrac{E_i \cdot A_{tree}}{L_{tree}}$	$A_{tree} = \pi \cdot r_{tree}^2$
Shear stiffness (k_{shear})	$\dfrac{G_{ij} \cdot A_{s,tree}}{L_{tree}}$	$A_{s,tree} = \dfrac{32}{37} \cdot A_{tree}$
Bending stiffness ($k_{bending}$)	$\dfrac{E_i \cdot I_{tree}}{L_{tree}}$	$I_{tree} = \dfrac{\pi \cdot r_{tree}^4}{4}$
Torsional stiffness ($k_{torsion}$)	$\dfrac{G_{ij} \cdot J_{tree}}{L_{tree}}$	$J_{tree} = \dfrac{\pi \cdot r_{tree}^4}{2}$

In the table, E_i represents the young's modulus of one of the principal fiber directions depending on the direction of the uniaxial load. G_{ij} represents the shear modulus of two of the principal fiber direction depending on the plane in which the shear force is present. The term A_s represents the reduced shear area, which is a calculated reduction of a cross-sectional area. Depending on the geometry of the cross-section, the effective shear area is different. Examples of shear stiffness for various cross-section is shown in table 8.2. For instance, from the table, it can be seen that the reduction factor for the shear area of a circular cross-section is $\dfrac{32}{37}$.

Table 8. 2 Shear stiffness for various cross-sections[52]

Combined with the tree growth model described earlier, it is then possible to investigate how the mechanical properties of a single tree vary with time. For illustration, the development of these cross-sectional properties at D.B.H (diameter of tree on 1.4m elevation) for Ficus Benjamina with respect to its age are illustrated from Figure 98 to Figure 101.
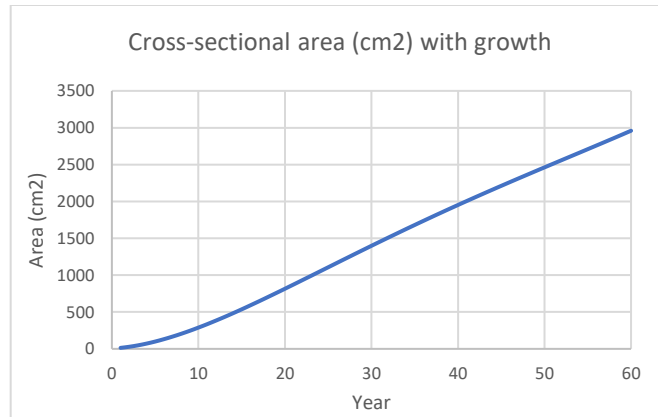
Figure 98. Development of cross-sectional area of Ficus Benjamina based on growth model
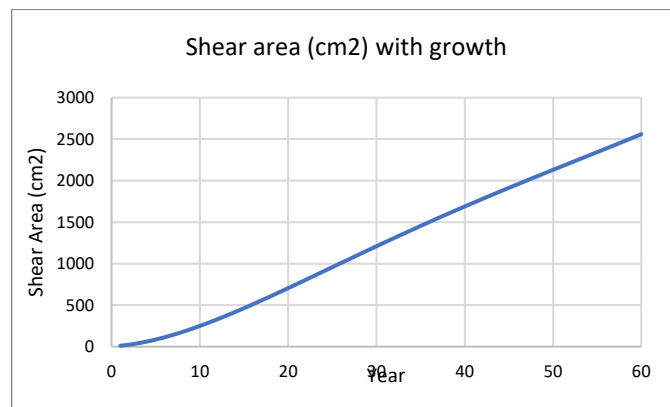
Figure 99. Development of shear area of Ficus Benjamina based on growth model
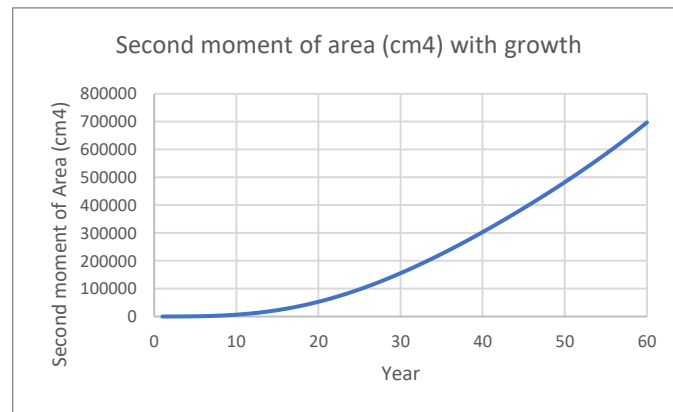
Figure 100. Development of second moment of area of Ficus Benjamina based on growth model
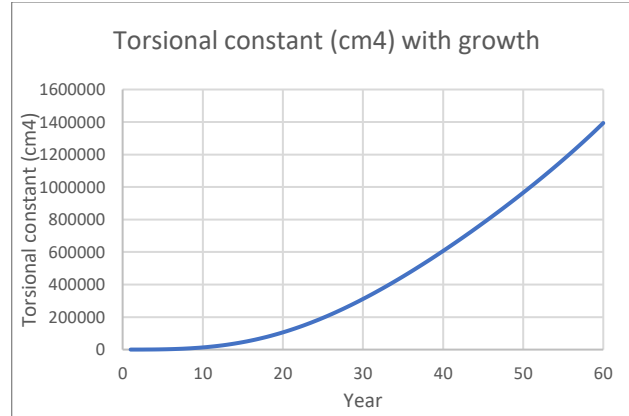
Figure 101. Development of torsional constant of Ficus Benjamina based on growth model

Crosswise connection

Besides the individual trees, the connection as a part of the structural system also plays an important role in the structural behaviour. Therefore, investigation must be made in terms of how growth affects the mechanical properties of the crosswise connection.

Similar to the tree elements, depending on the load sources, when utilized as a load-bearing element, the connection can also be subjected to various forces, including axial force, shear force, bending moment, and torsional moment. Thus, it is of interest to identify the magnitude of corresponding stiffness, which is summarized in Table 8.3.

Table 8. 3 Mechanical properties of elliptical crosswise connection

Mechanical parameter	Expression	Cross-sectional parameters
Axial stiffness (k_{axial})	$\dfrac{E_i \cdot A_{con}}{L_{con}}$	$A_{con} = \pi \cdot a \cdot b$
Shear stiffness (k_{shear})	$\dfrac{G_{ij} \cdot A_{s,con}}{L_{con}}$	$A_{s,con} = \dfrac{1}{\dfrac{1}{6} \cdot \left[6 + \dfrac{2(a^2 + b^2)}{3a^2 + b^2} \right]} \cdot A_{con}$
Bending stiffness $(k_{bending})$	$\dfrac{E_i \cdot I_{major,con}}{L_{con}}$	$I_{major,con} = \dfrac{\pi}{4} \cdot a^3 \cdot b$ $I_{minor} = \dfrac{\pi}{4} \cdot b^3 \cdot a$
Torsional stiffness $(k_{torsion})$	$\dfrac{G_{ij} \cdot J_{con}}{L_{con}}$	$J_{con} = \dfrac{\pi \cdot a^3 \cdot b^3}{a^2 + b^2}$

From the table, the subscript 'con' refers to connection. It is also worth explaining that the expression used to obtain shear area is based on the use of general beam theory proposed by Renton[53], which applies to all regular prismatic systems.

Similarly, the development of crosswise connection's mechanical properties with growth can be computed, shown from Figure 102 to Figure 106.
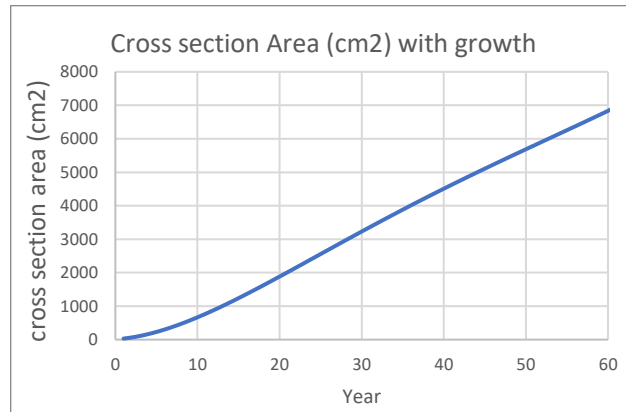
Figure 102. Development of cross-section area of crosswise connection
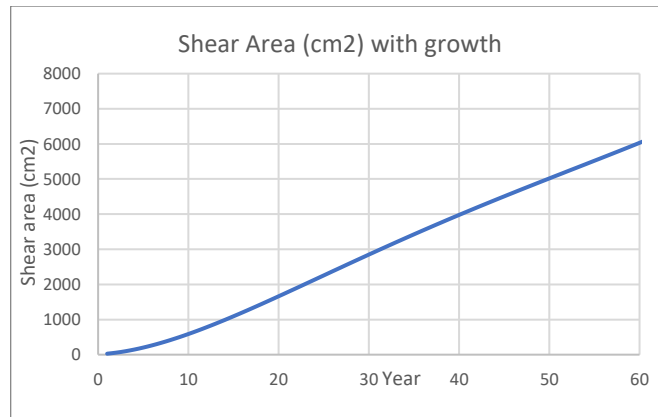
Figure 103. Development of shear area of crosswise connection
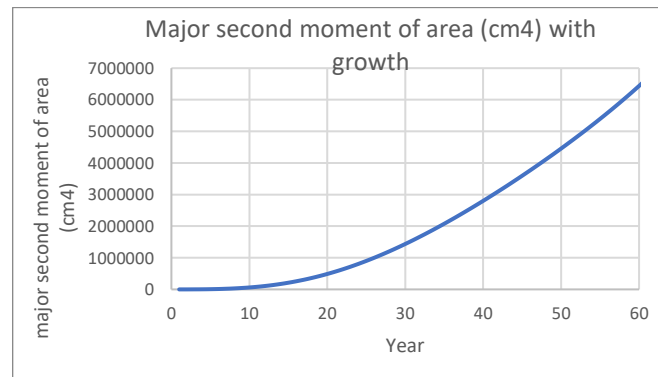
Figure 104. Development of second moment of area about major axis of crosswise connection

89
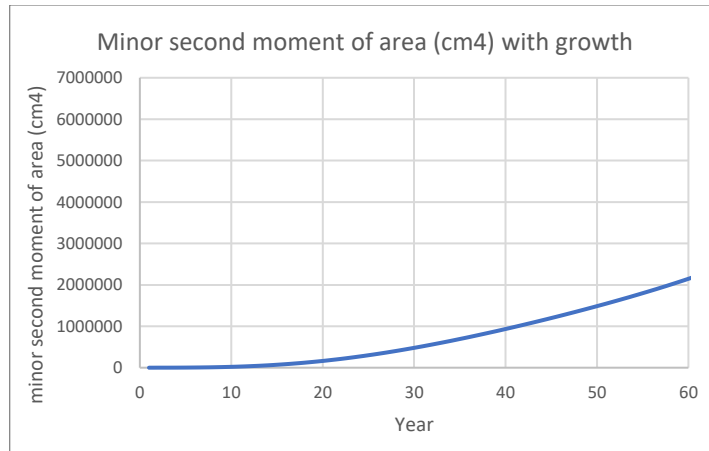
Figure 105. Development of second moment of area about minor axis of crosswise connection
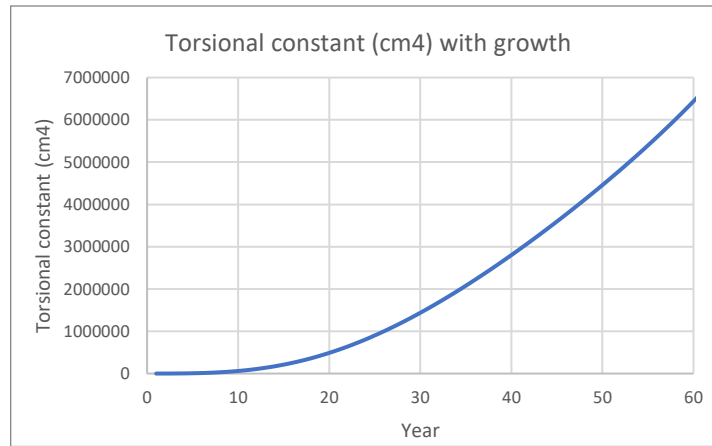
Figure 106. Development of torsional constant of crosswise connection

From section 1.3, it has been discussed that inosculation typically happens if the contact between two trees occurs early on during growth, because thicker barks make it more difficult for the fusion to take place. Therefore, it can be said that crosswise connections possess much higher bending stiffness and torsional stiffness, because the length of the element is much shorter compared to the length of individual trees.

8.4 Material property

Following the assumption made in section 1.1, orthotropic material properties with transverse isotropy are assigned to the trees and the connections. Since the material properties of Ficus Benjamina are not known, a reference wood material of Sitka Spruce is used here, which is the same species used in the experimental design in chapter 5, the finite element modelling approach in chapter 6, and the wireframe modelling approach in chapter 7.

As mentioned in section 7.1, in Karamba 3D, the longitudinal direction of any beam element is recognized as parallel to grain by default. It is suitable for the tree elements in the model, but it would cause an undesired error to the connecting beam element because the longitudinal axis of the connecting beam is no longer parallel to the grain. Therefore, manual adjustment is needed again. Table 8.4 and 8.5 illustrate the linear elastic material properties of tree elements and connecting elements, respectively.

Table 8. 4 Material properties for diagonal trees

Parameter	magnitude
$E_1 = E_L$	8500 Mpa
$E_2 = E_3 = E_R$	663 Mpa
$G_{12} = G_{13} = G_{LT}$	544 Mpa
$G_{32} = G_{RT}$	25.5 Mpa

Table 8. 5 Material properties for crosswise connections

Parameter	magnitude
$E_1 = E_3 = E_R$	663 Mpa
$E_2 = E_L$	8500 Mpa
$G_{12} = G_{32} = G_{LT}$	544 Mpa
$G_{13} = G_{RT}$	25.5Mpa

8.5 Load action

To ensure the safety of the structure, it is necessary to check the strength of each element with code standards under a specific load combination. The following sub-sections are used to define the different load actions and load combinations for the analysis.

8.5.1 Load combination

When analyzing critical structural elements, or solving for the minimum size of the elements, design load factors and load combination must be defined prior to the analysis. The design values of the load effect (Ed) shall be determined by combining all the load actions altogether.

$$\Sigma \gamma_{G,j} G_{k,j} + \gamma_P P + \gamma_{Q,1} \Psi_{0,1} Q_{k,1} + \Sigma \gamma_{Q,i} \Psi_{0,j} Q_{k,i} \qquad (8.8)$$

, where G_k and Q_k are the characteristic value for permanent action and leading variable action, respectively. γ_G and γ_Q are the partial factor for permanent action and variable action, respectively. Ψ_0 is the participation factor applied to variable action depending on the category of the building.

Partial factors vary depending on different limit state designs. For instance, under ultimate limit states, the load actions are magnified by partial factors as it concerns the safety of people and/or the safety of the structure; while for serviceability limit states, the load actions are not magnified by partial factors as it concerns the functioning of the structure or structural member under normal use and the comfort of people. The research focuses on the effect of the chosen structural system on its strength and safety; therefore, the serviceability limit state is neglected in the scope of the research.

According to EN 1990, several criteria are included in the ultimate limit state design. For instance, EQU regards the design check when the loss of static equilibrium of the structure or structural element is concerned; STR regards the design check when failure or excessive deformation of the structure or structural element is concerned; GEO relates to the design when excessive ground deformation is concerned, and finally, FAT relates to the fatigue failure of the structure or structural elements. For the purpose of this research, STR is chosen as the ultimate limit state design guide.

Ultimate limit state design is also dependent on the consequence class of the structure. Considering that the tower serves as a public space for people to gather, the consequence class is defined as CC3. According to Eq.6.10 from Table A1.2 in EN 1991, with the precondition defined above, the load factors to be considered during the analysis are listed in Table 8.6:

Table 8. 6 ULS Load combination based on STR criteria

Load factor	Magnitude
$\gamma_{G,j}$	1.35 for when permanent action is unfavourable
	0.9 for when permanent action is favourable
$\gamma_{Q,1}$	1.5
Ψ_0	0.7 for imposed load in buildings
	0.6 for wind loads on buildings

Therefore, the load combination to be considered is:

$$1.35 \cdot (G_{permanent}) + (1.5) \cdot (0.7) \cdot Q_{live\ load} + (1.5) \cdot (0.6) \cdot Q_{wind} \qquad (8.9)$$

8.5.2 Self weight of trees

The weight of the trees increases during growth, and the magnitude of the weight is correlated with the urban tree growth model described in section 2.2. However, from the USDA database, the weight is presented as the dry weight for the trees, while in reality, water occupies a major portion of the total tree weight. As a conservative assumption, half of the tree weight will be occupied by the weight of the water[54].

It is also important to note that, due to the tapering shape of the tree, the magnitude of load distribution of different segments along the height is different. Therefore, it is essential to assign the correct weight to the corresponding elements when assembling the model. In the model, for the parts of the tree elements that are already incorporated in the diagrid scheme, the self weight will be assigned as distributed loads along its member; while for the crown that is growing on top of the structure, the weight will be applied as a point load.

With the density of the tree being uniform along its entire height, the distribution of self weight of each segment is calculated based on its percentage of volume to the entire tree. For the elements incorporated in the diagrid scheme, they are treated as truncated cones, shown in Figure 107(a), with D_i as the diameter of the thicker end, D_{i+1} as the diameter of the thinner end, and L_i as the length of the segment, whereas the cantilevered crown is treated as a regular cone, shown in Figure 107(b).
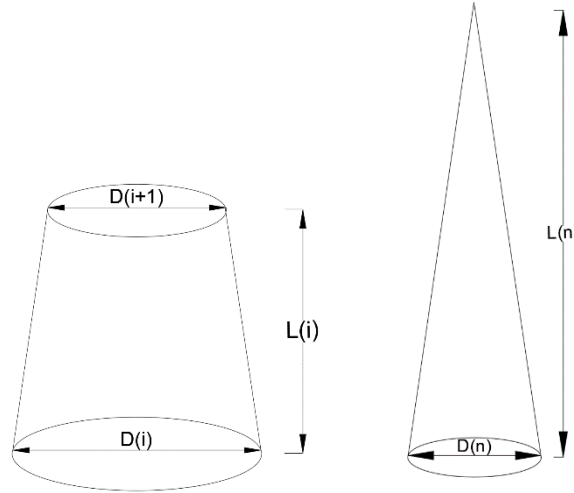
Figure 107. (a) truncated cone shape assigned to trees that are a part of the diagrid structure (b) cone shape assigned to cantilevered crown

The volume of a truncated cone is calculated as:

$$V = \frac{1}{3}\pi \left[\left(\frac{D_i}{2}\right)^2 + \left(\frac{D_i}{2} \cdot \frac{D_{i+1}}{2}\right) + \left(\frac{D_{i+1}}{2}\right)^2 \right] \cdot L_i \qquad (8.10)$$

The volume of a regular cone is calculated as:

$$V = \frac{1}{3}\pi \cdot \left(\frac{D_n}{2}\right)^2 \cdot L_n \qquad (8.11)$$

For illustration, the procedure in determining the self-weight distribution along diagonals for the tree tower having grown for 30 years is illustrated in Appendix 10.4.

8.5.3 Imposed lived load

After the trees have grown to a sufficient strength, the tower will be used as a public gathering facility. Therefore, according to Eurocode 1991-1, the imposed live load will be listed as category C3: congregation area without obstacles for moving people. Thus, the live load on the deck is $4\ KN/m^2$.

With the live load and floor plan defined in section 8.2.1, and the assumption that the total live load is equally shared by the perimeter beams, it is possible to determine the minimum dimension for the perimeter beams. With the calculation procedures illustrated in Appendix 10.5, it is decided that IPE-80 is a sufficient size for the perimeter beams.

8.5.4 Wind load

Taking Baubotanik Tower as an example, as the plants grow and as the weather alters throughout the year, there will be times that the façade of the structure be fully covered by tree crowns, especially in spring and summer time. According to the analysis made in section 8.2.3, during the 'construction' of the tower, wind is an important load source which would generate bending moment to the elements below them.

Figure 108. Crown coverage of Baubotaink Tower[6]

To increase the safety margin and for simplicity, the porous areas in the tree crown will be neglected, and the structure will be treated as a cylinder in wind analysis.

Eurocode 1991-1-4 NB provides tabulated data of wind pressure with corresponding height; however, it is decided to incorporate the wind pressure calculation procedure provided in the standard into the parametric script. As described in section 2.2, the tree height varies year by year according to the growth model provided by USDA. Therefore, by substituting the corresponding height to the calculation procedure provided by the standard, a more accurate wind

pressure can be obtained. The calculation procedures of wind load effect on circular cylinder elements according to EN 1991-1-4:2005+A1:2010 Section 7.9.2 is illustrated in Appendix 10.6

8.6 Results

With the analysis carried out with the structural model defined in the previous sections, this section is dedicated to show how the objectives set in the beginning of the chapter are met. Investigation is conducted in terms of how the chosen structural scheme has achieved the objective in minimizing the torsional effect at the connection.

As discussed in chapter 3, undesired errors can be resulted from wrongly assuming that the connections have rigid rotational stiffness. Therefore, in this section, further analysis is conducted to investigate how the torsional stiffness of the crosswise connection would affect the structural behaviour of the tree tower.

Lastly, structural verification is conducted with strength unity check. With such analysis procedures, designers can predict in terms of when the growing trees and tree connections will be strong enough to support all the loads from the structure.

8.6.1 Minimizing torsion at the connection

It has been discussed in chapter 4 that due to the nature of the crosswise connection, torsion is an inevitable stress state. It is worth mentioning again that the objective of the design case study is to incorporate the diagrid structural scheme so that, by minimizing the bending moment of the diagonals, the torsional effect in the connection could be subsequently minimized. The results shown in this section aims to illustrate the effect of the chosen diagrid structural scheme in minimizing torsion at the connections.

As the structure grows, Figure 110 to 112 illustrate the bending moment in the diagonals of a specific location shown in Figure 109. With the building configuration, there are six connections at each elevation (3m, 6m, and 9m). For the same elevation, the location with the greatest bending moment is selected for analysis.
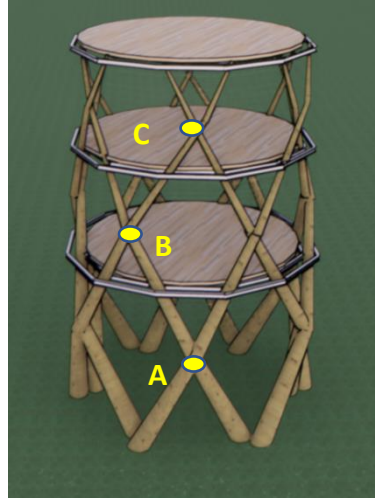
Figure 109. Points of interest for diagonals for analysis
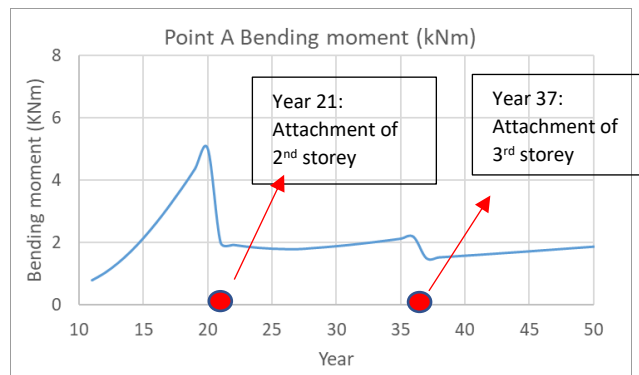
Figure 110. Development of bending moment at Point A
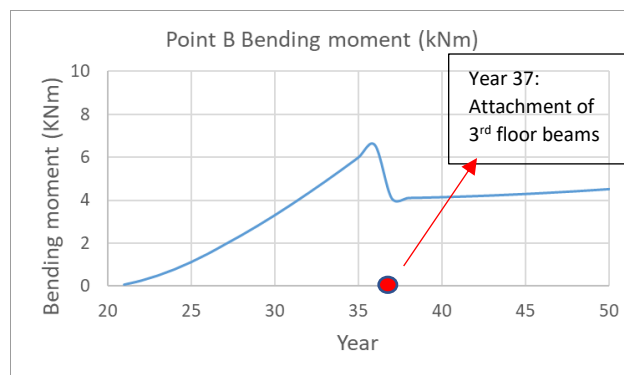
Figure 111. Bending moment of Element 2 at Point B
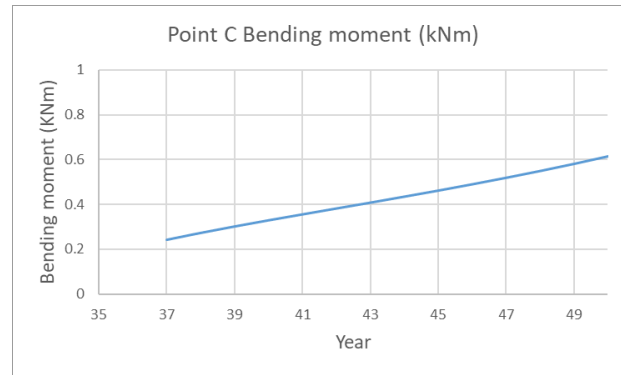
Figure 112. Bending moment of Element 3 at Point E

From the figures above, it can be discovered that, whenever the trees have grown to the next storey height, and are connected with the floor beams (2nd floor in year 21, and 3rd floor in year 37), there is a noticeable reduction in terms of the bending moment along the diagonals.

For instance, for the first connection at 3-meter, the bending moment occurred at Point A keeps increasing from Year 11 until Year 21. At Year 21, the bending moment at Point A then decreases from 5 kNm to 2 kNm, at about 60%. Then it stays almost constant from Year 21 until Year 37, when another reduction of bending moment occurs, from 2.189 kNm to 1.507kNm, at about 31%.

Similar behaviours are found for the second connection at 6-meter, where the bending moment at Point B increases from Year 21 until Year 37. At Year 37, the bending moment at Point B reduced from 6.57 kNm to 4.1 kNm, at about 37.6%. The bending moment at that location stays almost constant after that.

Having proved that the bending moment along the diagonals is reduced by incorporating diagrid structural system, investigation is conducted in terms of how the torsion at the connection is reduced as the result of the reduction in bending moment.

Torsion at the connection is reflected by the torsional moment in the link element that connects the neighboring tree elements. Again, out of the six link elements at the same elevation, the one with the greatest torsion is presented from Figure 113 to 115.
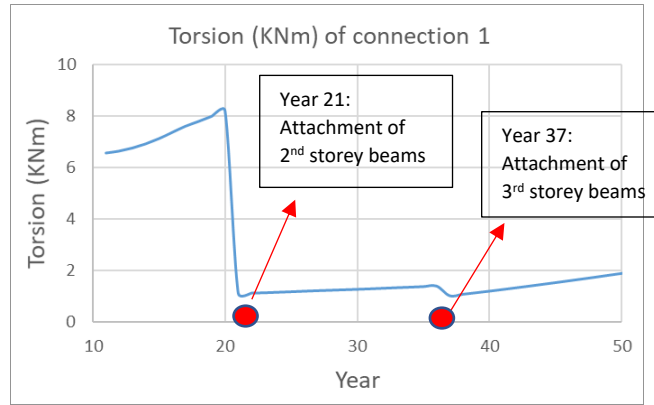
Figure 113. Torsion at the first connection on 3-meter elevation
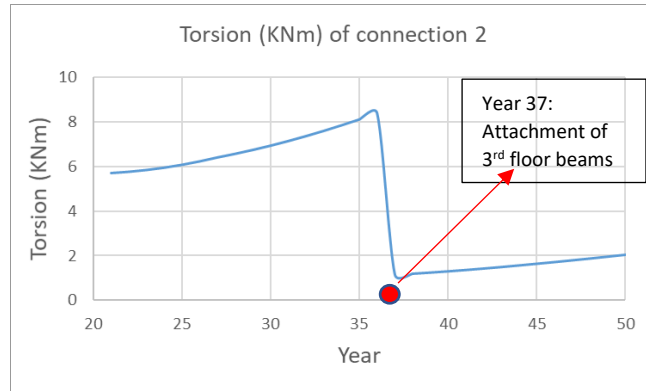
Figure 114. Torsion at the third connection on 6-meter elevation
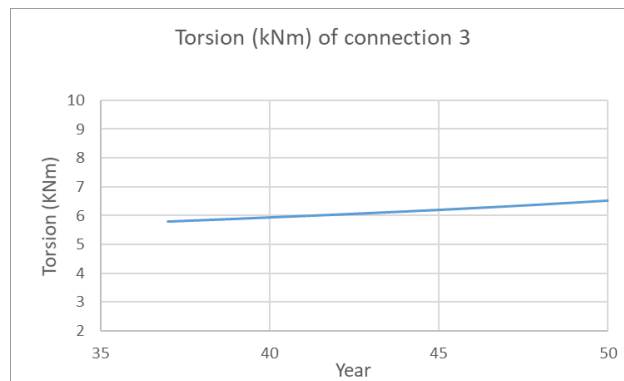
Figure 115. Torsion at the first connection at 9-meter elevation

From these Figures, it can be discovered that, torsion at the connection experiences a sudden reduction whenever the trees have grown to the next storey height, where new floor beams are attached: For the first connection at 3-meter, torsion keeps increasing from Year 11 tunil Year 21, when a reduction occurs from 8.19 kNm to 1.12 kNm, at about 86.3%, then it keeps increasing until Year 37, when a reduction occurs from 1.4 kNm to 1.02 kNm, at about 27.1%. Similar behaviours occur at the second connection, where the torsion keeps increasing from Year 21 until Year 37, where a reduction occurs from 8.38 kNm to 1.25 kNm, at about 85.1 %. It can be observed that the development of torsion in the connection exhibit similar behaviours with the bending moment at the same location.

Detailed discussion for such behaviours can be found in Section 8.7.

8.6.2 Effect of torsional stiffness on the structural behaviour

As mentioned in section 3.1, accurately determining the rotational stiffness of moment-resisting connections in a structure is essential, as it affects both the strength and serviceability of structures[33]. To investigate the effect of torsional stiffness on the structural behaviours of the tree tower, a comparison is made by assuming that the connection is fully rigid in resisting torsional moment; this is done by assigning a relatively high dummy rotational stiffness to the connecting element. After running the model with the assumed dummy stiffness, the results obtained are shown in Figure 116.
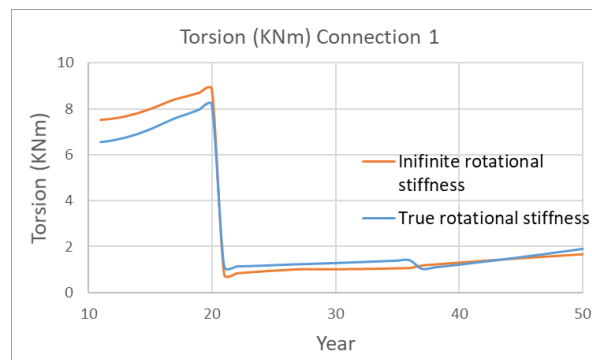
Figure 116. Comparison of Torsion at the first connection at 3-meter elevation, with semi-rigid spring element and rigid spring element

Numerically speaking, looking at the peak torsion, which occurs in Year 20, it is discovered that the torsional moment at the connection is 8.18 kNm when incorporating the actual rotational stiffness; however, when assuming a stiff rotational stiffness, the torsional moment is overestimated to 8.86 kNm, at about 8.3 percent. Although the overestimation is not that much, it is also discovered that the degree of overestimation is related to the length of eccentricity between the tree elements. To investigate such behaviour, analysis is conducted by varying the eccentricity from 10mm to 100mm at an increment of 10mm. The result is shown in Figure 117.
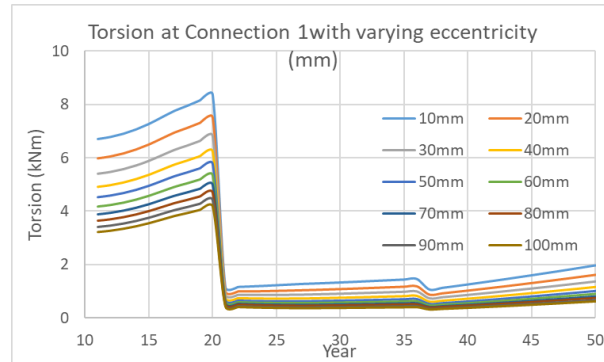
Figure 117. Development of torsional moment at Point A with various eccentricity modelled for the connection

From the figure, it can be observed that, for the connection with eccentricity of 100 millimetres, the peak torsion in Year 20 is 4.18 kNm. Therefore, by wrongly assuming that the rotational stiffness is infinite, the overestimation is as much as 112%.

Detailed discussion for such behaviours can be found in Section 8.7.

8.6.3 Ultimate limit state (STR) check

Having investigated the benefit of applying such structural scheme to the tree tower, the next step is to perform the unity check on the structural elements with the governing load combination to make sure that the load resistance is greater than the load effect. It has been mentioned earlier in section 8.5.1 that STR is followed as the ultimate limit design check for the structure and structural elements. Under STR guideline, the design should satisfy the following criteria:

$$E_d \leq R_d$$

, where E_d is the load action on the structural elements, while R_d is the resistance of the material.

Since the target of interest involves both the tree diagonals and the tree connections, it is essential to differentiate the different stresses that could occur on those elements, and the corresponding strength properties need to be checked.

For the diagonal tree elements, the strength criteria needed to be checked include axial stress, bending stress, and torsional shear stress. The need for checking the torsional shear stress has been discussed in chapter 7: when incorporated with crosswise connections in a structure, torsional moment in the trees' own longitudinal axis occurs.

Normal shear stress is neglected because it refers to the shear perpendicular to the grain. As explained in section 1.1.2.2, due to the orientation of wood fiber, it is very difficult for wood to fail in shear perpendicular to grain before another failure mode occurs. The stresses and strength criteria for tree diagonals are summarized in table 8.7.

Table 8. 7 Load actions to be checked for diagonal tree elements

Tree diagonals	Load effect	Resistance	Criteria
Axial stress	$\sigma_{c,0,d} = \dfrac{N}{A}$	$f_{c,0,d} = \dfrac{f_{c/t,0,k} k_{\text{mod}}}{\gamma_M}$	$f_{c,0,d} \geq \sigma_{c,0,d}$
Bending stress	$\sigma_{m,d} = \dfrac{M}{W}$	$f_{m,0,d} = \dfrac{f_{m,0,k} k_{mod}}{\gamma_M} k_h$	$f_{m,0,d} \geq \sigma_{m,d}$
Bending + axial	$\sigma_{c,0,d} = \dfrac{N}{A}, \sigma_{m,d} = \dfrac{M}{W}$	$\left(\dfrac{\sigma_{c,0,d}}{f_{c,0,d}}\right)^2 + \dfrac{\sigma_{m,d}}{f_{m,d}}$	$\left(\dfrac{\sigma_{c,0,d}}{f_{c,0,d}}\right)^2 + \dfrac{\sigma_{m,d}}{f_{m,d}} \leq 1$
Torsional shear stress	$\sigma_{v,d,\text{torsion}} = \dfrac{Tr}{J}$	$f_{v,torsion} = \dfrac{f_{v,k} k_{mod}}{\gamma_M}$	$f_{v,d} \geq \sigma_{v,d,torsion}$

, where

$f_{c,0,d}$ is the design compressive strength of wood parallel to the grain

$f_{m,0,d}$ is the design bending strength of wood

$f_{v,torsion}$ is the torsional shear strength of wood

k_{mod} is the modification factor for service class and load duration. $k_{mod} = 0.7$ for solid timber in service class 3 under short term loading.

γ_M = material safety factor. $\gamma_M = 1.3$ for solid timber

$k_h = depth\ factor = 1$

For the connection element, two strength properties need to be checked: axial stress and torsional shear stress. The check for bending and shear is neglected because it is important to note that, although modelled as a separate element, the connection is a part of the tree diagonals. Therefore, as an element to transfer forces, there is no need to check bending and shear, as they are already checked in the diagonal tree elements.

It is essential to perform the check on the axial stress of the connection because, due to the orientation of wood fiber, the axial force acts perpendicular to the grain, which is the weakest strength property of wood.

As explained in chapter 4, torsion of the connecting element is resisted by the rolling shear modulus and strength, which is also one of the weakest properties of wood. Therefore, it is also essential to perform such check so that the strength of the connection can be ensured. As discussed in section 1.1.2.2, suggested by Eurocode 5[22], rolling shear strength is approximately equal to twice the tensile strength perpendicular to the grain.

The stresses and strength criteria for tree connections are summarized in table 8.8.

Table 8. 8 Load actions to be checked for crosswise connection

Crosswise connection	Load effect	Resistance	Criteria
Axial stress	$\sigma_{c/t,90,d} = \dfrac{N}{A}$	$f_{c/t,90,d} = \dfrac{f_{c/t,90,k} k_{mod}}{\gamma_M}$	$f_{c/t,0,d} \geq \sigma_{c/t,90,d}$
Torsional shear stress	$\sigma_{v,d,torsion} = \dfrac{2 \cdot T}{A \cdot b}$	$f_{v,rolling} = 2 \cdot f_{t,90,d}$	$f_{v,rolling} \geq \sigma_{v,d,torsion}$

,where

$f_{c/t,90,d}$ is the design compressive/tensile strength perpendicular to the grain.

$f_{v,rolling}$ is the design rolling shear strength of wood.

The strength characteristics are taken as Sitka Spruce from Wood Handbook[20], illustrated in Table 8.9. It is essential to note that, from the publication, strength properties of wood are given in 2 different moisture content. 12% of moisture content refers to most engineering-timber elements, while 'green' refers to the wood that is fully saturated with water. Therefore, since the wood under analysis is a living organism, the latter is the obvious choice.

Table 8. 9 Strength properties of Spruce Sitka

MoR (MPa)	$f_{c,0}$ (MPa)	$f_{c,90}$ (MPa)	$f_{v,0}$ (MPa)	$f_{t,90}$ (MPa)	$f_{v,torsion}$ (MPa)	$f_{v,rolling}$ (MPa)
39	18.4	1.9	5.2	1.7	5.2	5.2*0.18=0.936

Diagonal tree elements

Based on the geometric definition of the growing tree tower, each tree is segmented into four diagonals (element 1 to element 4 shown in Figure 118), which will be the target for the unity check. It is to be noted that each diagonal is further segmented into 64 shorter segments, as suggested in section 8.3.1. All segments are analyzed for the unity check, and the most critical segment is presented for discussion in the following sections.
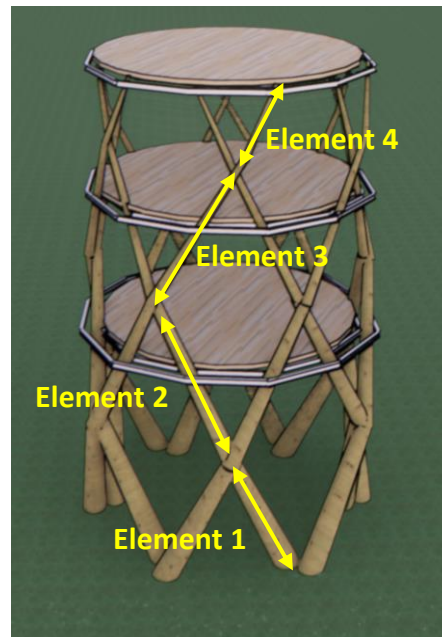
Figure 118. Numbering of elements for analysis

Bending stress vs. Bending strength

Unity check for diagonal tree elements in bending is done by checking the bending stress vs. the bending strength. The unity check criteria need to be fulfilled is:

$$\frac{f_{m,0,d}}{\sigma_{m,d}} < 1$$

Bending stress can be calculated with the following expression:

$$\sigma_{m,d} = \frac{M}{W}$$

, with W as the first moment of area of the tree elements. Being a circular element, W can be calculated as:

$$W = \frac{\pi d^3}{32}$$

, and the bending strength of wood, based on the formula provided in Table 8.9, is

$$f_{m,0,d} = \frac{f_{m,0,k} k_{mod}}{\gamma_M} k_h = \frac{39 \cdot 0.7}{1.3} = 21 \ Mpa$$

With the increasing size of cross-section due to tree growth and the varying bending moment action along the structural element, unity check is tracked for all elements during the 50 years period, which is 13 years after the tree tower is considered to be completed. The results are collected and illustrated in Appendix 10.7.1.

Axial stress vs. axial strength

Since all diagonal elements are subjected to compressive stress, unity check for tree elements in axial stress is done by checking the axial stress vs. compressive strength. The unity check criteria need to be fulfilled is:

$$\frac{\sigma_{c,0,d}}{f_{c,0,d}} < 1$$

For a circular element subjected to axial force, the axial stress equals to:

$$\sigma_{c,0,d} = \frac{N}{A}$$

, and the bending strength of wood, based on the formula provided in Table 8.9, is

$$f_{c,0,d} = \frac{f_{c,0,k} k_{mod}}{\gamma_M} = \frac{18.4 \cdot 0.7}{1.3} = 9.91 \ Mpa$$

The results are collected and illustrated in Appendix 10.7.2.

Torsional shear stress vs. shear strength

Unity check for tree elements subjected to torsion around its own longitudinal axis is done by checking the following unity criteria:

$$\frac{\sigma_{v,d,torsion}}{f_{v,d,torsion}} < 1$$

For a circular element subjected to torsional moment, the shear stress equals to:

$$\sigma_{v,d,torsion} = \frac{Tr}{J}$$

, with J as the torsional constant. Being a circular element, J can be calculated as:

$$J = \frac{\pi d^4}{32}$$

As discussed earlier, the torsional strength of wood about its longitudinal axis can be approximated as the shear strength parallel to the grain. Therefore, the torsional shear strength equals to

$$f_{v,d,torsion} = \frac{f_{v,0} \cdot k_{mod}}{\gamma_M} = \frac{5.2 \cdot 0.7}{1.3} = 2.8 \; Mpa$$

The results are collected and illustrated in Appendix 10.7.3.

Combination of axial and bending action

Unity check for tree elements in the combination of axial and bending action is done by checking the following unity criteria:

$$\left(\frac{\sigma_{c,0,d}}{f_{c,0,d}}\right)^2 + \frac{\sigma_{m,d}}{f_{m,d}} \leq 1$$

The results are collected and illustrated in Appendix 10.7.4.

Crosswise connection

For the crosswise connection, as described earlier, the unity check to be conducted include axial stress and torsional shear stress. All six connections on each elevation (3m, 6m, 9m), shown in Figure 119 are analyzed for the unity check, and the most critical one is presented for discussion in the following sections.
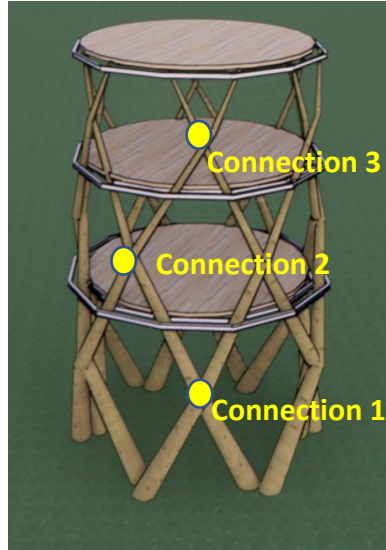
Figure 119. Numbering of crosswise connection

Torsional shear stress vs. rolling shear strength

As discussed earlier, due to the orientation of wood fiber, the torsion around the connection's longitudinal axis is resisted by the rolling shear modulus and strength. Therefore, unity check for connection elements subjected to torsional moment is done by checking the following unity criteria:

$$\frac{\sigma_{v,d,torsion}}{f_{v,d,rolling}} < 1$$

For an elliptical element subjected to torsional moment, the maximum shear stress occurs at the two ends of minor radius, which equals to:

$$\sigma_{v,d,torsion} = \frac{2 \cdot T}{A \cdot b}$$

, with A and b as the area and the minor radius of the ellipse, respectively.

As discussed earlier, the rolling shear strength can be approximated as twice the tensile strength perpendicular to the grain. Therefore, the torsional shear strength equals to

$$f_{v,d,torsion} = \frac{2 \cdot f_{t,90} \cdot k_{\text{mod}}}{\gamma_M} = \frac{2 \cdot 1.7 \cdot 0.7}{1.3} = 1.83 \; Mpa$$

The results are collected and illustrated in Appendix 10.7.5.

Axial stress vs axial strength

When the connection elements are subjected to axial force, depending on the direction of the forces, either tensile force perpendicular to grain or compression force perpendicular to the grain is subjected to the connection. Therefore, unity check for connection elements subjected to axial force is done by checking the following unity criteria:

$$\frac{\sigma_{c,90,d}}{f_{c,90,d}} < 1 \; or \; \frac{\sigma_{t,90,d}}{f_{t,90,d}} < 1$$

, and the axial strength of wood, based on the formula provided in table 8.8, is

$$f_{c,90,d} = \frac{f_{c,90,k} \cdot k_{\text{mod}}}{\gamma_M} = \frac{1.9 \cdot 0.7}{1.3} = 1.02 \; Mpa$$

$$f_{t,90,d} = \frac{f_{t,90,k} \cdot k_{\text{mod}}}{\gamma_M} = \frac{1.7 \cdot 0.7}{1.3} = 0.92 \; Mpa$$

The results are collected and illustrated in Appendix 10.7.6.

8.7 Discussion

In this section, discussion is made based on each section from section 8.6.

On minimizing torsion in the crosswise connection

Discussion is first made regarding the results obtained from section 8.6.1. From the results, the reduction of bending moment at Point A can be explained in the following context: From Year 11 to Year 21, the bending moment along the diagonal elements is caused by wind load on the cantilevered trees growing above the first floor's floor beams, as illustrated in Figure 120(a), which increases with the growing tree height. When the growing trees reach the second storey at 7.5m, which happens in Year 21, the horizontal wind load on the first floor is then transferred to the trees with axial action, thus leading to the reduction of bending moment. From Year 22 onwards, the bending moment at Point A stays almost constant because the wind does not have a large impact on it anymore.

Similarly, for Point B, from Year 22 to Year 36, the increase in bending moment is caused by wind load on the cantilevered trees growing above the second floor's floor beams, as illustrated in Figure 120(b). When the growing trees reach the second storey at 10.5m, which happens in Year 37, the horizontal wind load on the second floor is then transferred to the trees with axial action, thus leading to the reduction of bending moment. From Year 37 onwards, the bending moment at Point B stays almost constant.

Finally, when the trees have grown to their designed height at 10.5m, the diagrid is completed, where all horizontal wind load is transferred to the diagonals with axial actions, shown in Figure 120(c).
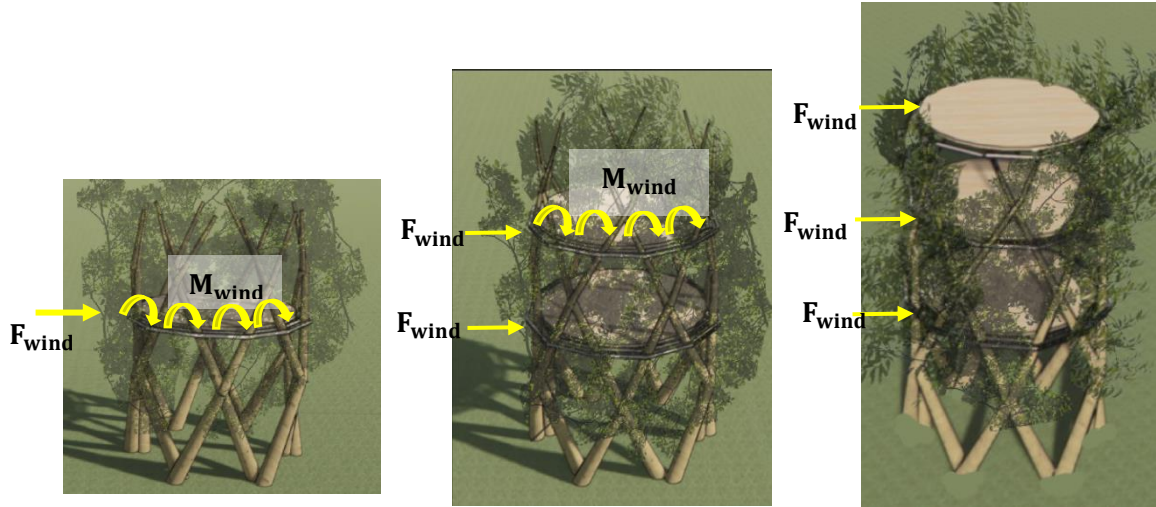
Figure 120. (a) Wind load scheme from Year 11 to 21 (b) Wind load scheme from Year 22 to 37 (c) Wind load scheme for the completed structure

The axial action mentioned above contributed by the diagrid system can be verified by the sudden increase of axial forces in the diagonal elements at the same locations, shown in Figure 122 and 123. It can be discovered from these figures that the axial force in element 1 increases from 25.1 kN in Year 20 to 44.1 kN in Year 21, at about 75.7%, the sudden increase occurs again from 57.8 kN in Year 36 to 75.8 kN in Year 37, at about 31.1%. Similarly, for element 2, the sudden increase in axial force occurs from 30.3 kN in Year 36 to 49.3 kN in Year 37, at about 62.7%.
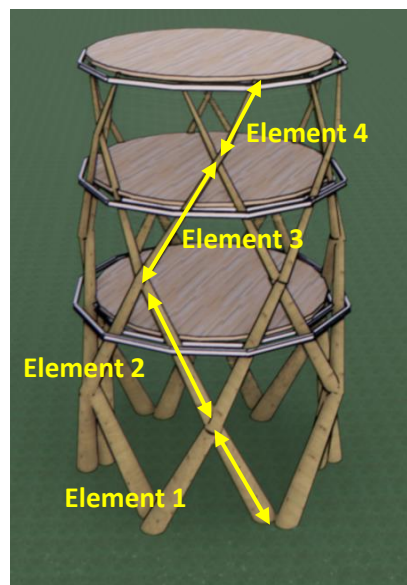
Figure 121. Element label for the tree diagonals
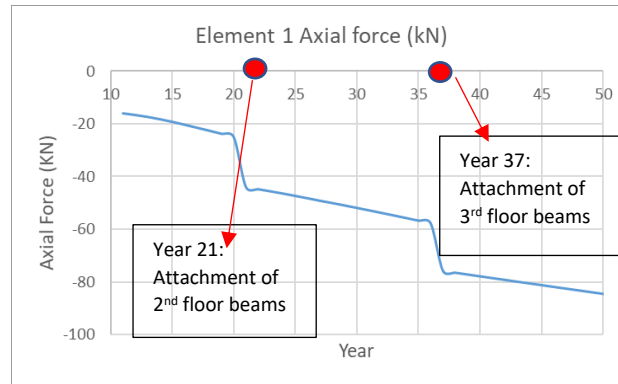
Figure 122. Axial force in Element 1
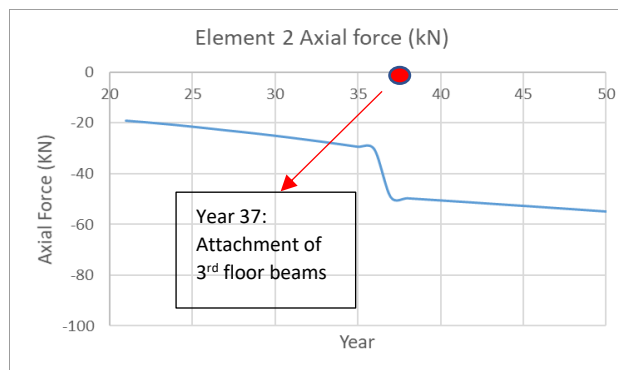
Figure 123. Axial force in Element 2

Therefore, it can be concluded that, by reducing the bending moment at the end of the diagonal elements with the diagrid structural scheme, torsion at the connection can also be effectively reduced.

On the effect of accurately modelling the torsional stiffness of crosswise connection

Next, discussion is made regarding the results obtained from section 8.6.2. It has been discovered that longer eccentricity would result in smaller torsional moment in the connection. Such behaviours can be referred to the discussion made in section 7.3, that the length of the eccentricity directly influences the torsional stiffness of the connection because of the term:

$$\frac{G_{RT} \cdot J}{L}$$

, where L represents the length of eccentricity. And it can be seen that, by increasing the eccentricity, the magnitude of the torsional stiffness decreases, therefore, it would attract less torsion in the connection.

On the Unity check on structural elements

From the figures provided from Appendix 10.7.1 to 10.7.6, it can be observed that, for the unity check of bending stress in the diagonals and the torsional stress in the crosswise connection, the magnitude experiences a reduction in the year when a new storey is completed. Such behaviour is similar to the results shown in section 8.6.1 in terms of the development of torsion in the connections, and the development of bending moment in the diagonals.

In terms of the strength of the structure, it can be observed that the most governing stress state is bending stress. From Appendix 10.7.1, it can be discovered that in Year 37 and 38, the top diagonal elements are not ready to take on that much bending stress, probably owing to the thinner stems and strong wind on higher altitude. However, it shows that in Year 39, the entire structure is ready for service, which is two years behind the initial planning, according to the growth model shown in section 8.2.2.

8.8 Parametric modelling of growing tree tower

With different demands and wishes from various parties involved in a building project, the building configuration could be subjected to changes. Since the readiness and strength of the structure built with growing trees and tree connections depend on time, to provide better insights to designers with more possibilities in the future, a parametric exploration is provided. The results will give designers an idea of how long it takes for the structure to acquire sufficient strength with the different building configurations. With the structural scheme proposed, several variables can be treated as parameters that could be modified, such as the floor radius of the tower, floor height, and the number of trees planted.

To conduct such analysis, only one out of the three parameters will be subjected to changes, while the other two will remain constant. Similar to the analysis made in the sections above, the structure is deemed to be completed when the following criteria are fulfilled:

- The structure is deemed to be completed when it reaches the third storey
- It takes two years for the perimeter beams to fuse with diagonal tree elements completely.
- Unity check of diagonal trees and crosswise connections are check following the procedures defined in section 8.6.3.

8.8.1 Number of trees planted

Investigation is made in terms of how the completion time of the structure is affected by the number of trees planted at the base. The analysis is performed on the tower built by 8, 10, 12, 14, and 16 trees, as shown in Figure 124. The other two parameters are fixed, which means that the floor height remains at three meters, and the floor radius remains at three meters.
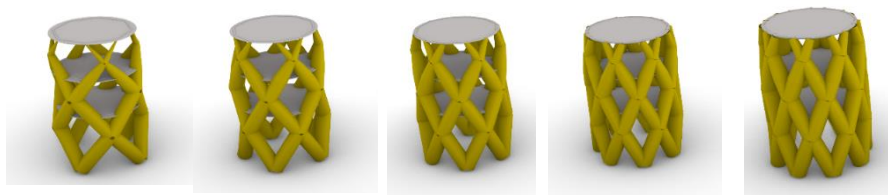
Figure 124. Diagrid tree tower with the number of trees as the parametric variable

Table 8.10 illustrates the results obtained from the parametric model. From the charts, yellow columns illustrate the time of completion by only considering the growth model of the tree species, and the assumption that the perimeter beam will be fully incorporated with the diagonal trees in two years. Green columns illustrate the delay of construction by considering the unity check of both diagonal trees and tree connections, the numbers in the green columns indicate the number of years that are delayed due to insufficient strength, and the terms inside the brackets indicate the strength property that governs the delay.

Table 8. 10 The year of completion for each storey based on the growth model and unity check

Trees planted	Completion Year based on the growth model			Years delay based on strength unity check		
	1st floor	2nd floor	3rd floor	1st floor	2nd floor	3rd floor
8	13	25	48	+3 (connection torsion)	+2 (tree bending)	+4 (tree bending)
10	12	23	41	/	/	+2 (tree bending)
12	11	21	37	/	/	+2 (Tree Bending)
14	11	20	35	/	/	+1 (Tree Bending)
16	10	20	34	/	/	+1 (Tree Bending + axial)

From the table, it can be observed that when more trees are planted at the base of the tower, the construction of the structure speeds up; this is because the inclination of trees decreases, which gives the trees a more 'straight' form, and the trees would reach the next storey sooner.

It can be seen from the results that, when the tower is constructed by 8 trees, the construction of first storey is delayed for three years due to insufficient torsional strength of crosswise connections. This is because when less trees are planted, each tree would share a larger portion of the wind load, which leads to the increase of bending moment along the tree diagonals, which then leads to larger torsion in the connections. Additionally, when less trees are planted,

the inclination of tree diagonals becomes larger, which means that the self weight of the trees causes more bending at the connection instead of axial force along the trees.

Similar to the results obtained from section 8.6.3, due to smaller cross-section and higher wind load at the top, the strength of the top storey is governed by bending on the highest diagonal trees on the third floor. It can also be observed that, with more trees planted, the completion of the structure based on strength unity check is much closer to the completion of structure based on tree growth model. This is because, with more trees planted, each diagonal tree and tree connection would be subjected to a smaller share of wind loads.

8.8.2 Storey height

Investigation is made in terms of how the completion time of the structure is affected by the storey height. The analysis is performed on the tower having storey height of 3m, 3.5m, and 4m, as shown in Figure 125. The other two parameters are fixed, which means that 12 trees are planted at the base, and the floor radius remains at three meters.


Figure 125. Diagrid tree tower with storey height as the parametric variable

Table 8.11 illustrates the results obtained from the parametric model. It can be understood intuitively that higher storey height would result in a slower completion time of the structure, and similar to the results obtained previously, the strength is governed again by the tallest diagonal trees at the top due to higher wind loads.

Table 8. 11 The year of completion for each storey based on the growth model and unity check

Storey height (m)	Completion Year based on the growth model			Years delay based on strength unity check		
	1st floor	2nd floor	3rd floor	1st floor	2nd floor	3rd floor
3	11	21	37	/	/	+2 (Tree Bending)
3.5	13	26	50	/	/	+2 (Tree Bending + axial)
4	15	31	66	/	+1 (Tree Bending + axial)	+2 (Tree Bending + axial)

8.8.3 Floor radius

Finally, investigation is made in terms of how the completion time of the structure is affected by the floor radius. The analysis is performed to the tower having floor radius of 3m, 4m, 5m, and 6m, as shown in Figure 126. The other two parameters are fixed, which means that 12 trees are planted at the base, and the storey height remains at three meters.
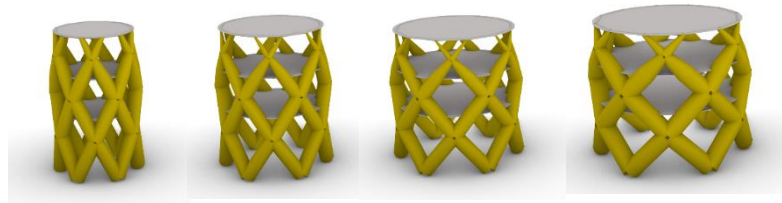
Figure 126. Diagrid tree tower with floor radius as the parametric variable

Table 8.12 illustrates the results obtained from the parametric model. It can be observed that a larger radius leads to a slower completion of the structure, which is intuitive, as it would take longer for a more inclined tree to reach to the next storey height. It is also discovered that, with larger floor radius, the completion of the first storey is highly delayed due to the insufficient torsional shear strength of the crosswise connection under torsion, which can be explained with the following reasons:

- A higher radius leads to a more significant live load onto the trees beneath the perimeter floor beams, which causes greater torsional effect on the connections.

- With more inclined tree diagonals, the self weight will result in more bending action at the connection, which further exacerbates the torsional effect at the connection.
- A larger building attracts greater wind loads, which further exacerbates the torsional effect at the connection

Once again, similar to the results obtained from section 8.6.3, the strength of the structure is governed by the highest diagonal trees under bending, due to its smaller cross-section and higher wind load at the top.

Table 8. 12 The year of completion for each storey based on the growth model and unity check

Floor radius (m)	Completion Year based on the growth model			Years delay based on strength unity check		
	1st floor	2nd floor	3rd floor	1st floor	2nd floor	3rd floor
3	11	21	37	/	/	+2 (Tree Bending)
4	12	24	44	+4 (connection torsion)	+1 (Tree Bending)	+4 (Tree Bending)
5	13	27	54	+12 (connection torsion)	+3 (Tree Bending)	+7 (Tree Bending)
6	15	32	67	+22 (connection torsion)	+8 (Tree Bending)	+13 (Tree Bending)

Conclusion

With minimizing the torsional effect in the connections as the main objective of the design case study, Chapter 8 investigated the feasibility of designing a living architecture utilizing growing trees and crosswise connections as the main load-bearing element. For its ability to resist both gravitational and lateral loads with axial action from diagonal elements, a diagrid structural scheme is a suitable system for structures built with growing trees and crosswise connections. Provided with results from section 8.6.1, implementing diagrid is indeed a viable solution to minimized the torsional effect of the crosswise connection.

Investigation is also made in terms of the importance of accurately determining the rotational stiffness of crosswise connection. From the results obtained from section 8.6.2, It is discovered that accurately determining the rotational stiffness of the crosswise connection is essential because by wrongly assuming that the connection provides infinite stiffness, overestimation of the torsional moment can occur. The degree of the overestimation is related to the eccentricity between the tree diagonals because it directly relates to the torsional stiffness of the connection. It is discovered that the shorter the eccentricity, the more it behaves like a connection with infinite rotational stiffness.

With a parametric design analysis discussed in section 8.8, it can be concluded that, with the verification procedure (unity check) defined in this chapter, designers are able to predict when the growing trees and connections are strong enough to support all the loads from the structure.

Part IV – Final Remarks

9.1 Conclusion

This thesis focuses on investigating the mechanical behaviours of a crosswise connection when used as a load bearing element, and the feasibility of conducting preliminary structural design and verification with growing trees and crosswise connections. Within a larger context of sustainable construction, this thesis serves as a small step towards such direction.

To investigate into this relatively new topic, the scope and methodology of conducting this project has been formulated in chapter 5 in the Introduction, and the parts of this thesis is divided in the following manner with its own objectives, as illustrated in the following charts.

Part-I Literature Study

Botanical study of living trees and crosswise connection

Part-II Mechanical behaviours of crosswise connection

Experimental Design

Finite Element Modelling approach

Wireframe Modelling approach

Part-III Design Case Study

Preliminary structural design and verification with growing trees and crosswise connections

Investigation is then carried out with the formulated outline, and this section serves to provide important conclusions with research made in each part of the thesis.

Part-I Botanical study of living trees and tree connections

To utilize a growing tree as a load-bearing element for structures, it is important to acknowledge its unique characteristics, which is the ability to mechanically optimize itself through adaptive growth based on the typical loading conditions. For instance, a tree is able to optimize its geometry based on the loading conditions exposed to it throughout its lifetime, adding more materials to the regions where stresses are greater. Such behaviours can be reflected by several pieces of evidences including the formation of reaction wood, and the ability of a growing tree to grow around other technical parts.

In terms of the inosculation process between two trees, from research, it can be concluded that, inosculation is triggered due to the bark breakage between the stems. From the bark breakage, microscopic events such as growth from phellogen and cambium are stimulated. During the inosculation process, fiber from both stems deviate and join together to form common growth rings. Such fiber deviation should be acknowledged in design purposes, because it is one of the sources of strength reduction of wood. And finally, for design purposes, it is important to acknowledge that the distance between piths of the stems (eccentricity) stays constant from the start of the fusion process.

Part-II Mechanical behaviours of crosswise connection

Under loading, two of the important stress states are tensile stress perpendicular to the grain, and rolling shear stress. As two of the weakest strength properties of wood, they should be treated with care by future designers. Additionally, due to its irregular geometry, when the connection is loaded, non-uniform stress distribution and stress concentration are found near the interface between the two stems, and the first sign of yielding failure is governed by the tensile strength perpendicular to the grain, which again is located along the interface.

When subjected to in-plane loading, due to the inevitable eccentricity in the connection, both in-plane and out-of-plane behaviours occur. For the in-plane deformation, except for the bending and shear deformation of the stem, part of the deformation is resulted from the torsional shear stress of the connection. Due to fiber orientation of the connection, such torsional shear stress causes rolling shear, which is one of the weakest strength properties of wood. For the out-of-plane deformation, it is resulted from torsional deformation of the stem around its own axis.

Finally, the length of eccentricity plays a vital role in the mechanical behaviours of the crosswise connection, as it directly influences the contacting surface area between the two stems, which is responsible for providing stiffness to the connection and transmitting forces from one stem to the other. With all other boundary conditions unchanged, a connection with a larger eccentricity results in larger in-plane deformation because it causes a smaller torsional stiffness for the connection. It also causes a larger out-of-plane deformation because of the larger moment arm between the neutral axis between the two stems.

Having investigated the mechanical behaviours of a crosswise connection, a wireframe modelling approach of such connection can be achieved by incorporating a separate beam element connecting the neutral axis between the two trees. Obtaining such model is helpful for design purposes, because a wireframe structural analysis for an entire building structure with trees as the main load bearing element can be conducted, and the building's overall behaviours can be captured.

With such modelling approach, an assumption is made, which is to assign the cross section of the connecting beam element with an elliptical shape. Comparing with the finite element modelling approach, although differences are found, its role in terms of providing stiffness and transmitting forces from one stem to the other can be realized. Finally, with the proposed modelling approach, it is necessary to manually adjust the orthotropic material properties of the connection element in the wireframe modelling platform, so that the fiber direction could match the correct local axis.

Part-III Design case study

Combining the knowledge regarding the growth model of trees as well as their tapering geometry, a building design case study with growing trees and crosswise connections is proposed. To properly model the structure, the growth model and the tapering geometry are useful tools to incorporate the time-dependent cross-sectional properties of the trees and tree connections.

For wireframe modelling software that does not incorporate tapering option to the structural elements, such as Karamba 3D, dividing the element into a certain number of segments with various dimension is an acceptable method. The exact number of segments required depends on the degree of the tapering as well as the length of the element.

The self-weight of growing trees needs to be defined with care during the design phase because of the tapering geometry of the trees. By assuming that the density along the entire tree height is constant, the self-weight for each tapering segment can be determined by its volumetric percentage.

With the verification procedures defined in the case study, designers are able to predict when the growing trees and connections will be strong enough to support the entire structure.

9.2 Recommendation for future study

The main focus of this thesis project is on investigating the mechanical behaviours of crosswise connection, which then leads to the study of the feasibility of utilizing crosswise connections in the preliminary design phase of a building structure made with growing trees. However, during the whole thesis projects, a number of assumptions are made, which deserve more attention and studies in the future so that a more comprehensive understanding regarding crosswise connection and its design opportunities can be obtained. Here follows a list for potential research topics:

- As discussed in the thesis, fiber deviation is a result of inosculation. As an important factor that influences the strength of wood, more research should be conducted in terms of how much influence it has on the strength properties of the connection.
- To investigate the rotational stiffness of the crosswise connection, it is ideal to apply pure bending to the connection. With the limitation of the loading machine, the load is designed to apply an inclined force to the stem, which does not generate pure bending to the connection. Therefore, the experiment set up can be further optimized.
- The finite element model is in this thesis is mainly used for analyzing the mechanical behaviours of the crosswise connection, which provides insights to the wireframe modelling. Therefore, linear elastic analysis is conducted. However, to obtain more insights such as a non-linear force vs. displacement curve, or the ultimate resistance of the connection, more research in terms of the non-linear material properties of the connection must be assigned to the elements.
- The geometry of crosswise connection in finite element modelling is constructed using two perfect cylinders, while it is not the case in reality. Therefore, more research in terms of representing the irregular geometry of a crosswise connection should be conducted in the future.
- In the design case study chapter, an assumption is made in terms of the fusion between trees and technical element such as a circular steel bar. Such assumption is based on the research made by Baubotanik research group; however, more research must be conducted in terms of the mechanical behaviour of such connection.

10. Appendix

10. 1 Allometric information of Ficus Benjamina from Year 1 to Year 60

Year	D.B.H (cm)	Tree height (m)	Volume (m3)	Dry weight (kg)
1	4.13231	1.662471	0.007522	3.460311
2	5.975	2.173015	0.017636	8.112482
3	7.77279	2.665294	0.032386	14.89772
4	9.52646	3.139949	0.051822	23.83835
5	11.23679	3.5976	0.075896	34.91197
6	12.90456	4.038849	0.104493	48.06693
7	14.53055	4.464277	0.13746	63.23164
8	16.11554	4.874449	0.17461	80.32072
9	17.66031	5.269909	0.215738	99.23933
10	19.16564	5.651187	0.260622	119.8863
11	20.63231	6.018793	0.309036	142.1566
12	22.0611	6.373222	0.360746	165.943
13	23.45279	6.714955	0.415517	191.1379
14	24.80816	7.044456	0.473117	217.6339
15	26.12799	7.362175	0.533316	245.3255
16	27.41306	7.668546	0.595889	274.1089
17	28.66415	7.963993	0.660616	303.8834
18	29.88204	8.248923	0.727286	334.5516
19	31.06751	8.523733	0.795695	366.0196
20	32.22134	8.788805	0.865646	398.1974
21	33.34431	9.044513	0.936955	430.9992
22	34.4372	9.291216	1.009443	464.3438
23	35.50079	9.529264	1.082944	498.1541
24	36.53586	9.758995	1.1573	532.3578
25	37.54319	9.980738	1.232363	566.8872
26	38.52356	10.19481	1.307998	601.679
27	39.47775	10.40153	1.384076	636.6749
28	40.40654	10.60118	1.460481	671.8211
29	41.31071	10.79407	1.537105	707.0681

30	42.19104	10.98047	1.613851	742.3713
31	43.04831	11.16067	1.690631	777.6903
32	43.8833	11.33493	1.767368	812.9892
33	44.69679	11.5035	1.843992	848.2365
34	45.48956	11.66665	1.920445	883.4046
35	46.26239	11.82461	1.996675	918.4703
36	47.01606	11.97764	2.07264	953.4142
37	47.75135	12.12596	2.148306	988.221
38	48.46904	12.2698	2.22365	1022.879
39	49.16991	12.40939	2.298652	1057.38
40	49.85474	12.54494	2.373304	1091.72
41	50.52431	12.67666	2.447604	1125.898
42	51.1794	12.80476	2.521557	1159.916
43	51.82079	12.92943	2.595175	1193.781
44	52.44926	13.05089	2.668478	1227.5
45	53.06559	13.16932	2.741492	1261.086
46	53.67056	13.28491	2.81425	1294.555
47	54.26495	13.39784	2.88679	1327.923
48	54.84954	13.5083	2.959156	1361.212
49	55.42511	13.61646	3.031401	1394.445
50	55.99244	13.72249	3.10358	1427.647
51	56.55231	13.82657	3.175757	1460.848
52	57.1055	13.92886	3.247997	1494.079
53	57.65279	14.02952	3.320376	1527.373
54	58.19496	14.12871	3.392971	1560.767
55	58.73279	14.22659	3.465866	1594.298
56	59.26706	14.32332	3.53915	1628.009
57	59.79855	14.41903	3.612917	1661.942
58	60.32804	14.51389	3.687266	1696.142
59	60.85631	14.60803	3.762301	1730.658
60	61.38414	14.7016	3.83813	1765.54

10.2 Script of Ficus Benjamina's growth model

```
        If string1 = "tropical ficus benjamina" Then
  a = 2.24394
  b = 1.91147
  c = -0.02323
  d = 0.00013
  a1 = 0.49558
  b1 = 0.28606
  c1 = -0.00089
  a2 = 0.20371
  b2 = 0.18713
  c2 = -0.00053
  dbh = a + (b * age) + (c * age ^ 2) + (d * age ^ 3)
  treeheight = a1 + (b1 * dbh) + (c1 * dbh ^ 2)
  htcb = a2 + (b2 * dbh) + (c2 * dbh ^ 2)
        If treeheight > 21 Then
    treeheight = 21
        End If
        If dbh > 108.41 Then
    dbh = 108.41
        End If
  volumn = 0.0002835 * dbh ^ 2.310647
  dryweight = volumn * 460
        End If
```

10.3 Script for tapering equation

```
diameterCrownBase = dbh + stemR * (htcb - bh)
crownLength = ht - htcb
topRate = diameterCrownBase / crownLength
simpleTaper = 0#

  If ((h >= bh) And (h < htcb)) Then
    simpleTaper = dbh + stemR * (h - bh)
  Else
    simpleTaper = (ht - h) * topRate
  End If
```

10.4 Calculation example for self-weight of 30-year-old Ficus Benjamina in the Growing Tree Tower

From Appendix 10.1, the dry weight of a single tree at the age of 30 is 742.37 kg. By assuming that water occupies half of the tree weight, the weight of one tree is 1481.74 kg. With the weight of one tree known, the correct magnitude of the self weight should be assigned to the segments according to the tapering shape.

In Year 30, the geometry of the tree tower is shown in Figure 127. With the procedure described above, diameter at four locations (D_1 to D_4) need to be defined. The tapering equations stated in section 2.3 are used here
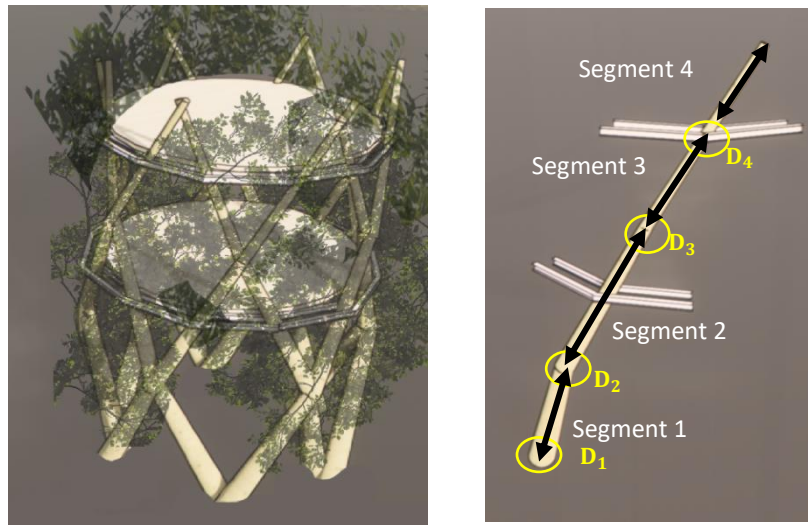
Figure 127. Tapering geometry of diagonal trees

It is reminded here again that depending on the location of the point of interest, one of the three equations (2.2 to 2.4) should be chosen to calculate the diameter of the stem. The boundary value for determining which equation to use is tree breast height (bh) and crown base height (htcb). Tree breast height (bh) is 1.4 meter, while crown base height (htcb) can be obtained from Appendix 10.1, which is 7.155m.

For D_1, located at h=0, which is below breast height (1.4m), equation 2.2 is used:

$$d_h = d\,b\,h + p_b \, * (h - b\,h)$$

$$= 42.191 + (-0.0625) * (0 - 1.4)$$

$$= 42.278 \; cm$$

For D_2, located at h=3m, equation 2.3 is used. It is also important to note that, h refers to the height of the tree, which is higher than the storey height due to the trees being tilted. With the building geometry, the full height of the trees at 3-meter elevation is 3.378 meters.

$$d_h = dbh + p_s * (h - bh)$$

$$= 42.191 + (-0.0202) * (3.378 - 1.4)$$

$$= 42.151 \; cm$$

For D_3, located at h=6m, equation 2.3 is used

$$d_h = dbh + p_s * (h - bh)$$

$$= 42.191 + (-0.0202) * (6.756 - 1.4)$$

$$= 42.083 \; cm$$

For D_4, located at h=7.5m, equation 2.4 is used. To utilize this equation, total tree height and crown taper rate should be computed. Form Appendix 10.1, tree height in year 30 is 10.98m. To obtain the crown taper rate, the diameter at the crown base, D_{cb}, and crown length, L_{crown}, should be calculated:

$$D_{cb} = d.b.h + p_s * (htcb - bh)$$

$$= 42.191 + (-0.0202) * (7.155 - 1.4)$$

$$= 42.075 \; cm$$

$$L_{crown} = ht - htcb$$

$$= 10.98 - 7.155$$

$$= 3.825 \, m$$

$$top\_ht\_rate = \frac{D_{cb}}{L_{crown}}$$

$$= \frac{42.075}{3.825} = 11$$

Finally, D_4 can be calculated using equation 2.4:

$$d_h = (ht - h)^* top\_ht\_\text{rate}$$

$$= (10.98 - 8.445) \cdot (11)$$

$$= 27.887 \, cm$$

Having calculated the diameter at the points of interest, and knowing the total weight of a single tree, it is then possible to calculate the magnitude of the distributed self weight for each segment based on the percentage of the volume of each segment. The numbering of the segment can be referred to Figure 128.
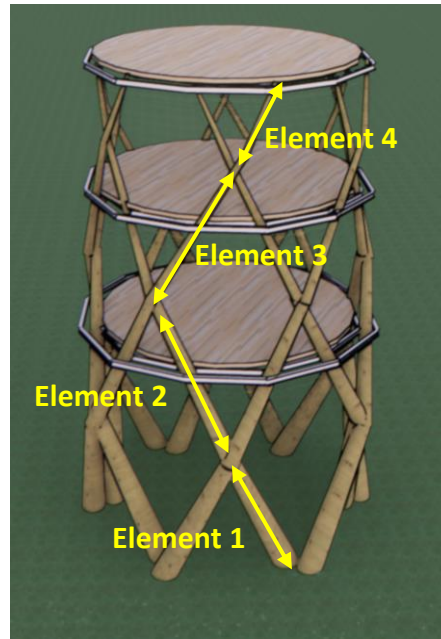
Figure 128. Element labelling for diagonal tree element

For segment 1:

$$V_1 = \frac{1}{3}\pi\left[\left(\frac{42.278}{2}\right)^2 + \left(\frac{42.278}{2} \cdot \frac{42.151}{2}\right) + \left(\frac{42.151}{2}\right)^2\right] \cdot 3.378$$

$$= 4.718 \cdot 10^5 \ cm^3$$

For segment 2:

$$V_2 = \frac{1}{3}\pi\left[\left(\frac{42.151}{2}\right)^2 + \left(\frac{42.151}{2} \cdot \frac{42.083}{2}\right) + \left(\frac{42.083}{2}\right)^2\right] \cdot 3.378$$

$$= 4.706 \cdot 10^5 \ cm^3$$

For segment 3:

$$V_3 = \frac{1}{3}\pi\left[\left(\frac{42.083}{2}\right)^2 + \left(\frac{42.083}{2} \cdot \frac{27.887}{2}\right) + \left(\frac{27.887}{2}\right)^2\right] \cdot 3.378$$

$$= 1.646 \cdot 10^5 \ cm^3$$

Finally, for the cantilevered,

$$V_4 = \frac{1}{3}\pi \cdot \left(\frac{27.887}{2}\right)^2 \cdot 3.378$$

$$= 5.162 \cdot 10^4 \; cm^3$$

With the volume of each segment calculated, the distribution of self weight of each segment can be calculated:

$$V_{total} = V_1 + V_2 + V_3 + V_4 = 1.159 \cdot 10^6 \; cm^3$$

$$w_1 = \frac{\frac{V_1}{V_{total}} \cdot F_{total}}{L_1} = \frac{\frac{4.718 \cdot 10^5 cm^3}{1.159 \cdot 10^6 cm^3} \cdot 14.565 \; kN}{3.378m} = 1.755 \; kN/m$$

Similarly, the self weight distribution of segment 2 and 3 can be calculated

$$w_2 = \frac{\frac{4.706 \cdot 10^5 cm^3}{1.159 \cdot 10^6 cm^3} \cdot 14.565 \; kN}{3.378m} = 1.751 \; kN/m$$

$$w_3 = \frac{\frac{1.646 \cdot 10^5 cm^3}{1.159 \cdot 10^6 cm^3} \cdot 14.565 \; kN}{3.378m} = 0.612 \; kN/m$$

Finally, the point load at the top of the structure resulted from the cantilevered tree elements can be calculated:

$$w_3 = \frac{5.162 \cdot 10^4 cm^3}{1.159 \cdot 10^6 cm^3} \cdot 14.565 \; kN = 0.649 \; kN$$
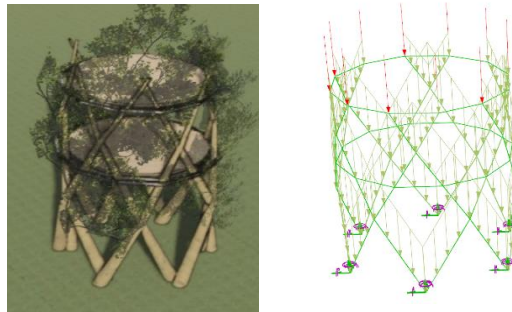
Figure 129. Self weight distribution

10.5 Calculation procedure for determining perimeter beam profile

With 12 sets of perimeter beams according to the floor plan, the point load from the floor beam to the perimeter beam applied at the center would be 1/12 of the total load.

$$Q_{live} = 4kN/m^2 * [\pi * (3m)^2] * (1/12) = 9.425\ kN$$

Assuming that IPE100 is used as floor beams, which have a total length of about 32 meters, an additional self weight from the floor beams is applied:

$$G_{floor\ beam} = 32(m)\ * \ 8.1\ kg/m\ * \ 9.81N/kg\ * \ (1/12) = 0.212\ kN$$

For the floor slab, a typical engineering hardwood flooring that weighs about 1.5 pounds per square foot, which is equivalent to 0.072 KPa, is used. An additional self weight from the floor slab should also be applied:

$$G_{floor} = 0.072\ KPa\ * \ [\pi * (3m)^2]\ * \ (1/12) = 0.17\ kN$$

With the applied loads known, the minimum size of the I-profile to ensure sufficient bearing capacity can be determined. It is to be noted that, with the fact that there are two I-profiles to be installed for each set of the perimeter beams, shown in Figure 130, the total load applied on each of the I-profile will be halved.
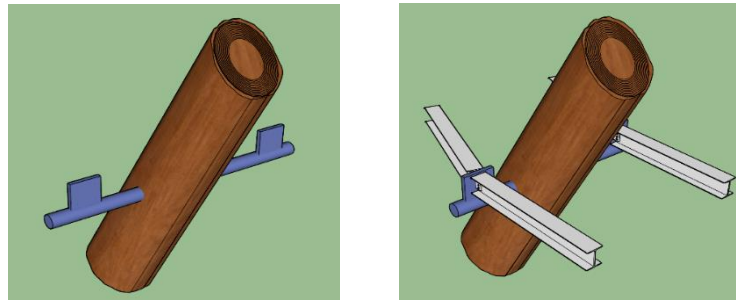
Figure 130.(a) Branch plate-to-circular section fused with tree (b) connected with I-profile beams

With the perimeter beams simply connected at the ends, the maximum bending moment occurs at the center can be obtained in the following manner:

$$F = \frac{1}{2}\left[1.35 \cdot (G_{permanent}) + (1.5) \cdot (0.7) \cdot Q_{live\ load}\right]$$

$$= \frac{1}{2}[1.35 \cdot (0.212kN + 0.17kN) + (1.5) \cdot (0.7) \cdot (9.425kN)]$$

$$= 5.206 \ kN$$

$$M_{Ed} = \frac{1}{2} \cdot F \cdot L$$

$$= \frac{1}{2} \cdot (5.206kN) \cdot (1.55m)$$

$$= 4.035 \ kNm$$

With the maximum designed bending moment determined, the minimum I-profile needed to ensure sufficient strength can be determined. IPE-80, which has an elastic bending moment resistance of 4.71 kNm, is selected for the perimeter beams.

10.6 Calculation procedure for wind pressure on a cylindrical building

Reference area and height

The reference height for the wind action z_e is equal to the maximum height above ground of the section being considered, as specified in *EN1991-1-4 §7.9.2(5)*. The reference area for the wind action A_{ref} is the projected area of the cylinder, as specified in *EN1991-1-4 §7.9.2(4)*. Therefore:

$z_e = z = 12$ m

$A_{ref} = b \cdot l = 6$ m $\cdot$ 12 m $= 72.00$ m²

Basic wind velocity

The basic wind velocity is calculated from the expression:

$$V_b = c_{dir} \cdot c_{season} \cdot V_{b,0}$$

135

,where $V_{b,0}$ is the basic wind velocity, in this scope of this thesis, $V_{b,0}$ is estimated to be 27 m/s. c_{dir} and c_{season} are directional factor and season factor. Recommended value is 1.0, therefore,

$$V_b = 1.0 \cdot 1.0 \cdot 27m/s = 27m/s$$

Basic velocity pressure

$$q_b = \frac{1}{2} \times \rho_{air} \times v_b^2$$

, where

$$\rho_{air} = 1{,}25 kg/m^3$$

$$q_b = \frac{1}{2} \times 1{,}25 \times 27^2 = 455.625\ N/m^2$$

Peak pressure

Following Eurocode EN-1991-1-4, peak wind pressure along the building can be calculated, which is illustrated below:

$$q_p(z) = [1 + 7I_v(z)] * \frac{1}{2} * \rho * v^2{}_m(z)$$

, where $v_m(z)$ is the mean wind velocity:

$$v_m(z) = c_r(z) * c_o(z) * v_b$$

c_r = orography factor, c_o= roughness factor:

$$c_r = k_r * ln\left(\frac{z}{z0}\right)$$

$$c_o = 1.0$$

k_r = terrain factor depending on the roughness:

$$k_r = 0.19\left(\frac{z_0}{z_{0,II}}\right)^{0.07}$$

, where $z_{0,II} = 0.05$, and according to EN-1991-1-4, for a structure built in city area, $z_0 = 1.0$m

$$k_r = 0.19(\frac{1}{0.05})^{0.07} = 0.234$$

I_v = turbulence intensity

$$I_v = \frac{k_l}{c_o(z) * ln\left(\frac{z}{z_0}\right)}$$

k_l is the turbulence factor

$$k_l = 1.0$$

Finally, the peak pressure is calculated as

$$q_p(z) = \left[1 + \frac{7k_l}{c_o(z) * ln\left(\frac{z}{z_0}\right)}\right] * \frac{1}{2} * \rho * v^2{}_b * k_r * ln\left(\frac{z}{z_0}\right)$$

$$q_p(z) = \left[1 + \frac{7}{ln\left(\frac{z}{0.05}\right)}\right] * \frac{1}{2} * 1.25 * 27^2 * 0.234 * ln\left(\frac{z}{0.05}\right)$$

$$q_p(z) = 106.616 * \left[1 + \frac{7}{ln\left(\frac{z}{0.05}\right)}\right] * ln\left(\frac{z}{0.05}\right)$$

The parametrical equation of wind pressure as a funtion of height is used for the analysis

10.7 Results from Unity Check for structural elements in the Growing Tree Tower

10.7.1 Tree diagonals – bending stress vs. bending strength
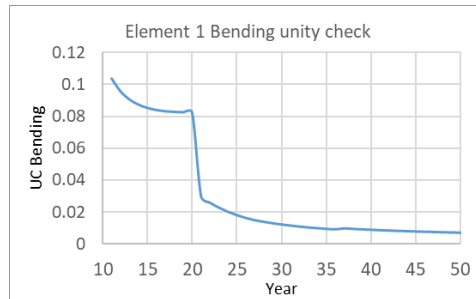
Figure 131. Bending unity check for Element 1
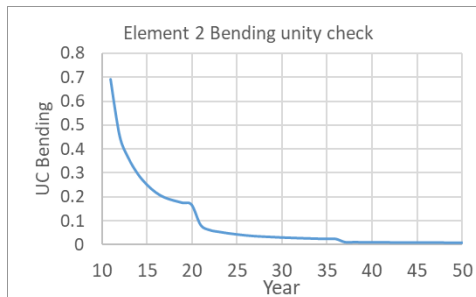
Figure 132. Bending unity check for element Element 2
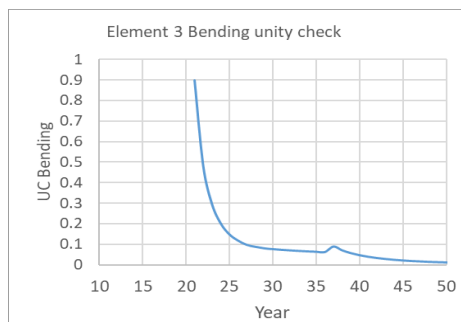
*Figure 133. Bending unity check for element Element 3*
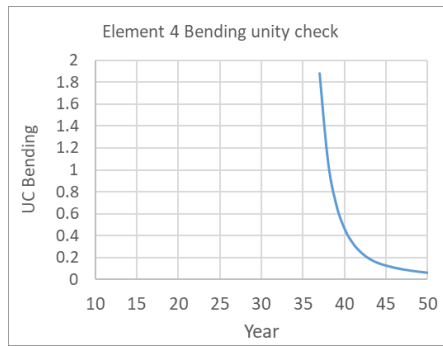
Figure 134. Bending unity check for element Element 4

## 10.7.2 Tree diagonals – axial stress vs. axial strength
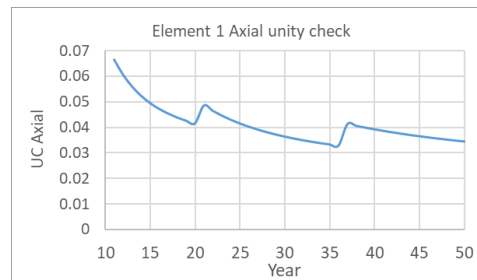

Figure 135. Axial unity check for element Element 1
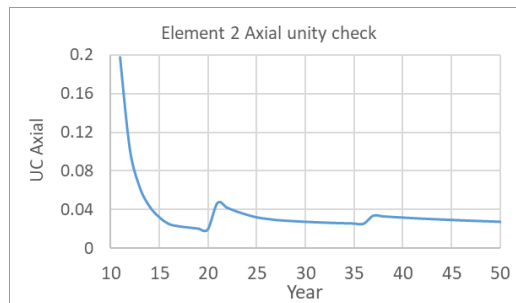
Figure 136. Axial unity check for element Element 2
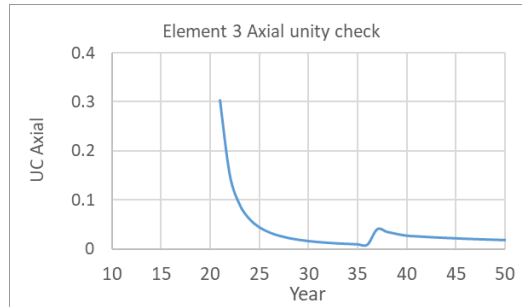
*Figure 137. Axial unity check for element Element 3*
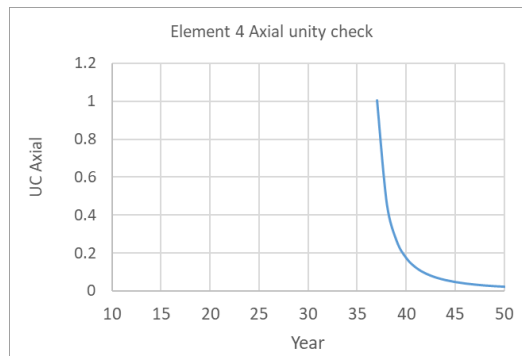
Figure 138. Axial unity check for element Element 4

10.7.3 Tree diagonals – torsional shear stress vs. shear strength
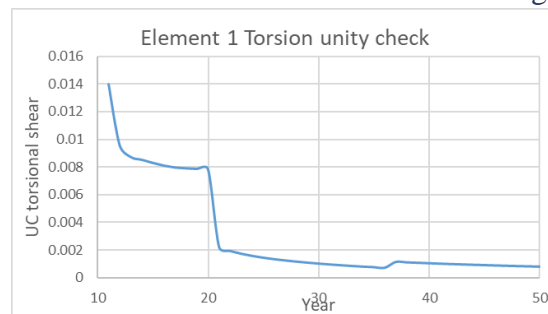

*Figure 139. Torsion unity check for element Element 1*
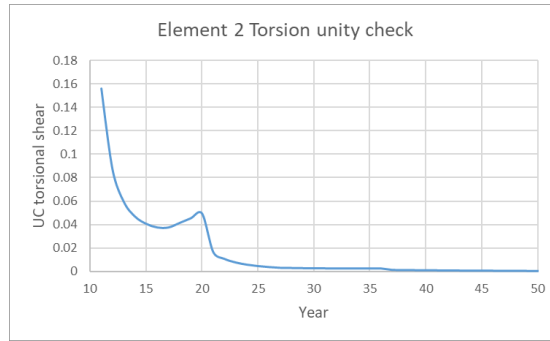
*Figure 140. Torsion unity check for element Element 2*
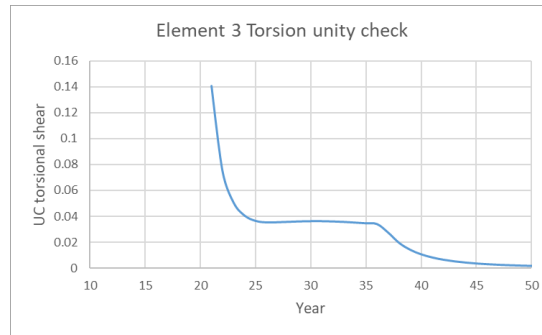

Figure 141. Torsion unity check for element Element 3
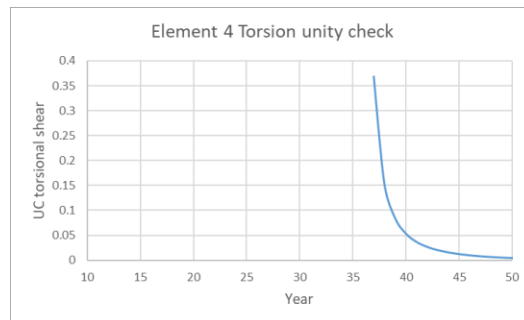
Figure 142. Torsion unity check for element Element 4

10.7.4 Tree diagonals – combination of bending and axial stress
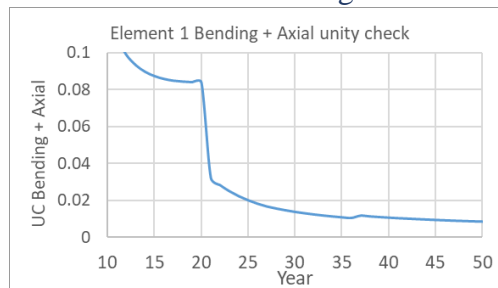
Figure 143. Combination of Bending and Axial unity check for element Element 1
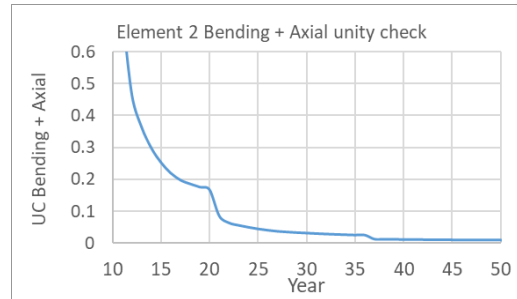
Figure 144. Combination of Bending and Axial unity check for element Element 2
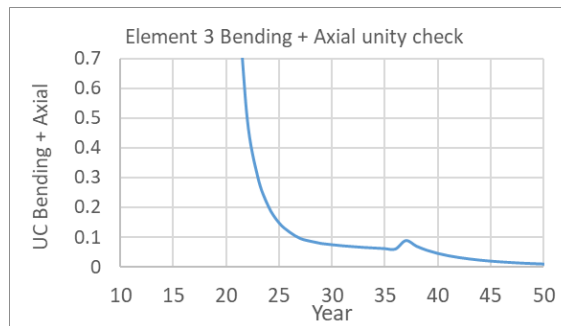

Figure 145. Combination of Bending and Axial unity check for element Element 3
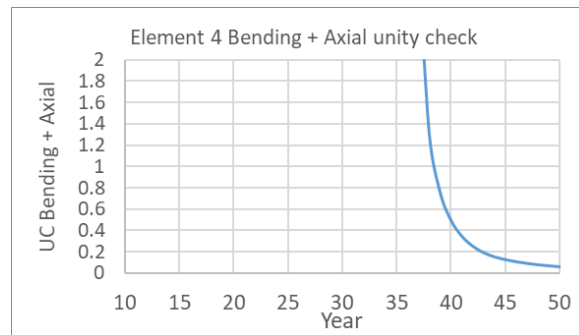

Figure 146. Combination of Bending and Axial unity check for element Element 4

10.7.5 Crosswise connection – torsional shear stress vs. rolling shear strength
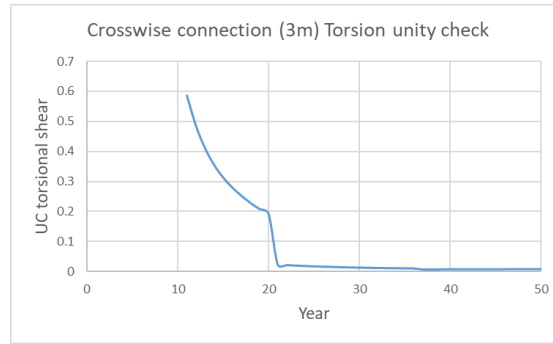
Figure 147. Torsion unity check for Connection 1
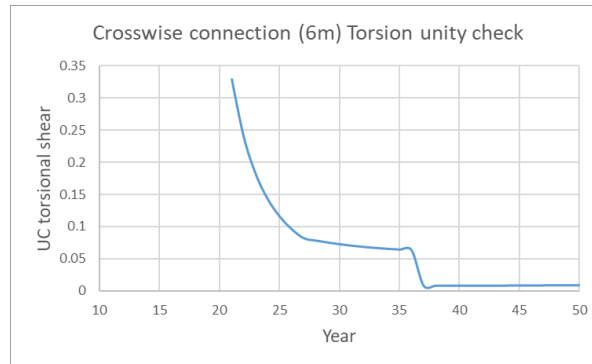
*Figure 148. Torsion unity check for Connection 2*
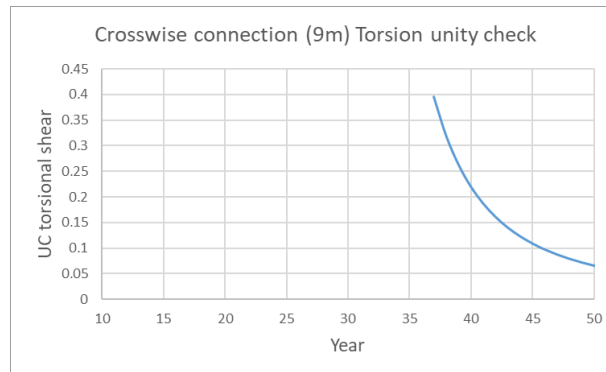

Figure 149. Torsion unity check for Connection 3

10.7.6 Crosswise connection – axial stress vs. axial strength
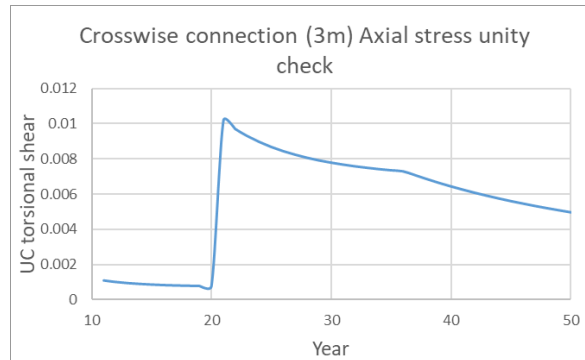
Figure 150. Axial unity check for Connection 1
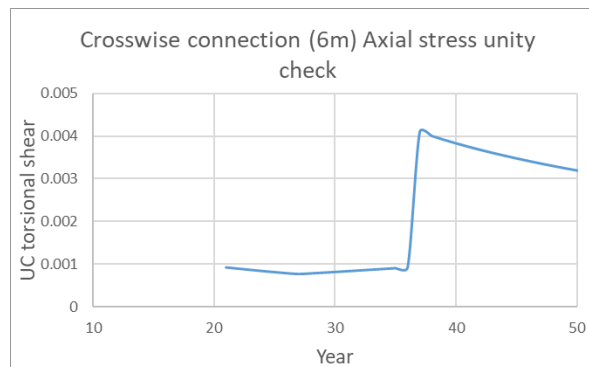
Figure 151. Axial unity check for Connection 2
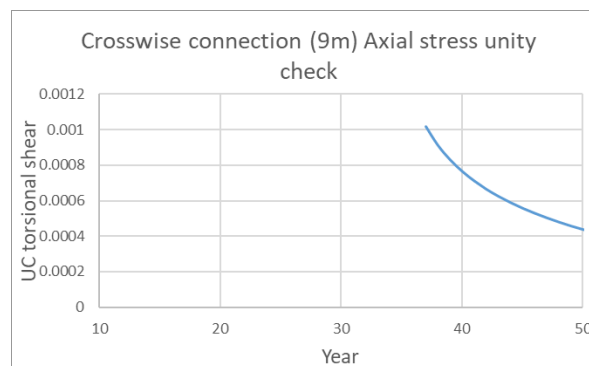
Figure 152. Axial unity check for Connection 3

11.Bibliography

[1]   O. Ortiz, F. Castells, and G. Sonnemann, "Sustainability in the construction industry: A review of recent developments based on LCA," *Constr. Build. Mater.*, vol. 23, no. 1, pp. 28–39, 2009.

[2]   F. R., V. Barranco, J. C. Galvan, S. Batlle, Sebastian FeliuFajardo, García, and David.C.G, "Introductory Chapter: Timber and Sustainability in Construction," *Intech*, vol. i, no. tourism, p. 13, 2016.

[3]   K. A. M. Kamar and Z. A. Hamid, "Sustainable construction and green building: The case of Malaysia," *WIT Trans. Ecol. Environ.*, vol. 167, pp. 15–22, 2012.

[4]   T. Vallas and L. Courard, "Using nature in architecture: Building a living house with mycelium and trees," *Front. Archit. Res.*, vol. 6, no. 3, pp. 318–328, 2017.

[5]   "The chair that grew: John Krubsack's first ever living chair - Walls with Stories." [Online]. Available: https://www.wallswithstories.com/interior/the-chair-that-grew-john-krubsacks-first-ever-living-chair.html. [Accessed: 15-Oct-2020].

[6]   F. Ludwig, "BAUBOTANIK - Designing Growth Processes University of Insbruck (Conference Paper) BAUBOTANIK - Designing Growth Processes," no. September, 2017.

[7]   C. Mattheck, *design in nature, Learning from trees*. 1392.

[8]   R. Chen, "Personal interview," 2020.

[9]   A. Nuijten, "Living Tree Buildings: A research into the possibilities and the load bearing capacity of living tree structures," 2011.

[10]   C. Winterman, "The description of anatomic features of self-growing connections in ficus trees to be able to determine mechanical properties," 2020.

[11]   R. K. Bamber, "Heartwood, its Function and Formation," 1976.

[12]   "DoITPoMS - TLP Library The structure and mechanical behaviour of wood - The structure of wood (II)." [Online]. Available: https://www.doitpoms.ac.uk/tlplib/wood/structure_wood_pt2.php. [Accessed: 31-Aug-2020].

[13]   "Epidermis | plant tissue | Britannica." [Online]. Available: https://www.britannica.com/science/epidermis-plant-tissue. [Accessed: 12-Jun-2020].

[14]   D. K. D. Coder, "Components of Periderm," vol. WSFNR14-13, no. Nov. 2014, pp. 1–18, 2007.

[15]   A. Shipsha and L. A. Berglund, "Shear coupling effects on stress and strain distributions in wood subjected to transverse compression," *Compos. Sci. Technol.*, vol. 67, no. 7–8, pp. 1362–1369, 2007.

[16]   M. Brabec, "Analysis of the Mechanical Behaviour of Wood By Means of Digital Image Correlation," 2016.

[17] B. H. Xu, A. Bouchaïr, and P. Racher, "Appropriate wood constitutive law for simulation of nonlinear behavior of timber joints," *J. Mater. Civ. Eng.*, vol. 26, no. 6, pp. 1–8, 2014.

[18] M. De Ridder *et al.*, "High-resolution proxies for wood density variations in Terminalia superba," *Ann. Bot.*, vol. 107, no. 2, pp. 293–302, 2011.

[19] R. D. Burdon, R. Paul Kibblewhite, J. C. F. Walker, R. A. Megraw, R. Evans, and D. J. Cown, "Juvenile versus mature wood: A new concept, orthogonal to corewood versus outerwood, with special reference to Pinus radiata and P. taeda," *For. Sci.*, vol. 50, no. 4, pp. 399–415, 2004.

[20] U. S. D. of A. F. Service, "Wood Handbook 1999," pp. 1–486, 2005.

[21] D. W. Green, "Wood: Strength and Stiffness," *Encycl. Mater. Sci. Technol.*, pp. 9732–9736, 2001.

[22] "Eurocode 5: Design of timber structures - Part 1-1: General - Common rules and rules for buildings," vol. 1, no. 2005, 2011.

[23] C. Mattheck and I. Tesari, "The mechanical self-optimisation of trees," *Inst. Phys. Conf. Ser.*, vol. 180, pp. 197–206, 2003.

[24] M. E. MILLNER, "Natural Grafting in Hedera Helix," *New Phytol.*, vol. 31, no. 1, pp. 2–25, 1932.

[25] M. Pramreiter, S. C. Bodner, J. Keckes, A. Stadlmann, C. Kumpenza, and U. Müller, "Influence of fiber deviation on strength of thin birch (Betula pendula Roth.) veneers," *Materials (Basel).*, vol. 13, no. 7, 2020.

[26] "UCAR Center for Science Education." [Online]. Available: https://scied.ucar.edu/activity/12606/student. [Accessed: 01-Sep-2020].

[27] C. J. Wood, *Understanding wind forces on trees*. 2009.

[28] E. G. Mcpherson, N. S. Van Doorn, and P. J. Peper, "United States Department of Agriculture Urban Tree Database and Allometric Equations," no. October, 2016.

[29] D. A. R. Tm, E. G. Mcpherson, N. S. Van Doorn, and P. J. Peper, "United States Department of Agriculture Urban Tree Database and Allometric Equations," no. October, 2016.

[30] H. A. Beltran, L. Chauchard, A. Iaconis, and G. M. Pastur, "Equações de afilamento e volume para tamanhos comerciais de nothofagus obliqua e N. alpina," *Cerne*, vol. 23, no. 3, pp. 299–309, 2017.

[31] D. R. Larsen, "Simple taper: Taper equations for the field forester," *Proc. 20th Cent. Hardwood For. Conf.*, pp. 265–278, 2016.

[32] T. Gečys and A. Daniūnas, "Rotational stiffness determination of the semi-rigid timber-steel connection," *J. Civ. Eng. Manag.*, vol. 23, no. 8, pp. 1021–1028, 2017.

[33] M. A. Bhatti and J. D. Hingtgen, "Effects of connection stiffness and plasticity on the service load behavior of unbraced steel frames," *Eng. J.*, vol. 32, no. 1, pp. 21–33, 1995.

[34] H. T. Thai and B. Uy, "Rotational stiffness and moment resistance of bolted endplate joints with hollow or CFST columns," *J. Constr. Steel Res.*, vol. 126, pp. 139–152, 2016.

[35]   "Eurocode 3: Design of steel structures - Part 1-8: Design of joints," vol. 1, no. 2005, 2011.

[36]   B. G. Johnston and E. H. Mount, "Analysis of building frames with semi-rigid connections, Trans:, ASCE, Vol. 107 (1942), p. 993, Reprint No. 53 (42-1)," vol. 107, no. 53, 1942.

[37]   F. J. Dávila-Arbona, J. M. Castro, and A. Y. Elghazouli, "Review of panel zone design approaches for steel moment frames," *14th World Conf. Earthq. Eng.*, 2008.

[38]   B. Rafezy and H. Gallart, "Evaluation of Steel Panel Zone Stiffness Using Equivalent End Zone (EEZ) Model," pp. 1–10, 2012.

[39]   W. P. De Wilde, "Structural optimisation of trusses," vol. 124, no. June, pp. 469–480, 2012.

[40]   "CSI Analysis Reference Manual."

[41]   M. He, H. Tian, and Y. Zhao, "Experimental study and rotational stiffness analysis of bolted timber connection," *2011 Int. Conf. Multimed. Technol. ICMT 2011*, pp. 3959–3963, 2011.

[42]   J. He, T. Yoda, H. Takaku, Y. Liu, A. Chen, and M. Iura, "Experimental and numerical study on cyclic behaviour ofsteel beam-to-column joints," *Int. J. Steel Struct.*, vol. 10, no. 2, pp. 131–146, 2010.

[43]   European Environment Agency (EEA), "Proceedings of International Conference on Advances in Steel Structures 11–14 December 1996, Pages 347-352," *Adv. Steel Struct. (ICASS 96)*, vol. 53, no. 9, pp. 1689–1699, 2019.

[44]   P. S. Prof, M. Veljkovic, and T. U. Delft, "Behaviour of steel-reinforced epoxy resin exposed to compressive-compressive cyclic loading in confined conditions," no. October, 2019.

[45]   F. Mirianon, S. Fortino, and T. Toratti, *A method to model wood by using ABAQUS finite element software Part 1. Constitutive model and computational ABAQUS details*. 2008.

[46]   T. Boake, *Diagrid structures*. 2013.

[47]   "Swiss Re Britain headquarters (The Gherkin), London." [Online]. Available: https://www.archinform.net/projekte/14020.htm. [Accessed: 26-Aug-2020].

[48]   "Flashback: Hearst Tower / Foster + Partners | ArchDaily." [Online]. Available: https://www.archdaily.com/204701/flashback-hearst-tower-foster-and-partners. [Accessed: 26-Aug-2020].

[49]   G. Milana, K. Gkoumas, and F. Bontempi, "Sustainability Concepts in the Design of High-Rise buildings: the case of Diagrid Systems," *Third Int. Work. Des. Civ. Environ. Eng.*, no. August, pp. 170–179, 2014.

[50]   T. M. Boake, "DIAGRIDS , THE NEW STABLITY SYSTEM : COMBINING ARCHITECTURE WITH ENGINEERING."

[51]   C. Sommerer and L. Mignonneau, "Living Systems: Designing growth in Baubotanik," *Fractals An Interdiscip. J. Complex Geom. Nat.*, pp. 1–23, 2011.

[52]   P. C. J. Hoogenboom and R. Spaan, "Shear stiffness and maximum shear stress of tubular

members," *Proc. Int. Offshore Polar Eng. Conf.*, vol. 2005, pp. 316–319, 2005.

[53] J. D. Renton, "Generalized beam theory applied to shear stiffness," *Int. J. Solids Struct.*, vol. 27, no. 15, pp. 1955–1967, 1991.

[54] "Ask Extension - What Percentage of the Mass of a Tree is Water? (General Questions)." [Online]. Available: https://web.extension.illinois.edu/askextension/thisQuestion.cfm?ThreadID=19549&catID =192&AskSiteID=87. [Accessed: 10-Nov-2020].